NUREG/CR-0009

TECHNOLOGICAL BASES FOR MODELS OF SPRAY WASHOUT OF AIRBORNE CONTAMINANTS IN CONTAINMENT VESSELS

A.K. Postma* R.R. Sherry**
P.S. Tam**

Benton City Technology*

Prepared for
U.S. Nuclear Regulatory Commission**

Available from
National Technical Information Service
Springfield, Virginia 22161
Price: Printed Copy $9.00 ; Microfiche $3.00

The price of this document for requesters outside of the North American Continent can be obtained from the National Technical Information Service.

NUREG/CR-0009

TECHNOLOGICAL BASES FOR MODELS OF SPRAY WASHOUT OF AIRBORNE CONTAMINANTS IN CONTAINMENT VESSELS

A.K. Postma* R.R. Sherry** P.S. Tam**

Manuscript Completed: October 1978
Date Published: October 1978

Benton City Technology*
R1, Box 1281
Benton City, WA 99352

Prepared for the
Division of Site Safety and Environmental Analysis
Office of Nuclear Reactor Regulation
U.S. Nuclear Regulatory Commission**

ACKNOWLEDGMENTS

The authors of the present report are indebted to the many researchers who have provided the technical knowledge on which spray models are based. W.F. Pasedag of the NRC staff played a key role in developing the models described herein and is the author of the SPIRT computer code which is used by the staff to analyze spray performance. This work was carried out under the contractual supervision of D.F. Bunch, Chief of the Accident Analysis Branch. His guidence and technical inputs are gratefully acknowledged.

PREFACE

The technological bases for containment spray systems are well understood and are supported by a vast quantity of theoretical and experimental work. Today, there is no doubt that properly designed spray systems are effective in removing airborne iodine; however, there has been an absence of a central, comprehensive document on the topic.

The absence of a report documenting NRC assessments of spray systems has caused occasional confusion for the utility applicants, architect-engineers, and consultants. The present report has been written to remedy this situation.

Contents of this report, including its appendices, describe models that have been found to be acceptable in licensing reviews to evaluate iodine removal capability of spray systems. While considerable effort has been expended to assure the technological accuracy of this work, there may be areas of disagreement with other workers in the field. The authors welcome all constructive criticisms of this report, and may use submitted comments as the basis for a future revision.

CONTENTS

LIST OF FIGURES

Page

LIST OF TABLES

Page

1.0 EXECUTIVE SUMMARY

1.1 The Problem

The Staff of the Nuclear Regulatory Commission has developed mathematical models for assessing the washout rate of airborne contaminants under postulated loss-of-coolant accident (LOCA) conditions. Heretofore there was no one document that summarized the technological bases of the models.

1.2 The Solution

In this report the models currently used by the staff are described in detail. The theoretical and experimental bases which underlie the models are reviewed, and model predictions are compared with experiments to demonstrate the conservatism inherent in the models.

1.3 Summary and Conclusions

Spray systems are included in containment vessels of water reactors as an engineered safety feature to suppress pressure and to scrub airborne contaminants in the unlikely event of a LOCA. The efficacy of spray scrubbing is important in the siting of power reactors because the spray removal rate directly affects the calculated radiation dose which could be received by people in the plant environs.

A large body of information is available to aid in

the assessment of spray performance. In this report the most relevant work is reviewed to show the technical bases for the spray models which are currently used by the NRC Staff.

Important conclusions and summary statements which are supported by this study are the following.

1. Mathematical models are available to conservatively predict the washout of the several physicochemical forms of iodine.
2. The models are supported by a large body of theoretical and experimental data.
3. For elemental iodine, the dominant airborne iodine specie, a stagnant film model has been adopted by the Staff. This model is a simplified form of the equation for absorption by a rigid sphere accounting for mass transfer resistance in both the gas and liquid phases.
4. Absorption of methyl iodide, the most persistent iodine form expected to be present in post-accident atmospheres, is predicted by a model in which it is assumed that both falling drops and wall films are stagnant.
5. Aerosol particle washout is predicted using a model in which conservative estimates of the single drop collection efficiency are obtained from large scale experiments.

NUREG-CR-0009

TECHNOLOGICAL BASES FOR MODELS OF SPRAY WASHOUT OF AIRBORNE CONTAMINANTS IN CONTAINMENT VESSELS

by

A.K. Postma
R.R. Sherry
P.S. Tam

2.0 INTRODUCTION

This report is a review of the technological bases underlying the washout models used by the Accident Analysis Branch to evaluate containment spray systems. Spray systems are installed in the containment vessels of water reactors to reduce containment pressure, remove heat from the containment and remove fission products which could be released from the core as a result of a postulated design basis loss-of-coolant accident (LOCA).

The maximum thyroid dose which an individual could receive following a LOCA is reduced by engineered safety features such as spray systems[1,2]. The magnitude to which potential doses are reduced by a spray system depends on how fast airborne fission products are washed from the containment atmosphere. The expected washout rates are predicted from mathematical models which account for the dominant removal mechanisms.

In order to assure that the safety of the public is adequately protected, models which are conservative are required. Such models must take into account all relevant physical phenomena to assure that removal mechanisms are adequately accounted for and thereby provide assurance that they are indeed conservative.

The spray systems of interest would operate only under postulated loss-of-coolant accident conditions. The performance of the containment system, including sprays, is typically evaluated by assuming that a significant fraction of the core inventory of fission products enters the containment atmosphere as an instantaneous source term[1,2]. This "site suitability" source term does not represent a realistic estimate of fission product releases, but rather serves as a tool for conservatively estimating radiation doses under accident conditions as required by NRC guidelines[1,2]. In reality, the emergency core cooling system would prevent the melting of fuel elements, and the only radioactive materials released to the containment system would be small quantities of fission gases which could escape from failed cladding.

Significant fractions of the core inventory of fission products can be released only under extremely low probability core-melt accidents. Thus fission product source terms of the magnitude postulated to evaluate spray system performance are possible only under low probability core-melt accidents which are more severe than design basis events. The use of the large "site suitability" source terms is useful because the doses from such a source term are obviously larger than

doses from any credible accident within the design-basis envelop.

3.0 OBJECTIVE

There is much theoretical and experimental information available on containment spray systems. Spray washout models used by NRC have been developed from the available technological base. However there is no one document that summarizes the technological bases of the models. This report is an attempt to provide such a summary.

4.0 BACKGROUND

As early as 1965, several reactor designs were proposed[3,4,5,6] in which containment sprays were designed to remove both heat and airborne fission products from the containment atmosphere in the unlikely event of a loss-of-coolant accident. Spray systems represent a class of gas scrubbers. Aqueous scrubbers similar to containment sprays are widely used in industrial applications and have been studied extensively over a period of more than 40 years[7,8,9,10].

It is important to recognize that there are differences as well as similarities between industrial scrubbers and containment building sprays. These are: (1). In a typical industrial scrubber the gas and liquid are in countercurrent flow and each makes one pass through the device, whereas in the containment building the same

body of air remains in the building for the entire time. (2). In the industrial absorber the contact time for gas is normally in the range of a few seconds, whereas in the containment building the contact time between gas and liquid is comparatively long and the liquid is recycled continuously. (3). In the containment building the mass of material to be absorbed is relatively small, and one can easily afford to use overwhelming excesses of chemical reagents to assure complete absorption. (4). In the containment building there are some problems unique to highly radioactive environments, such as radiolysis of the spray solution.

The performance of sprays in containment applications has been studied extensively throughout the world. In the U.S., the former U.S. Atomic Energy Commission sponsored research designed to provide the understanding needed to predict fission product removal under accident conditions. Major efforts in the 1960's included pilot plant testing and spray solution evaluations at Oak Ridge National Laboratory[11,12,13] and large scale containment system experiments at Battelle-Northwest[14]. Industry sponsored work was directed to spray system design[15] and to the efficacy of particular spray solution compositions[16,17,18,19].

Foreign work in the 1960's was limited to theoretical work and small scale tests. Results obtained in Japan[20] and Sweden[21] are consistent with those from American programs. More recent results from Italy[22] provide large scale test data which are consistent with results from CSE tests in the U.S..

As applications of sprays have developed, spray solutions of several chemical compositions have been used. These include boric acid, boric acid made basic

with sodium hydroxide (caustic spray), sodium hydroxide/sodium thiosulfate, and boric acid containing hydrazine at trace level concentrations. The effects of these chemical additives on spray effectiveness will be discussed in this report.

Iodine washout by sprays is complicated by the fact that it may exist in three states: elemental iodine, organic iodides, and particulate iodine. The most persistent of these forms, organic iodides, was shown by Eggleton and Atkins in 1964[23] to be composed mainly of methyl iodide. The fractional abundance of each of these three forms would vary with accident conditions. For a site suitability source term released into the containment vessel, the percent of each of the three species of iodine is conservatively estimated to be 91:4:5[1,2]. The absorption characteristics of the three species will be treated in following sections. In addition to these three iodine species, hypoiodous acid, HOI, was discovered subsequent to completion of most experimental programs. Its properties are not well known; hence the NRC approach has been to include hypoiodous acid with the organic iodide fraction. This is conservative because HOI is more readily absorbed by water sprays than organic iodides.

5.0 MODELS FOR SPRAY WASHOUT

Fission product washout in a containment vessel can be described mathematically by a first order differential equation which equates the rate of mass accumulation in

the containment atmosphere to the difference between source and removal rates:

$$V \frac{dC_i}{dt} = G_i - \Sigma R_{ij} C \qquad (1)$$

where V = volume of gas space, m^3,
C_i = concentration of ith fission product in gas phase, kg/m^3,
G_i = ith fission product input rate, kg/hr,
R_{ij} = jth removal rate constant for the ith fission product (R_{ij} is assumed to be first order with respect to concentration), m^3/hr.

For realistic calculations both time-dependent source and removal terms should be considered in modelling the spatial and temporal fission product distributions in multicompartment containment buildings. However, for a conservative analysis of the design basis LOCA an instantaneous source term may be assumed. For an instantaneous source, the time-dependent generation terms, G_i, in Eq. (1) are replaced by an initial condition on C_i at time zero. The washout equation may then be written as

$$\frac{dC_i}{dt} = \Sigma \lambda_{ij} C_i \qquad (2)$$

where $\lambda_{ij} = \frac{R_{ij}}{V}$ = the jth removal rate constant for the ith fission product specie, hr^{-1}.

The first order removal process defined in Eq. (2) applies until equilibrium between fission product concentrations in the containment atmosphere and the containment liquid mass is approached. At this point Eq. (2) is no longer valid and $\frac{dC}{dt}$ approaches zero. A simple and conservative method of handling the approach to equilibrium is to use the first order washout equation until a cut-off concentration level is reached. After the cut-off concentration level is reached washout is neglected.

The washout model based on an instantaneous source term and a cut-off concentration to account for equilibrium effects may be obtained by integrating Eq. (2) with respect to time:

$$C_i = C_{io} e^{-\lambda_i t} \qquad (3)$$

where $\lambda_i = \sum_j \lambda_{ij}$

$C_{io} = C_i$ at time = 0,

and imposing the condition $\lambda_i = 0$ for $C_i \leq C_{i_{cut\text{-}off}}$.

In Eq. (3) λ_i is the total removal constant resulting from all removal mechanisms for the ith fission product specie.

Each fission product specie would have its own lambda and cut-off concentration level. Consequently Eq. (3) must be solved for each iodine specie independently. The following subsections describe the calculational methods used to predict λ_i's for particular containment systems and fission product species.

5.1 Models For Absorption of Elemental Iodine

Elemental iodine is the dominant iodine specie in post-accident containment atmospheres. It is removed at an appreciable rate by both spray drop absorption and by wall deposition. Models for these two removal processes are described as follows. For simplicity, subscripts indicating the iodine species are dropped in the development of equations in this section.

5.1.1 Absorption by Spray Drops

The removal rate of any absorbable specie may be equated to the product of concentration increase and spray flow rate:

$$RC = F(C_{\ell o} - C_{\ell i}) \qquad (4)$$

where RC = removal rate, k_g/hr,
C = airborne iodine concentration, k_g/m^3,
R = spray removal rate constant, m^3/hr,
F = spray flow rate, m^3/hr,
$C_{\ell o}$ = concentration of solute in spray drops leaving atmosphere, k_g/m^3,
$C_{\ell i}$ = concentration of solute in liquid entering atmosphere, k_g/m^3.

For spray liquid which has not been exposed to the containment atmosphere previously (i.e. during the injection phase of spray operation), $_{\ell i} = 0$ and $C_{\ell o}$ may be related

to the equilibrium partition coefficient, H, through the use of an absorption efficiency, E, defined by:

$$C_{\ell o} = HE(C) \qquad (5)$$

where H = equilibrium partition coefficient applicable to spray absorption,
E = fractional approach to equilibrium by spray drops during a single pass,
C = concentration of solute in gas phase, k_g/m^3.

Eq. (4) and (5) may be used together with Eq. (2) to relate λ to the spray parameters:

$$\lambda_s = \frac{FHE}{V} \qquad (6)$$

where λ_s = washout λ due to the spray, hr^{-1},
V = volume of sprayed region, m^3.

The absorption efficiency, E, may be computed by several models. The models differ in degrees of conservatism and simplicity, and hence represent alternatives useful in specific applications.

Stagnant Film Model

The stagnant film model is based on absorption through both a gas film and a liquid film. This model is conservative because it neglects mixing within the drop. In this

model, E is computed by

$$E = 1-\exp-\left[\frac{6k_g t_e}{d\left(H+\frac{k_g}{k_\ell}\right)}\right] \qquad (7)$$

where k_g = gas film mass transfer coefficient, cm/sec,
t_e = drop exposure time, sec,
d = drop diameter, cm,
k_ℓ = liquid film mass transfer coefficient, cm/sec.

The gas phase mass transfer coefficient, k_g, may be computed from the Ranz-Marshall approximation[24] to the Frossling equation[25]:

$$k_g = \frac{D}{d}\left(2+0.6Re^{0.5}Sc^{0.33}\right) \qquad (8)$$

where D = diffusivity of solute in gas phase, cm^2/sec,
Re = Reynolds number for falling drop,
Sc = Schmidt number for solute in gas phase.

On the liquid side of the drop interface, the film coefficient is predicted by Griffiths'[26] approximation to the rigid drop[27] absorption equation:

$$k_\ell = \frac{2\pi^2 D}{3d} \qquad (9)$$

where D = diffusivity of solute in liquid, cm^2/sec.

Eq. (9) is a conservative formulation of the rigid drop equation in that it predicts lower rates of absorption than the rigid drop equation[28].

Since Eq. (9) is a simple, conservative predictor of the drop absorption efficiency, it is the equation used by the staff to evaluate containment spray washout using the site suitability instantaneous source term. (See Appendix A for a listing of the computer code SPIRT 10.)

Rigid Drop Model

The rigid drop model is similar to the stagnant film model in that it represents a mathematical solution to absorption by a stagnant sphere, accounting for gas phase and liquid phase mass transfer resistance. Dankwerts'[27] equation for drop absorption can be written in terms of the absorption efficiency, E, as[28]:

$$E = 1 - \sum_{n=1}^{\infty} \frac{6Sh^2 \exp(-\alpha_n^2 \theta)}{\alpha_n^2 \left(\alpha_n^2 + Sh(Sh-1) \right)} \qquad (10)$$

where $Sh = \frac{k_g a}{HD_\ell}$

$$\theta = \frac{D_\ell t_e}{a^2}$$

α_n = nth root of $\alpha_n \mathrm{Cot}\alpha_n + (Sh-1) = 0$

a = drop radius, cm.

Numerical comparisons of the stagnant film and rigid drop models[28] show that the stagnant film model typically underpredicts the E values as compared to the rigid drop model by less than 16%. This minor difference may not justify the use of the more complex rigid drop formulation.

Well-Mixed Drop Model

In the well-mixed drop model, mass transfer resistance inside the drop is neglected. The solute concentration on the liquid side of the gas/liquid interface is equated to the average concentration in the drop. While liquid phase mass transfer resistance is neglected, gas/liquid equilibria are properly accounted for in this model. The drop absorption efficiency may be expressed as[28]

$$E = 1-\exp-\left[\frac{6k_g t_e}{dH}\right]. \qquad (11)$$

By comparison with the stagnant film E, Eq. (7), Eq. (11) would apply where k_ℓ was large (small drops or circulating drops) or where H was large compared to k_g/k_L (reactive liquid).

Numerical values of E predicted from Eq. (11) are as much as a factor of two higher than values of E predicted from the stagnant film model. For H values larger than 10^5, all three models yield similar predictions.

The well-mixed drop model is not currently employed

by the staff, but could find application in realist analyses of spray performance.

5.1.2 Deposition of Iodine on Interior Containmen Surfaces

Surface deposition of iodine occurs as the result of several transport processes which occur in series. Regions of transport include: the bulk gas phase, the gas boundary layer, the liquid film, and the solid wall surface. Of these, transport in the gas boundary layer has been shown to be the controlling step[29].

Several models have been proposed to describe fission product removal due to surface deposition. Of these, the Knudsen-Hilliard[30] model and the Yuille-Baston[31] model appear to be in good agreement with available experiments. The Knudsen-Hilliard model views deposition as a gas film transport process to vessel surfaces. The gas film mass transfer coefficient is predicted from natural convection heat transfer correlations by a mass transfer-heat transfer analogy. The Yuill-Baston model is based on the penetration theory for mass transfer, and uses a natural convection heat transfer model to estimate gas flow velocities. Of the two models, the Knudsen-Hilliard model offers several advantages and has been adopted by the staff.

In the Knudsen-Hilliard model, the bulk gas in the containment atmosphere is assumed to be well-mixed by natural convection, by steam flows, and by spray operation. A gas boundary layer is established adjacent to

containment surfaces. For a laminar boundary layer the mass transfer coefficient across the gas boundary layer is predicted by

$$\frac{k_g L}{D} = 0.59(Gr\ Sc)^{\frac{1}{4}} \qquad (12)$$

where k_g = film mass transfer coefficient,
L = length measured along deposition surface,
D = diffusivity of iodine in gas phase,
Gr = Grashov number,
Sc = Schmidt number.

For turbulent boundary flow, the mass transfer coefficient is predicted using

$$\frac{k_g L}{D} = 0.13\ (Gr\ Sc)^{1/3} \qquad (13)$$

The transition from laminar flow to turbulent flow occurs at a critical Grashov number. Important variables in the Grashov number include length, L, and temperature difference between the gas and the wall surface. Therefore the plate length at which the flow transition occurs depends on thermal conditions in the containment vessel.

Hilliard and Coleman[32] found that Containment System Experiment tests were best explained by assuming that transition from laminar to turbulent flow occured ten feet from the top of the test vessel. This value was in good agreement with predicted transition lengths. These transition lengths apply for thermal conditions which occur after blowdown transients are over, and

where heat transport takes place with gas film temperature differences of 1^0F to 2^0F. They would conservatively apply to post-LOCA situations consistent with spray operation.

The iodine removal rate constant for a particular compartment in the containment is given by

$$\lambda_n = \frac{k_g A}{V} \tag{14}$$

where λ_n = removal rate constant due to surface deposition,
k_g = average mass transfer coefficient,
A = surface area for wall deposition,
V = volume of contained gas.

As is described in section 6.1.9, the value of k_g should not exceed 0.137 cm/sec. This maximum value is based on CSE tests, and its use assures that the predicted deposition rates remain within the range where the Knudsen-Hilliard model applies.

5.1.3 Overall Absorption Rate

The overall removal rate is the sum of that due to spray operation and natural convection plate-out:

$$\lambda = \lambda_s + \lambda_n \tag{15}$$

Thus the airborne concentration at any time, t, after the release of an instantaneous source term is

$$C = C_o\, e^{-(\lambda_s + \lambda_n)t} \qquad (16)$$

An alternative calculational approach, which has been used in the past, is to apply an instantaneous plate-out factor of 2 to the source term and set λ_n equal to zero. This latter approach is discussed later in this report.

5.1.4 Effect of Spray Solution Composition

Elemental iodine is only moderately soluble in water. Thus for many aqueous solutions the equilibrium partition coefficient, H, depends mainly on chemical equilibria in solution. A first step in iodine hydrolysis involves formation of HOI, I^- and H^+:

$$I_2 + H_2O \rightleftarrows HOI + H^+ + I^- \qquad (17)$$

This reaction can be shifted to the right by removing HOI, H^+, or I^- through chemical reactions. When any of the reaction products is removed the partition coefficient, H, is increased.

Many containment spray systems contain an injection system for adding sodium hydroxide. NaOH enhances iodine uptake by reducing the H^+ concentration and shifting Eq. (17) to the right. Reactive additives such as hydrazine and sodium thiosulfate owe their effectiveness to destruction of HOI, an alternative way to shift Eq. (17) to the right.

Experimental data are required to determine the

numerical value of H for a particular spray solution. The value of H which governs spray absorption is the "instantaneous" value which is attained in time periods short compared to drop fall times. Slower reactions would aid absorption on a longer time scale, but their effect must be accounted for with models which account for a finite reaction rate of iodine in solution.

Spray solutions which have been characterized in terms of the iodine partition coefficient include: (a) sodium hydroxide[28], (b) hydrazine[17,33], sodium thiosulphate[14,19,33,34], and boric acid without other additives[18,33].

5.2 Models For Absorption of Organic Iodides

Methyl iodide is slightly soluble in water, and reacts slowly with pure water. Therefore its absorption rate is governed by mass transfer resistance in the liquid phase. This is different from elemental iodine which is more soluble in water, and also undergoes very rapid hydrolysis through ionic reactions.

For slightly soluble gases which are relatively inert chemically, the absorption rate is strongly influenced by the presence of reactive additives which destroy the dissolved solute. Models for the absorption rates of drops, wall films, and sump pools will be described in detail.

Absorption by a stagnant drop with a surface resistance may be predicted from a solution of the diffusion equation written in spherical coordinates

$$\frac{\partial C}{\partial t} = \frac{D}{r^2}\left[\frac{\partial}{\partial r}\left(r^2 \frac{\partial C}{\partial r}\right)\right] - R \qquad (18)$$

subject to the surface condition

$$D \frac{\partial C}{\partial N} = k_g (C_g - C_{gi}) \qquad (19)$$

where N = outward directed normal at the surface of the drop,
D = diffusivity in the liquid,
R = destruction rate per unit volume by chemical reaction.

A solution to Eq. (18), subject to the boundary condition (19) and assuming C is initially zero within the drop, has been given by Danckwerts[27]. The total amount of absorption in time t is obtained by integrating the flux over the area and time. The final equation for the amount of solute gas absorbed by a drop is

$$Q = 8\pi h^2 C^* Da^2 \sum_{n=1}^{\infty} \frac{\alpha t(k+D\alpha_n^2) - D\alpha_n^2\left(\exp[-t(k+D\alpha_n^2)] - 1\right)}{(k+D\alpha_n^2)^2\left(a\alpha_n^2 + h(ah-1)\right)} \qquad (20)$$

where $h = \frac{k_g}{HD}$, cm^{-1},

$C^* = HC_g$ = solute conc. on liquid side of interface, kg/cm^3,

α_n = nth root of $(a\alpha)\mathrm{Cot}(a\alpha) + ah - 1 = 0$, cm^{-1},
k = first order reaction rate constant, sec^{-1},
t = exposure time, sec,
a = drop radius, cm,
D = diffusivity of solute in liquid, cm^2/sec,
Q = total amount of solute absorbed during exposure time t, kg.

The boundary condition, Eq. (19), has been assumed to apply at all points on the surface of the drop. Also the reaction rate, R, was taken to be that for a first order reaction, kC.

If gas phase resistance is small, h becomes large. In the limit as h approaches infinity, Eq. (20) becomes

$$Q = 8\pi aDC^* \sum_{n=1}^{\infty} \frac{ka^2 + \dfrac{Dn^2\pi^2}{k + \dfrac{Dn^2\pi^2}{a^2}} \left(1-\exp\left[-t\left(k + \dfrac{Dn^2\pi^2}{a^2}\right)\right]\right)}{ka^2 + Dn^2\pi^2} \qquad (21)$$

This equation would be expected to apply for absorption of slightly soluble substances such as methyl iodide unless the reaction rate constant, k, were very large. For very large values of the reaction rate gas phase resistance is appreciable. A simple test of the applicability of Eq. (21) is to compare Q calculated from Eq. (21) with Q predicted for zero liquid phase mass transfer resistance. If the value of Q calculated from Eq. (21) is less than a few percent of the rate limit by gas phase resistance,

it may be concluded that Eq. (21) is a good approximation to Eq. (20).

Eq. (21), the equation which would apply for many reactive spray solutions used to absorb methyl iodide, is not amenable to evaluation by hand calculations. Numerical evaluations are given in reference 29.

Both Eq. (20) and Eq. (21) can be written in terms of absorption efficiency, E. Since E is equal to the attained solute concentration divided by the equilibrium concentration, $E = 3Q/4\pi a^3 C^*$.

5.2.2 Wall Film Absorption

The flow characteristics and absorption by liquid films have been extensively studied during the past 25 years. Based on theoretical and experimental studies, the general characteristics of wetted wall flow may be stated as follows. At low flow velocities, laminar flow persists, the velocity profile is parabolic, and the free surface velocity is 3/2 the average velocity. At Reynolds numbers in the range 5-25, waves begin to appear on the surface, though the flow is substantially laminar. At Reynolds numbers of 250-500 the flow becomes turbulent.

Absorption into a wetted wall film is described mathematically by Eq. (22):

$$\frac{\partial C}{\partial t} + V_x \frac{\partial C}{\partial x} + V_y \frac{\partial C}{\partial y} + V_z \frac{\partial C}{\partial z} = D\left(\frac{\partial^2 C}{\partial x^2} + \frac{\partial^2 C}{\partial y^2} + \frac{\partial^2 C}{\partial x^2} \right) - R \quad (22)$$

where C = concentration of solute in liquid, kg/m^3

t = time, sec,

V_x = fluid velocity in x direction, m/sec,

V_y = fluid velocity in y direction, m/sec,

V_z = fluid velocity in z direction, m/sec,

D = diffusion coefficient of solute in liquid, m^2/sec,

R = destruction rate per unit volume by chemical reaction = kC, kg/m^3 sec,

x,y,z = distances measured along the three rectangular space coordinates,

k = first order reaction rate constant, sec^{-1}.

The total absorption rate for methyl iodine is obtained by integrating the absorption rate per unit area $D \left.\frac{\partial C}{\partial x}\right|_{x=0}$ over the surface area. Analytical solution is possible only for relatively simple flow regimes. A simple flow regime of practical use is that corresponding to fully developed one dimensional laminar flow. For this case, the velocity profile is derived to be

$$V_z = V_{max} \left(1-\left(\frac{x}{\delta}\right)^2\right) \quad x \leq \delta \tag{23a}$$

$$V_x = 0 \tag{23b}$$

$$V_y = 0 \tag{23c}$$

where V_{max} = velocity at gas/liquid interface,

z = distance parallel to plane of film, measured in direction of liquid flow,

x = distance measured perpendicular to plane of film measured from surface of film toward solid surface,

δ = thickness of liquid film.

Using this velocity profile, and neglecting diffusion in the y direction, Eq. (22) becomes

$$V_{max}\left[1-\left(\frac{x}{\delta}\right)^2\right]\frac{\partial C}{\partial z} = D\frac{\partial^2 C}{\partial x^2} - kC \qquad (24)$$

The initial and boundary conditions must be chosen consistent with the physical problem being modeled by Eq. (24).

For short laminar films, the solute does not have time to penetrate far into the film, and hence absorption takes place as though the film were infinite in thickness. The differential equation for this case involving the penetration theory approximation, is obtained from Eq. (24) by setting x equal to zero.

$$V_{max}\frac{\partial C}{\partial z} = D\frac{\partial^2 C}{\partial x^2} - kC \qquad (25)$$

Since x is taken to be zero, the fluid velocity is assumed to be equal to V_{max} at all positions. Thus Eq. (25) may be written in terms of exposure time,

$$t = \frac{z}{V_{max}} . \qquad (26)$$

The solution to Eq. (25) is given by Danckwerts[35] as

$$q = C^* \frac{D}{k} \left[(kt + \tfrac{1}{2}) \cdot \operatorname{erf}(kt) + \frac{kt}{\pi} e^{-kt} \right] \quad (27)$$

where C^* = concentration in liquid at the gas-liquid interface,

q = amount absorbed per unit area up to time t.

Most experimental data obtained for laminar flow in short wetted wall columns agree with predictions based on the penetration theory. Serious discrepancies however may be encountered if the absorption process causes interfacial turbulence[36]. Interfacial turbulence enhances absorption compared to predictions based on the penetration theory.

A lower limit to the absorption may be calculated from a solution of Eq. (24) for $\frac{\partial C}{\partial z} = 0$

$$0 = D \frac{d^2C}{dx^2} - kC. \quad (28)$$

For this steady state model, the boundary conditions are

$$C = C^* \text{ at } x = 0,$$

$$\frac{dC}{dx} = 0 \text{ at } x = \delta.$$

The second of these boundary values is based on the assumption that there is no net transfer of methyl iodide to the solid wall. The absorption rate per unit area of interface is

$$q = C^* \sqrt{kD} \tanh \left(\sqrt{\frac{k}{D}} \delta \right) \quad (29)$$

Eq. (29) would yield lower limit estimates of the absorption rate because transient absorption has been neglected, and uptake at the solid wall has been taken as zero.

For the films encountered in containment vessels, predictions based on Eqs. (27) or (29) do not differ greatly. As shown later in this report, experimental results can be explained using the lower limit Eq. (29), hence this equation is used by the staff to evaluate methyl iodide absorption by films of reactive solution.

5.2.3 Absorption by Sump Pool Liquid

Uptake of methyl iodide in sumps in a PWR containment system can be important compared to spray and wall film absorption for spray solutions which react slowly with methyl iodide. For the slow reaction regime, exposure of liquid in the form of sprays and wall films merely cause it to attain saturation with respect to the gas phase. If no additional reaction occurred, recirculated liquid would enter saturated in methyl iodide, and no further absorption would occur. Residence time of liquid in the pool is relatively long, permitting relatively slow reactions to destroy absorbed methyl iodide.

A material balance made on the spray liquid can be used to relate the methyl iodide washout rate to the pool reaction rate. For the pool, the following CH_3I material balance can be written

$$\text{Input Rate} = F\,HC_g, \tag{30a}$$

$$\text{Output Rate} = F\,C_\ell + kV_\ell C_\ell, \tag{30b}$$

$$\text{Accum. Rate} = 0 \text{ for steady state absorption,} \tag{30c}$$

$$\text{and } F\,HC_g = FC_\ell + kV_\ell C_\ell. \tag{30d}$$

where F = volumetric spray flow rate entering pool, m^3/sec,
k = reaction rate constant, sec^{-1},
C_ℓ = CH_3I conc. in pool liquid, kg/m^3,
V_ℓ = volume of pool liquid, m^3.

A similar material balance made on the gas phase leads to

$$FC_\ell = FHC_g + V_g\left(\frac{dC_g}{dt}\right). \tag{31}$$

If Eq. (31) is solved for C_ℓ, the methyl iodide concentration in the liquid, and the result substituted into Eq. (30) and the resulting equation solved for C_g, the result is

$$C_g = C_{go} \exp -\left[\frac{F\,k\,H\,t}{V_g\left(\frac{F}{V_\ell} + k\right)}\right] \tag{32}$$

where C_{go} = airborne methyl iodide concentration at time zero, kg/m^3,
F = spray flow rate, m^3/sec,
V_g = volume of gas phase, m^3,
V_ℓ = volume of liquid, in containment sump, m^3,
k = first order reaction rate constant, sec^{-1}.

Eq. (32) would be applicable for cases where k is too low to appreciably enhance absorption during a single pass of

spray drops or wall film through the containment atmosphere. This case obtains for water sprays which contain no special additive for methyl iodide, hence would apply to boric acid, buffered boric acid, and sprays made basic with sodium hydroxide.

5.2.4 Effect of Spray Solution Composition

Pure water reacts very slowly with methyl iodide, and methyl iodide is only slightly soluble in water. Therefore, the spray removal rate is small unless reactive chemicals are added to the spray solution.

Methyl iodide reacts in aqueous solution by substitution reactions[37] in which a nucleophylic agent replaces the methyl radical. Schwendiman, et al.[37] have summarized reaction rates available prior to 1968. These are reproduced in Table I.

Of the reactants listed in Table I, only four, the two forms of hydrazine, sodium thiosulfate, and perhaps sodium sulfite, appear to be practical additives for enhancing methyl iodide absorption. The others react too slowly to give an appreciable enhancement compared to water alone.

Schwendiman, et al.[37] also studied other reactions from a theoretical viewpoint, and concluded from data obtained in methanol that certain exotic chemicals would react much faster with methyl iodide than hydrazine or thiosulfate. These chemicals included sodium selenophenoxide, triethylphosphine, and sodium thiophenoxide. It is unlikely that such chemicals would be usable because

TABLE I. Summary of Reaction Rates of Methyl Iodide in Aqueous Solutions[37]

Reactant	k**	Activation Energy (kCal/mole)	Temperature Range Studied (°C)	k Extrapolated at 120°C
H_2O	1.4×10^{-9}*	>24.8	30-93	0.00006
F^-	7.08×10^{-8}	25.2	-	0.002
Cl^-	3.3×10^{-6}	21.97	-	0.025
Br^-	4.16×10^{-5}	19.31	-	0.11
OH^-	6.36×10^{-5}	22.22	30-70	0.55
SCN^-	3.58×10^{-4}	19.95	25-35	1.2
I^-	4.71×10^{-4}	17.58	-	1.6
CN^-	5.76×10^{-4}	20.47	20-55	2.5
N_2H_4	1.1×10^{-3}	20.2	25-65	10
Ag^+	2.61×10^{-3}	19.4	15-45	7
1,1 dimethyl hydrazine	7.7×10^{-3}	18.4	25-35	13
$S_2O_3^=$	3×10^{-2}	18.88	10-25	70
$SO_3^=$	3.3×10^{-2}	-	25	-

* Calculated from first order rate constant using H_2O concentration = 55 moles/liter

** Bimolecular reaction rate constant at 25°C (liter $mole^{-1}$ sec^{-1})

they are relatively insoluble in water, and react rapidly with oxygen.

Hasty and Sutter[38] have presented more recent data on the kinetics of the reaction of methyl iodide

with sulfite, thiosulfate, and bisulfite ions. Their results are consistent with the data shown in Table I.

5.2.5 Overall Absorption Rate

A model formulated from absorption theory for stagnant drops and stagnant wall films is described as follows. The overall washout λ for reactive sprays is

$$\lambda = \lambda_{drops} + \lambda_{wall\ film} \tag{33}$$

The washout rate constant for spray drop, λ_{drops}, may be written as

$$\lambda_{drops} = \frac{F\ H\ E}{V} \tag{34}$$

where F = spray flow rate, m^3/sec,
H = methyl iodide partition coefficient,
E = fractional saturation achieved during single pass,
V = volume of containment gas space, m^3.

The numerical value of E should be obtained from Eq. (21) using the relation $E = 3Q/4\pi a^3 C^*$. In selecting a drop size, it would be best to break the drop size spectrum into increments, and integrate Eq. (34) over the spectrum. If a mean drop size is to be used, the volume median diameter is recommended because it will provide a conservative estimate of washout rate[39].

The washout rate constant for wall films, $\lambda_{wall\ film}$

may be expressed as

$$\lambda_{\text{wall film}} = \frac{q\ A}{V\ C_g} \tag{35}$$

where $\frac{q}{C_g} = \frac{\text{absorption rate per unit area}}{\text{gas phase concentration}}$, m sec^{-1},

A = surface area of wall film, m^2,

V = volume of gas space, m^3.

The numerical value of q/C_g should be calculated from Eq. (29) which applies to stagnant films of finite thickness. From Eq. (29), q/C_g is given by

$$\frac{q}{C_g} = H\sqrt{kD}\quad \tanh\left(\sqrt{\frac{k}{D}}\ \delta\right) \tag{36}$$

where H = partition coefficient = C^*/C_g,

k = first order reaction rate constant, sec^{-1},

D = diffusivity of methyl iodide in water, m^2/sec,

δ = thickness of wall film, m.

Film thickness, δ, may be predicted from laminar flow theory, which relates the film thickness to the film flow rate and the fluid viscosity. The film thickness is given by[39]

$$\delta = \left[\frac{3\nu\ \Gamma}{g}\right]^{1/3} \tag{37}$$

where δ = film thickness on vertical wall,

ν = kinematic viscosity of water film,

Γ = film flow rate per length of perimeter,

g = acceleration due to gravity.

In summary, the washout rate of methyl iodide by reactive sprays such as 1% thiosulfate, can be calculated from Eq. (33), using Eqs. (34) and (35) to evaluate the λ's.

For slowly reacting sprays, a simpler model may be used because the reaction rate is too slow to enhance absorption during a single pass. Solutions which fit this catagory are pure or buffered boric acid, and basic borax solutions containing sodium hydroxide. Eq. (32) applies for these sprays. The spray lambda implicitly defined by Eq. (32) is

$$\lambda = \frac{F\ k\ H}{V_g \left(\frac{F}{V_\ell} + k \right)} \qquad (38)$$

where F = total spray rate, m^3/sec,
V_g = volume of gas space, m^3,
V_ℓ = volume of spray liquid in containment vessel sump, m^3,
k = first order reaction rate constant, sec^{-1}.

5.3 Models For Aerosol Particle Washout

5.3.1 Washout by Spray Drops

The removal of aerosol particles by sprays is a more complex process than gaseous absorption because a number of mechanisms contribute significantly to capture. In a review of particle washout by containment sprays, Ritzman et al.[29] list the following important mechanisms.

- Brownian diffusion
- Diffusiophoresis
- Interception
- Inertial impaction

The relative importance of each of the contributing mechanisms depends on spray and aerosol properties. Ritzman, et al.[29] have evaluated each of these mechanisms for typical LWR containment conditions for a 1210 micron diameter spray drop.

The dominant mechanisms for capture of particles in the 0.1 micron to 1.5 micron range are diffusiophoresis and interception. For particles with diameters larger than about two microns, inertial impaction becomes the dominant mechanism. Brownian diffusion controls capture of particles smaller than about 0.1 micron diameter.

The spray removal rate for aerosols can be related to spray parameters and to the single drop collection efficiency by considering the spray to be an assembledge of single drops. The relating equation is[40]:

$$-\frac{dC}{C} = \lambda_s dt = \frac{3hFE}{2\ dV}\ dt \qquad (39)$$

where C = aerosol concentration, kg/m^3,
λ_s = spray removal rate constant, $sec.^{-1}$,
h = drop fall height, m,
F = spray flow rate, m^3/sec,
E = single drop collection efficiency,
d = mean spray drop diameter, m,
V = volume of contained gas phase, m^3.

The quantities h, F, and V are parameters of the containment system design. The drop diameter, d, is determined by the spray nozzle design and operating conditions, and is subject to direct experimental measurement. The most difficult-to-determine parameter in Eq. (39) is the single drop collection efficiency, E,

After considering alternative approaches, it was determined that use of experimental washout rate data from large scale containment tests provided the firmest basis for arriving at a simple conservative model for washout of particulate fission products.

From a review of available large scale test results on aerosol washout, a conservative estimate of particulate iodine washout can be obtained by choosing (E/d) = 0.1 cm^{-1} for C/C_o values from 1 to 0.01, and 0.01 cm^{-1} for C/C_o values smaller than 0.01[40]. Mathematically this can be stated in terms of washout λ's:

$$\lambda = \frac{3hF}{2V} \ (0.1 \ cm^{-1}) \quad \text{for } 0.01 \leq C/C_o \leq 1.0 \qquad (40)$$

$$\lambda = \frac{3hF}{2V} \ (0.01 \ cm^{-1}) \quad \text{for } C/C_o \leq 0.01 \qquad (41)$$

In the above expressions C/C_o represents the ratio of airborne concentration, C, at time t to initial concentration, C_o, computed for an instantaneous release at time zero.

5.3.2 Deposition of Particles on Surfaces

Airborne particles are known to be removed by a number of mechanisms even if sprays do not operate[32]. Dominant among these is gravity settling[32] onto horizontal surfaces. Wall plating occurs by diffusion, by thermophoresis, by diffusiophoresis, and by turbulence in the wall boundary layer. All of these mechanisms lead to removal rates which are small compared to the spray removal rate, and therefore surface deposition of particles has usually been neglected in site evaluations.

5.4 Absorption of Hypoiodous Acid

The physical properties of HOI which govern its absorption rate have not been firmly established. Consequently calculations of washout λ's are not possible. However the known properties of HOI (its solubility in water) indicate that its removal rate would fall between that of elemental iodine and that of methyl iodide. HOI has been lumped with methyl iodide to assure conservative washout predictions.

6.0 DISCUSSION OF TECHNICAL BASES FOR WASHOUT MODELS

In this section the technical bases which underlie the NRC washout models are discussed. This discussion will help elucidate the NRC position on the various models employed to compute spray washout in containment vessels.

6.1 Elemental Iodine

6.1.1 Effect of Iodine Concentration on Removal Rate

The model assumes first order behavior which requires the removal processes to be independent of gas phase iodine concentration. Physical properties such as density, viscosity, and diffusivity are known to be independent of iodine concentration at the very low iodine concentrations involved in containment atmospheres[42]. However the overall iodine equilibrium partition coefficient is controlled largely by liquid phase chemical reaction equilibria, and the degree of completion of these reactions is a function of iodine concentration. For example, the theoretical study of iodine hydrolysis by Eggleton[43] shows that the overall partition coefficient varies greatly with iodine concentration. While experimental measurements of iodine partition coefficients applicable to spray washout[18,33,44] tend to be larger numerically than predicted by the Eggleton theory[43] the data follow the predicted trend in that partition coefficients decrease in magnitude with increasing concentration. Nonconservative errors can be avoided if the numerical value of the partition coefficient is chosen as the minimum value achieved for the range of iodine concentrations which is possible.

6.1.2 Instantaneous Release Versus Continuous Source of Iodine

The removal process is analyzed under the assumption

that all of the iodine which becomes airborne does so instantaneously at time zero. While this assumption is met for practical purposes by gap iodine releases[45], fuel melt and vaporization releases would occur over a time period. For example realistic assessments of core melt accidents[45] showed that most of the iodine would be released over a time period of 30 minutes or more. This minimum time duration is determined by the time required to melt the core by fission heat in the absence of core cooling. Experiments have demonstrated that the major iodine release occurs when UO_2 melting occurs[45].

In order to determine the factor of conservatism caused by the puff release assumption, the two hour average concentration was computed as a function of source release time, t_R, and the washout λ. For a puff release at time zero the two hour average concentration is

$$\text{Puff Release Avg.} = \frac{C_o\ (1-e^{-2\lambda})}{2\lambda} \qquad (42)$$

where C_o = initial atmospheric concentration
λ = spray removal rate constant hr^{-1}.

For a continuous source term lasting a time, t_R, the two hour average concentration was computed to be

$$\text{Continuous Release Avg.} = \frac{C_o}{2\lambda}\left[1 - \frac{1}{\lambda t_R}\left(1-e^{-\lambda t_R}\right)e^{-\lambda(2-t_R)}\right] \qquad (43)$$

where C_o = total mass released/gas volume,
t_R = time of constant source.

The degree of conservatism resulting from the puff source term was computed by dividing Eq. (42) by Eq. (43). Results of the calculation are shown graphically in Figure 1.

The puff and continuous source terms lead to appreciably different results only for small washout lambdas. Since typical PWR lambdas are 5 hr^{-1} or greater, the puff release assumption introduces a factor of conservatism of 1.10 at most for a two hour calculational period.

6.1.3 Effect of Initial Drop Velocity on Absorption

In the previously discussed models for absorption by falling drops, it was assumed that spray drops fall vertically at the terminal velocity for the full fall height. This assumption simplifies the estimation of the exposed surface area for mass transfer and the mass transfer coefficient.

In a containment vessel, spray drops enter at various angles with respect to the vertical direction. After traveling a relatively short distance, the horizontal component of velocity becomes negligible, and the drops then fall vertically at terminal velocity with respect to the containment atmosphere. Thus the theoretical assumption will not be precisely met for the following reasons. (1) The drops enter with a horizontal velocity component, and hence will have trajectories longer than the fall height. This factor tends to increase the absorption effectiveness for a drop as compared to a straight line trajectory. (2) The drops initially have a higher than

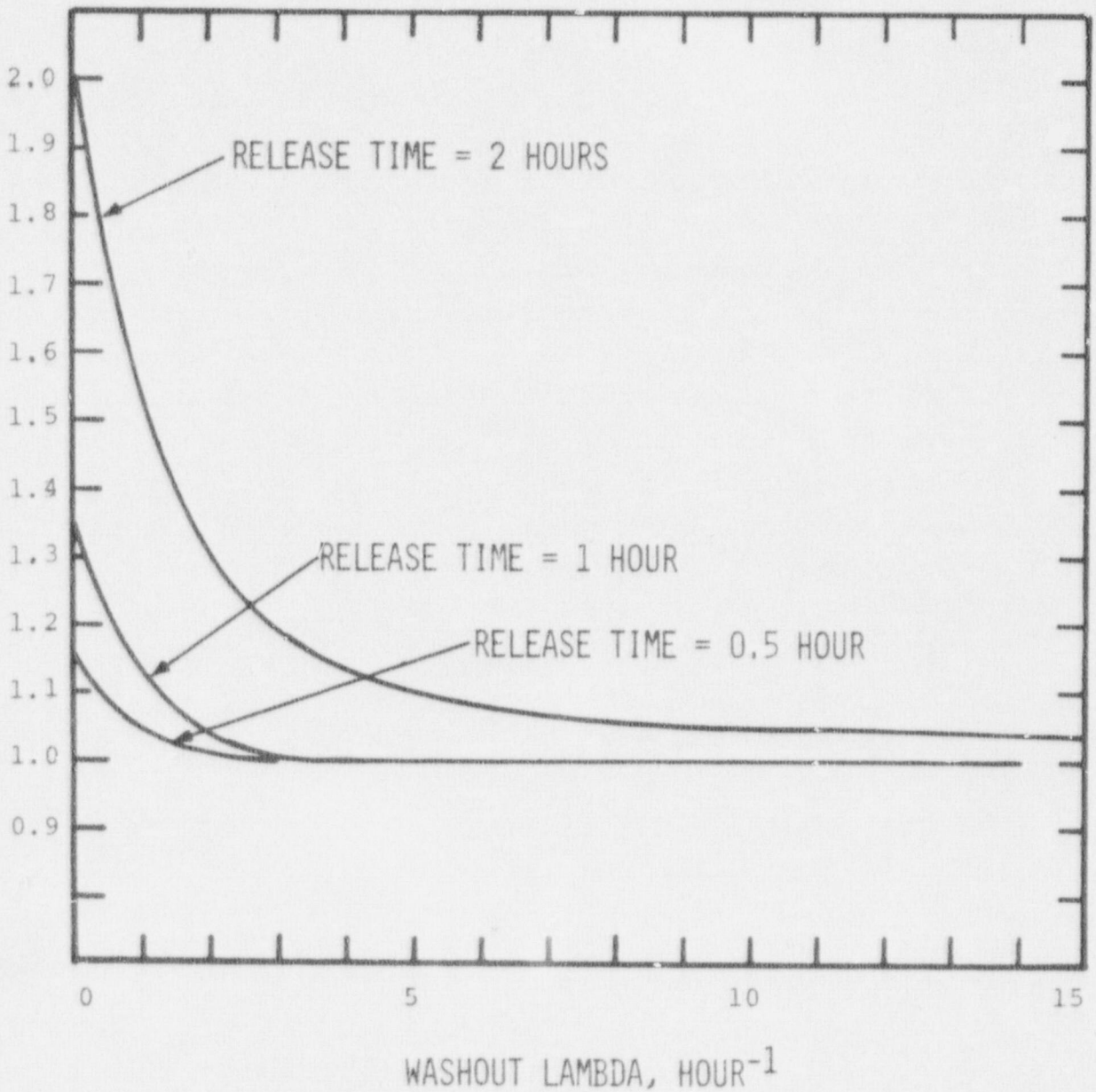

FIGURE 1. Comparison of Airborne Concentrations For Puff Release and Continuous Fission Product Source Terms

terminal settling velocity which reduces the exposure time and increases the mass transfer coefficient. The decrease in exposure time more than offsets the increased mass transfer coefficient, hence the higher initial velocity tends to reduce the absorption rate. Thus a terminal settling velocity model would tend to overpredict the absorption rate, though as shown later, the effect is small. (3) The gas phase is not stagnant. Particularly in the region near the spray nozzles, the gas phase is highly turbulent. Thus, over a segment of its trajectory, the drop falls at velocities higher than would be predicted for a stagnant gas. Since the containment atmosphere has a net vertical velocity of zero, the decreased exposure time for a part of the drops would be balanced by an increase in exposure time for the remainder of the drops, and therefore the net effect of gas phase currents is expected to be negligible. This factor is one of several which are best evaluated through large scale experiments. Agreement between experiment and absorption theory confirms that such factors have a negligible influence on absorption rate.

The effect of initial downward velocity has been evaluated using a perfect sink absorption model[28]. For conservatism, it was assumed that the drop trajectories were vertical.

Mathematically, the total iodine absorbed by a falling drop may be written as

$$\text{mass absorbed} = \int_{t=o}^{t=t_e} k_g \; A \; C_g \; dt =$$

$$\int_{t=o}^{t=t_e} C_g . \pi d^2 . \frac{D}{d} . (2 + 0.55 \; Re^{0.5} Sc^{0.33}) dt \qquad (44)$$

where d = drop diameter,
D = gas phase diffusivity,
Re = Reynolds number for drop,
Sc = Schmidt number for drop,
t_e = drop exposure time.

For the terminal velocity model, the mass transfer coefficient is taken as constant and the fall time is equated to the fall height divided by the settling velocity. The mass absorbed by a drop would thus be

$$\text{mass absorbed} = C_g . \pi d^2 . \frac{D}{d} . (2 + 0.55\ Re^{0.5} Sc^{0.33}) . t_e \qquad (45)$$

where Re = Reynolds number evaluated at terminal velocity.

The iodine absorbed by a terminal velocity drop and that absorbed by a drop entering the containment vessel with a velocity of 62 ft/sec were compared by evaluating the ratio of Eq. (44) to Eq. (45). Results of this evaluation[28] are shown in Figure 2. The results shown in Figure 2 apply for drops projected downward without any horizontal velocity component. This assumption maximizes the calculated effect of initial velocity, and for the hollow cone spray nozzles typically used in containment vessels, the ratio portrayed in Figure 2 would be even closer to unity.

The fall height in the main containment region is approximately 100 feet and mean drop size is in the neighborhood of 1000 μ. From Figure 2, the downward initial velocity decreases the calculated absorption by 5%. This is a conservative estimate because the horizontal velocity component and drop saturation effects have

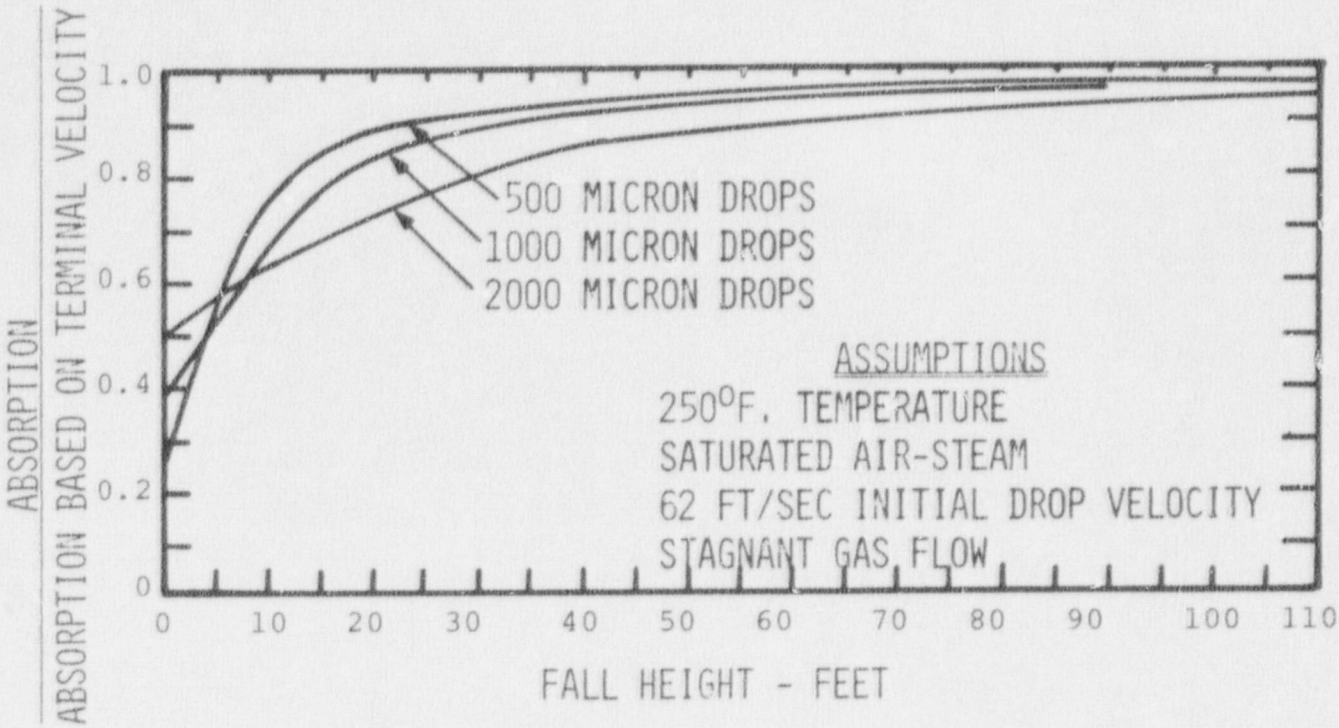

FIGURE 2. Effect of Initial Downward Velocity on Drop Absorption Efficiency

been neglected. This degree of error is too small to merit additional detailed analyses except in special cases such as where spray headers are located in areas where the fall height is less than approximately 20 feet.

6.1.4 Use of Stagnant Film Model For Liquid Resistance

The Griffith model[26] for liquid phase mass transfer

is used to calculate liquid phase mass transfer resistance in the stagnant film model:

$$k_\ell = \frac{2\pi^2}{3} \frac{D_\ell}{d}. \qquad (9)$$

This equation results from an approximation to the rigid drop diffusion equation[27]:

$$\frac{C - C_o}{C_i - C_o} = 1 - \frac{6}{\pi^2} \sum_{n=1}^{n=\infty} \frac{1}{n^2} \exp\left[\frac{-n^2 \pi^2 D_\ell \, t_e}{a^2} \right] \qquad (46)$$

where C = average concentration in drop at time t,
C_i = concentration at drop surface,
C_o = initial concentration in drop,
D_ℓ = diffusivity in liquid,
a = radius of drop,
t_e = drop exposure time.

If the first term of the series is factored out, and the remaining terms evaluated at t = o, there results

$$\frac{C - C_o}{C_i - C_o} = 1 - \exp - \frac{\pi^2 D_\ell \, t_e}{a^2} \qquad (47)$$

If this equation is differentiated with respect to time, and the rate of change in average concentration multiplied by drop volume is equated to a mass transfer coefficient times a surface area and concentration difference, the result is

$$\frac{dm}{dt} = \frac{2}{3} \pi^3 d \, D_\ell \, (C_i - C) = k_\ell \pi d^2 \, (C_i - C) \qquad (48)$$

where m = mass of solute in drop.

From Eq. (48) k_ℓ may be obtained as

$$k_\ell = \frac{2}{3} \frac{\pi^2}{d} D_\ell \tag{9}$$

This representation is approximate because of the series truncation procedure used. We have re-derived the expression for k_ℓ, accounting for the series terms dropped in Griffith's approach. The result is

$$k_\ell = \frac{2\pi^2 D_\ell}{3d} - \frac{d}{6} \frac{f'(t)}{f(t)} \tag{49}$$

where f(t) varies from $\frac{\pi^2}{6}$ at t = o to 1 as t becomes long, and f'(t) has a value of $-\infty$ at t = o and approaches o at long times. The correction factor is infinite at zero time but becomes negligible at long times. It is apparent that the Griffith's approximation is conservative in that it predicts lower absorption than would be predicted by the full series for stagnant drop absorption.

The Griffith model was compared to the exact treatment for a rigid drop by calculating the drop absorption efficiency predicted by both models. The results were normalized by dividing by the drop absorption for a well mixed drop.

For the stagnant film treatment of liquid phase mass transfer we derived

$$E = 1 - \exp - \left[\frac{6 \, k_g \, t_e}{d\left(H + \frac{k_g}{k_\ell}\right)} \right] \tag{7}$$

where E = fractional saturation acheived by drop,

$$k_\ell = \frac{2\pi^2 D_\ell}{3d} .$$

Eq. (7) represents the stagnant film drop absorption model.

For the stagnant drop, the drop absorption efficiency, E, is given by

$$E = 1 - \sum_{n=1}^{\infty} \frac{6\ sh^2 \exp\ (-\alpha_n^2 \Theta)}{\alpha_n^2 \left[\alpha_n^2 + sh(sh-1)\right]} \qquad (10)$$

where $sh = \frac{k_g\ a}{H\ D_\ell}$,

$$\Theta = \frac{D_\ell\ t_e}{a^2}$$

α_n = nth root of $\alpha_n \cot\alpha_n + (sh-1) = 0$,

a = drop radius.

Finally, the well mixed drop model gives E as

$$E = 1 - \exp - \left[\frac{6\ k_g\ t_e}{dH}\right] \qquad (11)$$

These three equations were evaluated for spray drops falling 90 feet in a steam-air environment at 250°F. Drop sizes used in the calculation were 500, 1000, 1500 micrometers. Partition coefficient was a parameter, varying from 10^2 to 10^6. Results are tabulated in Table 2 and shown graphically in Figure 3.

As postulated, the stagnant film model predicts lower absorption rates than the rigid drop model. The maximum difference in stagnant versus well mixed models

TABLE 2. Comparison of Stagnant Film Model, Rigid Drop Model and Well Mixed Drop Absorption Model

	$\frac{E_{\text{Stagnant Film Model}}}{E_{\text{Well Mixed Model}}}$			$\frac{E_{\text{Rigid Drop Model}}}{E_{\text{Well Mixed Model}}}$		
	Drop Diameter			Drop Diameter		
H	500 μ	1000 μ	1500 μ	500 μ	1000 μ	1500 μ
100	1.00	0.89	0.51	1.00	0.93	0.69
500	1.00	0.83	0.47	1.00	0.89	0.64
1,000	1.00	0.76	0.50	1.00	0.85	0.66
5,000	0.98	0.82	0.73	0.99	0.88	0.83
10,000	0.97	0.88	0.83	0.98	0.93	0.91
10^5	0.99	0.99	0.98	1.00	0.99	0.99
10^6	1.00	1.00	1.00	1.00	1.00	1.00

occurs for the largest drops, and at partition coefficients smaller than 1000. For partition coefficients greater than 5000, the discrepancy between the well mixed model and the rigid drop model is less than 17% for 1500 μ drops. For partition coefficients greater than 5000, the stagnant film model predicts an absorption efficiency 27% smaller than that predicted by the well mixed model. This 27% difference occurs for 1500 μ drops. For smaller drops, the difference is smaller, demonstrating the relatively minor influence of using the Griffith model as compared to the rigid drop model.

From the foregoing discussion of liquid phase mass transfer, it is concluded that use of the Griffith model

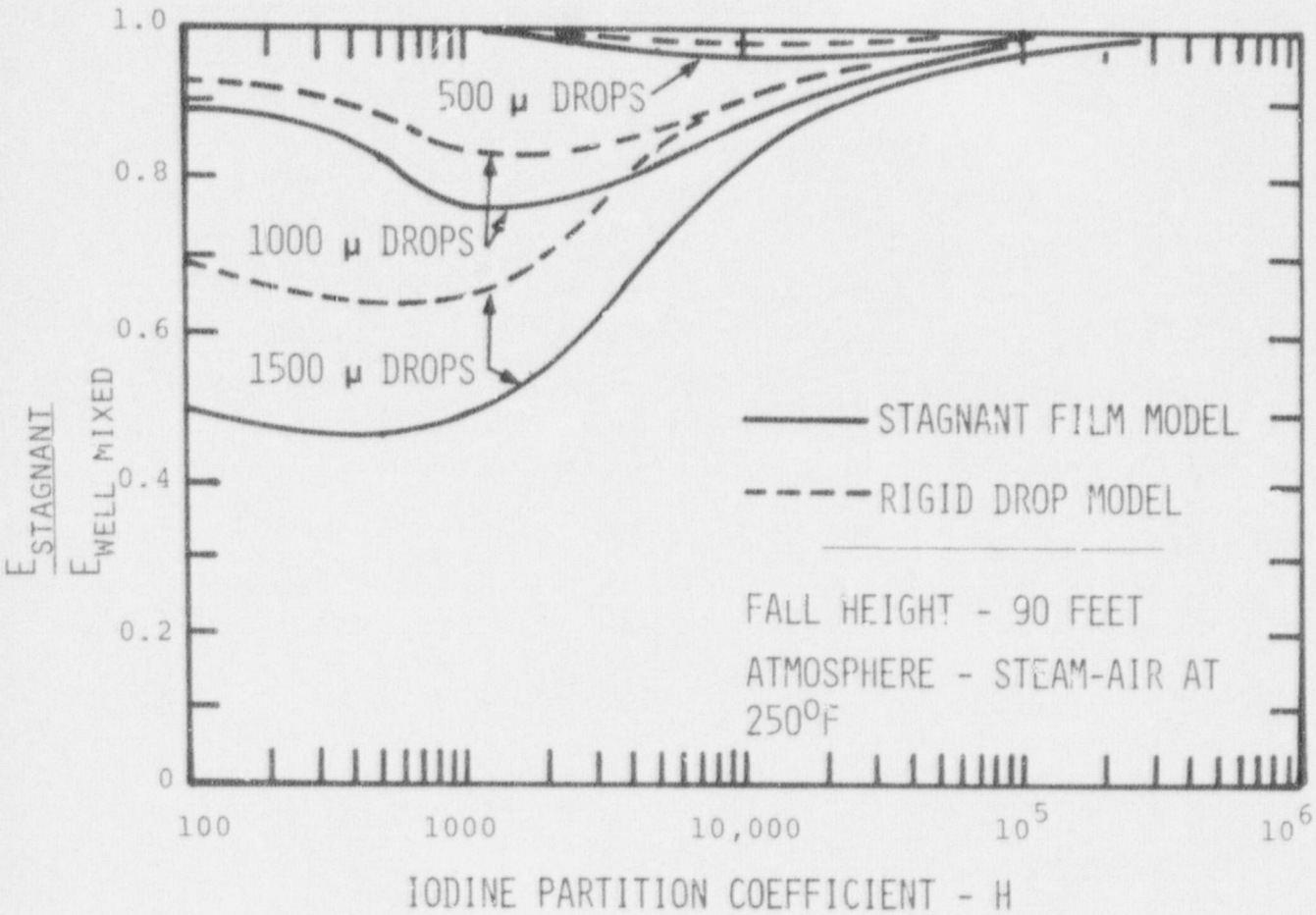

FIGURE 3. Comparison of Absorption Efficiency For Two Stagnant Drops Models

for estimating k_L is a conservative approximation to the rigid drop model. Both models are conservative because they neglect mixing within falling drops.

6.1.5 Effect of Drop Coalescence on Absorption

A conservative estimate of drop coalescence may be obtained from an analysis of all theoretically possible collisions between the spray drops in the containment. The theoretical maximum effect of coalescence is obtained if it is assumed that each of these collisions will result in coalescence, i.e., a single larger drop equal in volume to the sum of the two colliding drops. The derivation of such a model is given by Pasedag and Gallegher[46]. The number of coalescences between drops of two different sizes in a height increment dz is given by:

$$n_{ij} = \pi E_{ij} P_i P_j (a_i + a_j)^2 \left(1 - \frac{U_j}{U_i}\right) dz \qquad (50)$$

where n_{ij} = number of coalescences between drop size groups i and j,

E_{ij} = collection efficiency for drop sizes i and j,

P_i = drop population per unit containment volume for size i,

a_i = radius of drops of group i,

U_i = velocity of drops of group i.

The derivation of this equation is based on the following assumptions:

a. The spectrum of drop sizes emitted from the nozzle is known, and can be represented by a finite number of discrete drop size groups.

b. The drop population of each of the several drop size groups is uniformly distributed within the space of the control volume of height dz.

c. The drops are spherical in shape and fall at their terminal velocity.

Eq. (50) is made amendable to digital computer programming by replacing the differential dz with a finite difference Δz. The computations are performed for each combination of drop sizes. The drop size distribution is then updated to account for the smaller drops lost, and the larger drops gained in the coalescence process, and the calculation is repeated for the next height increment.

In this manner, a drop size distribution as a function of height in the containment (or distance from the nozzle) is obtained. The maximum effect of coalescence on the spray drop size spectrum, therefore, is evident in the distribution of the last step, immediately above the operating deck. A conservative estimate of the maximum reduction in the spray effectiveness is obtained by assuming that this size distribution exists throughout the containment.

The results obtained from this calculation are shown in Figure 4 as a function of spray flow rate and fall height for a drop size distribution emitted by a spray nozzle commonly used in containment vessels. Since most containment systems use spray rates in the range of 0.0005 and 0.0025 gpm/ft^3, it is evident that the maximum possible effect of coalescence would reduce the spray effectiveness by less than 15%.

This coalescence model predicts a reduction of up to 13% for the highest flow test in CSE (0.0071 gpm/ft^3 and 38 ft fall height). No reduction in spray effectiveness due to coalescence could be seen from test results[48].

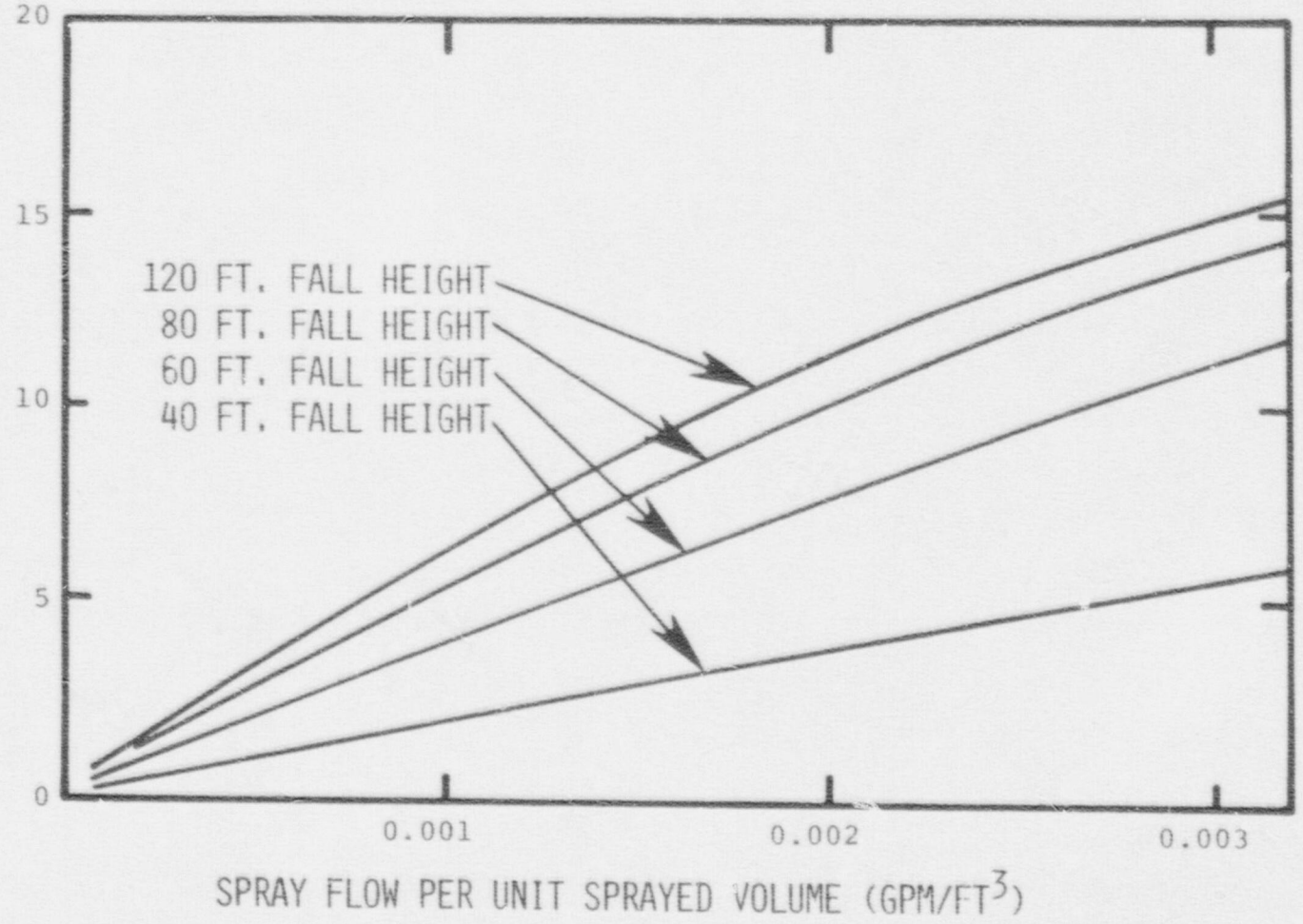

FIGURE 4. Effect of Drop Coalescence on Spray Removal of Elemental Iodine by Caustic Spray

This large scale test result supports the model. However since the test results had a precision of about 10%, the experiments cannot be used to numerically evaluate the degree of conservatism inherent in the coalescence model.

The drop size distribution before and after coalescence is shown in Figure 5. As expected, the distribution is broadened toward the larger size range.

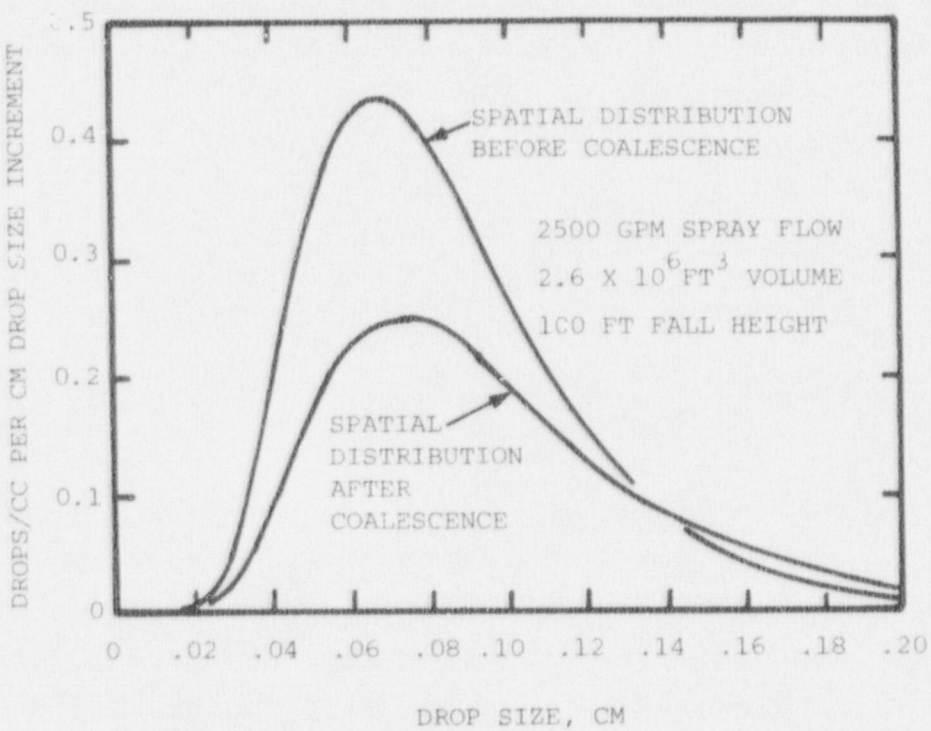

FIGURE 5. Effect of Coalescence on Drop Size Distribution

The coalescence model used by the staff[47] over-predicts the effect of drop coalescence due to the following assumptions:

- Each drop-drop impact is assumed to result in coalescence, i.e. a drop collection efficiency of 100% is used.
- Aerodynamic forces which tend to lower the drop impaction efficiency are neglected.
- Mass transfer calculations are made using the drop size distribution achieved at the end of the fall path.

Due to the conservative nature of the model[47] its use assures that the effects of drop coalescence will be treated conservatively.

6.1.6 Effect of Steam Condensation on Iodine Absorption

Spray drops entering a hot containment vessel atmosphere will condense steam until the drop warms to the atmosphere temperature. The condensation of steam onto the drops can affect mass transfer in three ways. First, the drops will grow in size, potentially decreasing their effectiveness. Second, one can postulate the buildup of a film of pure condensate on the outside of the drop, which could act as a diffusion barrier to iodine. Third, there would be a sweeping flow of steam toward the drop which would increase the gas phase mass transfer coefficient.

The significance of each of these three effects is discussed below.

Increase in Drop Diameter by Condensation

The maximum amount of water which can condense on a drop is determined by the temperature difference between the entering drops and the containment atmosphere. For a containment atmosphere temperature of 250^0F and for water entering at 70^0F, the temperature rise is equal to or less than 180^0F. A heat balance on the drop gives

heat of condensation = sensible heat increase

$$\lambda_c M_c = \frac{\pi}{6} d^3 \rho C_p \ (180) \qquad (51)$$

where λ_c = specific heat of condensation, BTU/lb,
M_c = mass of condensate, lb,
d = drop diameter prior to condensation, ft,
ρ = drop density at initial conditions, lb/ft^3,
C_p = specific heat of drop, BTU/lb^{0}F.

$$M_c = \frac{30 \pi d^3 \rho C_p}{\lambda_c} \qquad (52)$$

Hence the final mass is

$$M = \frac{\pi}{6} d^3 \rho + \frac{30 \pi d^3 \rho C_p}{\lambda_c} \qquad (53)$$

and the final size is

$$d_f = d \left[1 + \frac{180\ C_p}{\lambda_c} \right]^{1/3} \qquad (54)$$

For water, taking C_p = BTU/^{0}F lb and λ_c = 1000 BTU/lb, d_f is about 6% greater than the initial size. This is probably a maximum estimate because the temperature difference could well be less than 180^{0}F, and not all heat is transferred by means of water condensation.

A 6% change in drop size is relatively unimportant. Calculations based on a perfect sink absorption model (H arbitrarily large) showed the absorption efficiency to vary approximately with the inverse 2.2 power of drop size. Since saturation effects would reduce the relative importance of drop size, the perfect sink calculation is more sensitive to drop size than would be the stagnant film model for typical containment applications. Because the spray λ increases linearly with spray flow rate, the net effect of steam condensation is to increase the λ. This can be shown as follows

$$\lambda = k \frac{F}{d^{2.2}} \qquad (55)$$

where k = a constant,
F = spray flow rate,
d = drop diameter,
λ = spray washout rate constant.

Because the number of spray drops is not changed by steam

condensation, the drop diameter will vary with the 1/3 power of the liquid flow rate. Therefore λ may be written as

$$\lambda = k' \frac{F}{\left(F^{\frac{1}{3}}\right)^{2.2}} = k' F^{0.27} \qquad (56)$$

Eq. (56) indicates that condensation, which increases F, will tend to increase the iodine washout rate provided the drop size does not enter the absorption efficiency calculation to a power higher than three. This is true for all practical cases involving containment sprays.

Effect of Build-Up of a Pure Water Layer

Chemical reactions play an important role in absorption in I_2. For this reason a layer of pure water on the surface of a drop could lower the absorption rate. From the preceding calculation, it was concluded that, at most, drops would increase in diameter by about 6%. Thus for a 1000 micron diameter drop, a pure water layer having a thickness of 30 microns might form at the surface. For a stagnant drop, diffusion calculations indicate that the surface concentration of a reactive reagent would reach 50% of the bulk concentration in a time of about 0.1 second. Since drop residence times are of the order of seconds, the condensate layer will not appreciably influence the absorption rate. For a 3 second fall time, it was predicted that the transfer rate would be reduced by about 3%. The model used in arriving at this estimate yields an

overestimate of the effect, because drop mixing was neglected, and because the absorption rate was assumed to be linearly related to the concentration of a dissolved reactive solute.

Increased Transfer Due to Sweep Effect

The gas phase mass transfer coefficient will be enhanced because of bulk motion toward the surface caused by condensing steam. This effect would obviously be negligible for organic iodides such as CH_3I because their transfer rate is controlled by liquid phase resistance. The degree of enhancement of gas phase transfer, for an airborne species which exhibited zero back pressure at the surface, was estimated from theory. The drop was assumed to fall at terminal velocity. The water condensation rate was calculated from Eq. (8) in conjunction with a heat transfer model based on a well mixed drop. The enhancement in the gas phase mass transfer coefficient was calculated using data presented by Bird, et al.[49]. The results of this calculation are presented in Table 3.

The data of Bird, et al.[49] used to obtain the predictions shown in Table 3 were calcualted from the penetration theory. Models based on film theory and boundary layer theory give comparable results. Although these models would not be expected to apply precisely to drops, significant discrepancies would not be expected for the present case.

From this analysis it is apparent that the increase in liquid flow rate and the increase in the mass transfer

TABLE 3. Predicted Enhancement of Gas Phase Mass Transfer Due to Water Condensation

Drop Diameter	Percent Enhancement*
500	0.5%
1000	2.5%
2000	10%

* Initial drop temperature 70°F and atmosphere temperature 250°F.

coefficient caused by steam condensation enhance the iodine absorption rate. The degree of enhancement is expected to equal or exceed the potential decrease in absorption rate caused by build-up of a pure water layer on the surface of the drop. Moreover, since all three effects are small no measureable influence on absorption would result from the condensing of steam onto spray drops in a containment vessel.

6.1.7 Physical Property Estimation

All spray models require input data for gas phase properties including diffusivity, viscosity, and density. If liquid phase mass transfer is important, liquid properties including diffusivity and density will also be required. In addition to these physical properties, correlations for friction factors and mass transfer coefficients for spheres must be used.

Fluid densities and viscosities are quite accurately known and errors in these quantities are expected to be less than 10% for steam/air mixtures. Errors of 10% might be expected in the friction factor correlation, and on the basis of scatter of mass transfer data for spheres[50] errors up to 20% might be expected in the gas phase mass transfer correlation. Diffusivity data are probably the least accurate of the inputs. Gas phase diffusivities are calculated from theory, and may be in error by 20%. Liquid phase diffusivities could be in error as much as 30%.

These errors are of a magnitude which is typical of those encountered in engineering calculations. The overall error caused by inaccuracies in these input data depends on how each variable enters into a specific model, and on the degree to which the individual errors tend to compensate. If large scale washout experiments were not available, then a detailed study of errors would be required in order to estimate potential errors in λ's predicted by models. However, in the present case, spray washout data are available, and the data offer the best available means for evaluating model error. Comparisons of experiments and theory are presented in a later section of this report.

6.1.8 Partition Coefficients For Spray Solutions

Elemental iodine reacts with water, forming a number of ionic species in solution. The partition coefficient, which is the ratio of total iodine concentration in the liquid to I_2 concentration in the gas phase, is numerically

determined by the physical sorption of I_2 and by rapid ionization reactions which occur in soltuion. At least eight reactions are involved when elemental iodine is dissolved in water[43]:

$$I_2(\text{gas phase}) \overset{K_1}{\rightleftharpoons} I_2(aq) \qquad K_1 = \frac{(I_2(aq))}{(I_2(\text{gas phase}))} \tag{57}$$

$$I_2(aq) + I^- \overset{K_2}{\rightleftharpoons} I_3^- \qquad K_2 = \frac{(I_3^-)}{(I_2(aq))(I^-)} \tag{58}$$

$$I_2(aq) + H_2O \overset{K_3}{\rightleftharpoons} H^+ + I^- + HOI \qquad K_3 = \frac{(H^+)(I^-)(HOI)}{(I_2(aq))} \tag{59}$$

$$I_2(a) + H_2O \overset{K_4}{\rightleftharpoons} H_2OI^+ + I^- \qquad K_4 = \frac{(H_2OI^+)(I^-)}{(I_2(aq))} \tag{60}$$

$$3I_2(aq) + 3H_2O \overset{K_5}{\rightleftharpoons} IO_3^- + 5I^- + 6H^+ \qquad K_5 = \frac{(IO_3^-)(I^-)^5(H^+)^6}{(I_2(aq))^3} \tag{61}$$

$$HOI \overset{K_6}{\rightleftharpoons} H^+ + IO^- \qquad K_6 = \frac{(H^+)(IO^-)}{(HOI)} \tag{62}$$

$$IO^- + I^- + H_2O \overset{K_7}{\rightleftharpoons} I_2OH^- + OH^- \qquad K_7 = \frac{(I_2OH^-)(OH^-)}{(IO^-)(I^-)} \tag{63}$$

$$IO^- + I^- \overset{K_8}{\rightleftharpoons} I_2O^{=} \qquad K_8 = \frac{(I_2O^{=})}{(IO^-)(I^-)} \tag{64}$$

The rates of the first four of these reactions are known to be fast. Rates of the last four reactions are not well known, but these latter four reactions could be important for long times. They would cause displacement of the equilibrium to favor the liquid phase.

Elemental iodine can be effectively absorbed because of the displacement equilibria. At least three chemical approaches can be used to enhance the iodine partition coefficient.

- add reductants to form I^-
- add oxidants to form IO_3^-
- shift hydrolysis equilibria by removing H^+

Sodium hydroxide, a commonly used spray additive, shifts hydrolysis equilibria by reducing (H^+). This would drive reactions (59), (61), and (62) to the right, thereby increasing the quantity of ionic iodine in equilibrium with $I_2(aq)$. The effect of such a change would be to increase the partition coefficient.

Hydrazine and sodium thiosulfate are reducing agents which convert $I_2(aq)$ to I^-. The mechanism for the reduction

reaction appears to involve the reduction of HOI[51], so these agents would also serve as hydrolysis shifters for Eq. (59) by removing HOI.

Eggleton[43] has presented numerical evaluations of H based on Eqs. (57) through (64). Results show that the partition coefficient increases with increasing pH and decreasing iodine concentration.

Experimentally derived partition coefficients are often found to be larger than those predicted by Eggleton's theory. One reason for this is the presence of trace level impurities which interact with dissolved iodine. For example in CSE test A-7[52] iodine was removed about as rapidly as in test A-6. Test A-7 used boric acid whereas test A-6 spray water was made basic (pH=9.5) by sodium hydroxide. A subsequent CSE test using highly purified boric acid[18] showed slower removal, consistent with a partition coefficient of 200. Tests conducted in Italy in PSICO[22] also indicated that boric acid without chemical additives was as effective as a spray solution containing sodium thiosulfate. We attribute this to impurities in the spray water.

While the sorption of iodine in water is understood, direct experimental data must be relied upon to select a partition coefficient for a particular spray solution.

Partition coefficients for plain boric acid solution without other chemical additives have been reported by Postma, et al.[18]. Based on the available information, it is concluded that H_o, the partition coefficient which controls spray absorption is about 200. H increases with time so that fairly large concentration reduction factors can be obtained as spraying recirculation is continued.

For sodium hydroxide solutions at pH of 9.5, available information suggests that H_o is greater than 5000[33,44]. Calculations made using an H_o value of 5000 will result in conservative estimates of iodine washout.

Hydrazine, in low concentration levels, has also been studied experimentally[17,33] and use of H_o equal to 5000 assures conservative predictions for hydrazine sprays.

Sodium thiosulfate at 1% by weight, has been studied by a number of investigators[16,19,33,52]. Of the spray solutions designed for use in containments, the basic thiosulfate solution is the most powerful from a chemical reduction standpoint. Use of an instantaneous partition coefficient of 100,000 appears to be justified.

6.1.9 Deposition of Iodine on Containment Surfaces

Surface deposition of iodine occurs as the result of several transport processes which occur in series. These are depicted in Figure 6.

Each of the transport steps shown in Figure 6 is potentially important in gas absorption, and each will be briefly discussed in relation to iodine absorption under accident conditions.

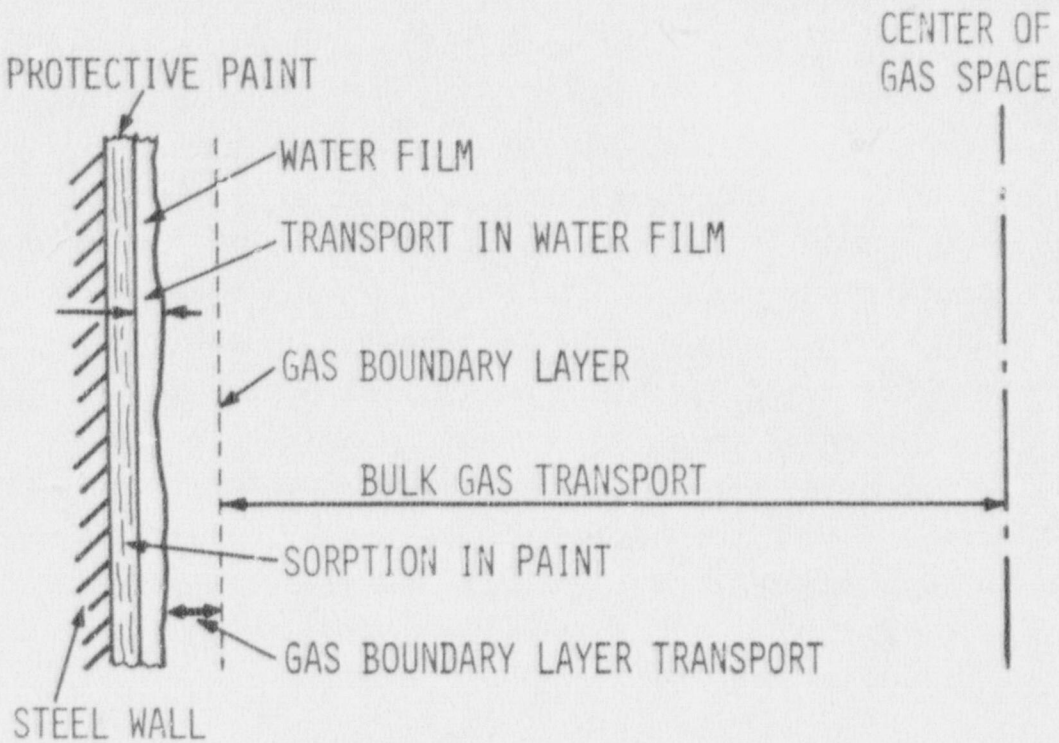

FIGURE 6. Schematic Representation of Iodine Surface Deposition

Mass Transfer in the Bulk Gas Phase

Transport of iodine molecules from the bulk of the gas space over to a boundary layer represents the longest transport step from a physical size standpoint. Such transport would be dominant if the bulk gas were stagnant. However, numerous experiments in containment vessels[30,32] have demonstrated that in a single compartment, the bulk gas phase is well mixed. The mixing is induced by thermal gradients, by operation of sprays or air cleaners, and by

thermally generated steam flows. As shown by large scale experiments[32] only very small thermal sources are required to mix a large vessel to the point where boundary layer transport dominates. Therefore, mass transfer through the bulk gas phase is not expected to be a controlling factor in iodine plateout in a single compartment of a containment vessel.

It should be noted that internal surfaces, such as those presented by shield walls, would trap iodine as well as the outer containment wall. In large scale CSE tests, the total exposed surface was about twice that afforded by the outer vessel walls, and all of the surface had to be accounted for to obtain agreement between theory and experiment[32]. Therefore the discussion of surface deposition presented here applies to all massive structures in the containment along which natural convective flows can freely develop.

Gas Boundary Layer Transport

Mass transport resistance through the gas boundary layer is expected to be important for absorption of all reactive gases where uptake at the wall is rapid. Since iodine is present in parts per million concentration levels, effects due to high concentrations on the boundary layer transport processes are insignificant. Based on a film model the iodine flux is defined by

$$N_A = k_g (C_{yb} - C_{gi}) \quad (65)$$

where N_A = iodine flux, $g/cm^2 sec$,
k_g = mass transfer coefficient, cm/sec,
C_{gb} = iodine concentration in bulk gas, g/cm^3,
C_{gi} = iodine concentration at gas-liquid interface, g/cm^3.

If the iodine is rapidly absorbed by the wall, then $C_{gb} >> C_{gi}$ and the gas boundary layer resistance controls the absorption rate. As will be shown later in this report, this is the case for deposition of elemental iodine in containment vessels.

Transport In Water Film

The surfaces inside a containment vessel following a LOCA will be covered in part by water, and therefore the water film may play a role in the overall deposition process. Water films could, theoretically, either enhance or retard iodine deposition, depending on the value of the iodine partition coefficient in the aqueous film. For reactive liquid films, absorption would be enhanced, ensuring that $C_{gi}/C_{gb} \simeq 0$. If the wall surface were completely covered by a water film, in which the iodine partition coefficient were a minimum value, the water could represent a minor diffusion barrier. However the following order of magnitude calculation indicates that the water film would be too thin to appreciably retard the iodine absorption process.

At steady state, the iodine absorption rate per unit area in the gas and liquid films is

$$I_2 \text{ flux} = k_g (C_{gb} - C_{gi}) = \frac{D_L (C_{\ell i} - C_{\ell w})}{\delta} \quad (66)$$

where D_L = iodine diffusivity in water, cm^2/sec,
δ = thickness of liquid film, cm.

The maximum impeding effect of the water layer would be present if $C_{\ell w}$, the iodine concentration in liquid at the wall, is zero. Setting $C_{\ell w} = 0$, and using the usual surface saturation ($C_{\ell i} = H\, C_{gi}$), Eq. (66) may be written as

$$\frac{C_{gb}}{C_{gi}} = \frac{D_L H}{k_g \delta} + 1 \quad (67)$$

where H = equilibrium partition coefficient.

Mass transfer resistance in the liquid phase will be unimportant if $C_{gb}/C_{gi} > 10$. This will occur if the reciprocal Sherwood number $D_L H/k_g \delta$ is greater than 9.

For a typical case: $D_L = 3 \times 10^{-4}$ ft^2/hr
$H = 5000$
$k_g = 8$ ft/hr
$\delta = 0.01$ cm $= 3 \times 10^{-4}$ ft

Using these values, $D_L H/k_g \delta \cong 625$. Therefore it is concluded that liquid phase mass transfer resistance will be negligible for elemental iodine sorption on surfaces.

A water film would absorb iodine regardless of whether the solid wall were adsorbing or non-adsorbing.

An order of magnitude estimate of the wall liquid absorption rate may be obtained by considering a strip of unit width along the wall extending from the top of the containment vessel to the operating floor. If the wall film liquid (originating from spray drops and steam condensate) becomes saturated with iodine the total quantity absorbed will be:

$$I_2 \text{ absorbed} = \Gamma H C_g \tag{68}$$

where Γ = wall film flow rate,
H = equilibrium partition coefficient,
C_g = gas phase concentration of I_2.

For a typical case, we estimate $\Gamma \tilde{=} 3$ ft^3/hr ft and $H = 5 \times 10^3$. The absorption rate, $3 \times 10^3 C_g$ ft^{3}hr^{-1} may be compared to absorption where the wall is a perfect sink, $k_g A C_g$. In this case A will be numerically equal to the height of the wall surface, approximately 100 ft.

$$\frac{I_2 \text{ absorbed by liquid film}}{I_2 \text{ absorbed for perfect sink case}} = \frac{(3)(5\times10^3)C_g}{(8)(100)C_g} = 18.75$$

From this calculation it appears that the wall liquid film alone is capable of absorbing all the iodine which could be transported to a wall which was a perfect sink for iodine.

Sorption of Iodine by Paint and Other Surfaces

Iodine deposition on painted surfaces, on concrete, and on stainless steel surfaces has been studied extensively in the United States and abroad. The broad picture which emerges from the many studies is that iodine sorbs onto the exposed surface, and then diffuses into the material where it is held by both irreversible chemical reaction and by physical solubility. The overall absorption capacity is typically much larger than required to absorb all the iodine transported to the wall. For example, a typical reactor core at equilibrium for a 1000 MW plant would contain some 25 kg of iodine[53]. Of the 50% which could be released from the core, less than 10% would be adsorbed by surfaces if sprays operate. Therefore only 25(0.5) (0.1), or 1.25 kg of iodine at most would be available for surface deposition. If this iodine were distributed uniformly on surfaces within the containment vessel above the operating deck, the surface density would be roughly

$\frac{1.25 \times 10^6 mg}{3.5 \times 10^8 cm^2} = 0.0035\ mg/cm^2$. This is a very low surface loading and is appreciably less than the sorptive capacity ($0.04\ mg/cm^2$) of the least sorptive paint (vinyl base) studied by Rosenberg, et al.[54]. For most paints used in containment vessels, the sorptive capacity is an order of magnitude higher than the value listed above for the vinyl paint. Therefore, it appears that the painted surfaces have the capacity to retain all the iodine which could be deposited on them. Similar results have been reported for other surfaces, including stainless

steel[54], mild steel[55] and concrete[55].

Review of Iodine Deposition Measurements

Deposition on Small Specimens

Results of an extensive research program on deposition of elemental iodine and methyl iodide on paints commonly used in containment vessels were reported by Rosenberg, et al.[54]. Several kinds of laboratory scale experiments were performed. First was a "screening chamber" in which 12 deposition coupons (1 inch square) could be exposed simultaneously to an iodine-containing atmosphere. The deposition coupons were supported from a glass shaft which was rotated at speeds of 1, 25, and 250 rpm to evaluate the effect of gas velocity on adsorption. The coupons were removed periodically from the chamber and the iodine deposit analyzed by means of gamma ray spectroscopy.

In a second apparatus, a single deposition coupon was suspended in a glass vessel so that iodine deposited from a flowing gas stream could be assayed continuously using a gamma ray scintillation probe.

Deposition under condensing steam conditions was measured within a cylindrical chamber (1 ft x 1 ft), the walls of which were warmed by a heating tape to control the condensation rate.

Iodine deposition from the liquid phase was measured by suspending coated discs (10 cm diameter) in liquid saturated with tagged iodine crystals.

Typical results from vapor phase sorption and desorption

tests are shown in Figure 7. Important features of the data in Figure 7 include the following. First, there is an initial rapid sorption rate which is constant with time. After several hours, the paint becomes saturated with iodine, and the sorption rate slows. The paint becomes completely saturated after about 10 hours and for longer times no additional deposition occurs. When iodine-free gas is passed across the specimen, a fraction of the iodine is desorbed, and the remainder is bound irreversibly.

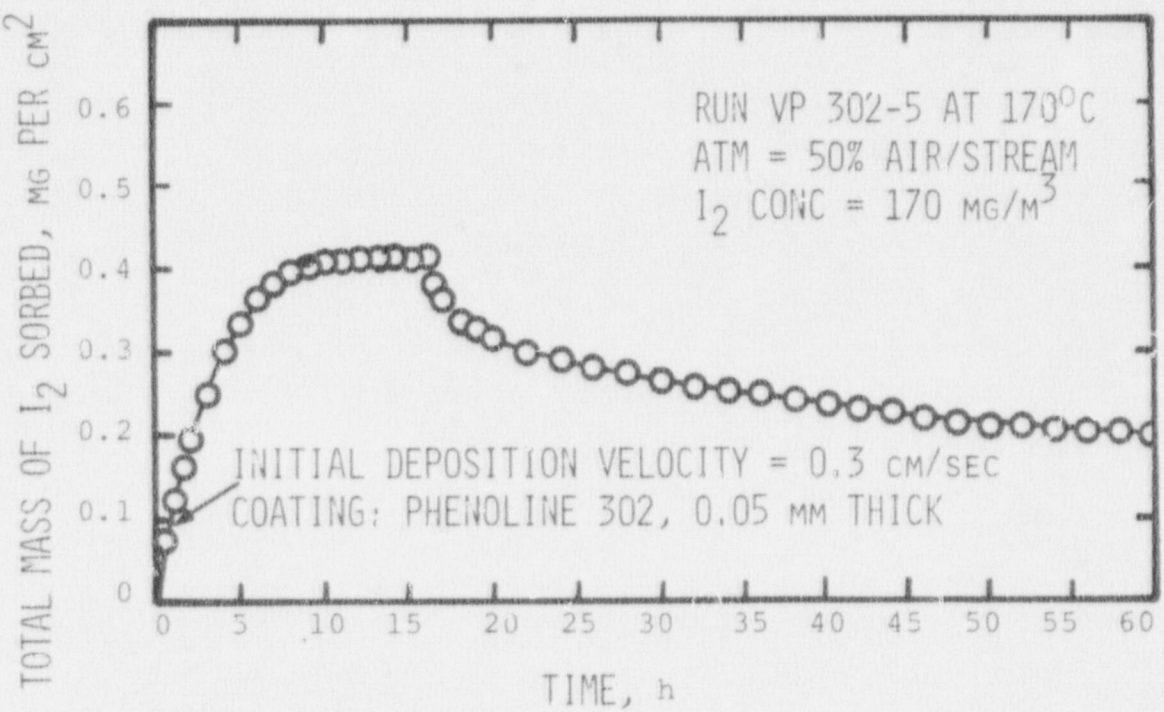

FIGURE 7. Typical Results of Vapor Phase Iodine Sorption-Desorption Experiments Reported by Rosenberg, et al.[54]

Experiments were conducted with the coatings described in Table 4.

TABLE 4. Commerical Coatings Studied by Rosenberg et al.[54]

Coating Name	Coating Class	Manufacturer
Amercoat 33 HB	Vinyl	Americoat Corp.
Amercoat 66	Epoxy	Americoat Corp.
Amercoat 1756	Acrylic latex	Americoat Corp.
Dimetcote No. 3	Inorganic zinc primer	Americoat Corp.
Carboline 3300	Acrylic latex	Carboline Co.
Phenoline 302	Phenolic	Carboline Co.
Phenoline 368	Phenolic	Carboline Co.
Carbo-zinc 11	Inorganic zinc primer	Carboline Co.
Turco Contam-Affix Rem	Vinyl	Turco Products, Inc.
Corlar 588	Epoxy	du Pont
Strathclyde	Iron Oxide primer	Federated Paints, Ltd.

Selected results obtained for vapor phase deposition at 115°C and 1 atm pressure are shown in Table 5.

These results show that for most coatings, the observed deposition velocity is larger than the value of the mass transfer coefficient predicted for the walls of the containment vessel, approximately 0.07 cm/sec. Therefore, for most of the paints, the wall may be considered a perfect sink for iodine even in the absence of an

absorptive liquid film. Also, the absorptive capacity, at a minimum, is an order of magnitude larger than required to adsorb the quantity of iodine which will be deposited on surfaces if sprays operate.

TABLE 5. Typical Iodine Sorption Results Reported by Rosenberg, et al.[54] for Vapor Phase Deposition at 115°C

Coating Name	Initial Deposition Velocity, cm/sec	Iodine Capacity at Saturation, mg/cm^2	Iodine Irreversibly Retained, %
Amercoat	0.0206	0.0744	55.1
Turco Contam Affix Rem	0.00984	0.0327	71.3
Amercoat	0.0389	0.271	40.6
Carboline 3300	0.101	0.223	39.3
Phenoline 302	0.148	0.458	67.6
Phenoline 368	0.184	0.697	86.5
Amercoat 66	0.491	0.976	56.6
Corlar	0.675	1.21	43.1
Dimetcote No.3	0.707	10.3	100.0
Carbo-zinc 11	0.678	9.70	99.4

The deposition velocities obtained in this small scale study would not be expected to apply directly to reactor containment vessels, but serve as guidelines and represent limiting cases for particular situations.

Measurements of iodine deposition on small test coupons have also been reported by Parker, et al.[56], by

Hilliard and Coleman[32], by Nebaker, et al.[57], and by Freeby, et al.[58]. The results of these latter studies are supportive of the work of Rosenberg, et al.[54], hence, will not be reviewed here.

Natural Transport Measurements In Small Vessels

Numerous tests of iodine plateout characteristics have been carried out in vessels having volumes of the order of one cubic meter. While these vessels are very much smaller than reactor containment vessels, the tests allow thermal and concentration effects to be realistically demonstrated.

Containment Research Installation (CRI)

The CRI system[56] consists principally of a stainless steel tank equipped with a removable liner to permit deposition to be studied for various surfaces. The vessel volume is 4.6×10^6 cm^3, and has an internal surface area of 1.34×10^5 cm^2.

Airborne iodine concentration in a typical test fell rapidly soon after release; then after the concentration had fallen by more than an order of magnitude, the concentration decreased more slowly. The results of tests carried out with a stainless steel liner are summarized in Table 6.

Two important results from the tests are the following. First, the iodine deposition rate is not strongly

dependent on the temperature of steam-air atmospheres or on the initial iodine concentration. Second, the deposition velocities observed are equal to or larger than 0.08 cm/sec, a magnitude expected for natural convection gas phase limited transport in this vessel.

Results obtained in the CRI after a liner covered with an Amercoat paint was installed are summarized in Table 7.

The results obtained with the Amercoat paint are in good agreement with those obtained with the stainless steel liner.

TABLE 6. Results of Iodine Tests Carried Out in CRI With a Stainless Steel Liner As Reported by Parker, et al. (56)

Experiment No.	Release Conc. mg/m^3	Maximum Temp. ^oC	Initial Conc. Half-Life min.	Initial I_2 Deposition Velocity*, cm/sec
100 I	4.8	25	0.35	1.14
103 I		25	3.4	0.117
104 I	6.7	125.5	1.6	1.25
107 S	3.4	110.5	4.5	0.089
110 SI	0.5	118	3.9	0.102
111 SI	0.05	115	3.0	0.133
114 H	0.27	111	4.6	0.087

* $V_d = \frac{0.693}{t_{\frac{1}{2}}} \cdot \frac{\text{Volume}}{\text{Area}} = \frac{23.9}{t_{\frac{1}{2}}}$ cm/sec

TABLE 7. Results of Iodine Tests Carried Out in CRI With an Amercoat Liner [59]

Experiment No.	Release Conc. mg/m^3	Maximum Temp. ^oC	Initial Conc. Half-Life min.	Initial I_2 Deposition Velocity*, cm/sec
115	0.0001	115	6	0.067
117	0.005	115	2.7	0.148
118	0.005	115	2.7	0.148
119	0.035	115	5	0.080
120	0.125	115	4.2	0.09

*$V_d = \frac{0.693}{t_{\frac{1}{2}}} \cdot \frac{\text{Volume}}{\text{Area}} = \frac{23.9}{t_{\frac{1}{2}}}$ cm/sec

Thus, iodine deposition proceeded at about the same rate in vessels having either painted walls or stainless steel walls.

Aerosol Development Facility (ADF)

The Aerosol Development Facility (ADF) [60] was used to obtain pilot data for the large tests carried out in the Containment Systems Experiment. Two different vessels were used in the ADF tests. The PAT vessel (painted aerosol tank) had a volume of 1.54 m^3, an internal surface area of 8.0 m^2, and had walls of carbon steel painted with Phenoline 300, a modified phenolic coating. The SAT vessel (stainless aerosol tank) had a volume of 0.90 m^3, a surface area of 5.2 m^2, and was made from 304 L

stainless steel. Surface deposition tests carried out in ADF tanks are summarized in Table 8.

Results obtained in the stainless steel vessel are in good agreement with those obtained in the painted vessel. Hilliard[60] concluded that the iodine deposition velocity (mass transfer coefficient) was governed by mass transfer resistance in the gas phase. In Runs SB-48 and SB-50, the steam flux was a factor of 10 below the value used in other experiments. The iodine removal rate was reduced by a factor of four due to this lower condensation rate.

The ADF results appear to agree well with those obtained at ORNL in the CRI. Agreement of results obtained with three types of surfaces supports the conclusion that gas phase resistance controlled the mass transfer rate.

Contamination-Decontamination Experiment (CDE)

The Contamination-Decontamination (CDE) facility was set up to provide piloting data for the LOFT experiment[57,58]. The test vessel was approximately 1.5 m in diameter by 1.5 m in height. It had a volume of 2.4 m^3 and a surface area of 10.7 m^2. As indicated in the name of this program, the emphasis was on the development of procedures for decontamination of surfaces exposed to fission products. Some data were obtained which can be used to estimate the initial iodine deposition velocity. Available data from the CDE are summarized in Table 9.

The removal rates for elemental iodine given in Table 9 are comparable to those obtained in ADF and CRI

TABLE 8. Iodine Plateout Tests Reported by Hilliard, et al.[60]

Run No.	Vessel Used	I_2 Release Conc. mg/m^3	Temp. ^oC	Initial I_2 Half-Life min	I_2 Deposition Velocity cm/sec	Atmosphere
IA-26	PAT	4.5×10^{-5}	70	7.0	0.031	Air
IA-32	PAT	1.8×10^{-4}	82	6.7	0.033	Steam
IA-33	PAT	1.6×10^{-4}	82	4.5	0.049	Air/Steam
IA-39	PAT	2.9×10^{-4}	82	4.5	0.049	Air/Steam
IA-40	PAT	2.3×10^{-4}	84	6.5	0.034	Air/Steam
IB-41	PAT	2.7×10^{-4}	84	10	0.022	Air/Steam
IB-42	PAT	2.7×10^{-4}	84	13	0.015	Steam/Argon
SA-23	PAT	0.52	79	4.0	0.055	Air/Steam
SA-28	PAT	3.3×10^{-4}	81	4.5	0.049	Air/Steam
SA-43	PAT	0.45	80	3.5	0.063	Air/Steam
SA-44	SAT	0.53	81	4.0	0.050	Air/Steam
SB-48	SAT	0.54	82	15	0.013	Air/Steam
SB-50	SAT	0.52	81	17	0.012	Air/Steam
SB-53	SAT	1.0	80	6	0.033	Air/Steam
SB-74	SAT	.52	81	5	0.040	Air/Steam
SB-78	SAT	0.97	80	8	0.025	Air/Steam

TABLE 9. CDE Iodine Deposition Rates[57,58]

CDE Run No.	Initial I_2 Removal $t_{\frac{1}{2}}$ min	Initial I_2 Deposition Velocity cm/sec
Composite of 6 Runs	8	0.065
Tracer Run 10	1-3	0.52 - 0.17
Tracer Run 11	1-3	0.52 - 0.17

at Battelle-Northwest and Oak Ridge National Laboratory, respectively.

From this review of small scale pilot scale tests, it is concluded that iodine deposits initially at a rate limited by gas phase mass transfer resistance. This initial rate continues until the airborne concentration decays by a factor of 100 or more, and then the removal rate decreases. The long term removal rate is typically less than 10% of the initial rate. If chemical reactions within liquid or solid surfaces had controlled iodine plate-out, then both iodine concentration and wall material would have influenced the removal rate. Since neither of these variables was important, one is forced to conclude that gas phase mass transfer resistance controlled the deposition rate during early stages.

Natural Transport Experiments in Large Vessels

A significant number of experiments at relatively large scale have been carried out in the United States and in Great Britain. These experiments are important because they show the degree to which a large gas volume can be considered well-mixed. They also provide data on the removal rate, so that predictions for full-sized containment vessels can be made with a reasonably small scaleup factor. Important tests are described as follows.

Containment Systems Experiment (CSE)

A total of six (6) natural transport tests were carried out as part of the Containment Systems Experiment Program carried out at Battelle-Northwest[32]. Two tests were carried out in an inner vessel (called the dry well) and four were done in the main containment vessel. The inner vessel was 11 feet in diameter and 30 feet in height, whereas the main vessel was 25 feet in diameter and 67 feet in height. Both vessels were painted internally with a phenolic resin paint, Phenoline 302*. The vessels were heated internally by live steam injection. In most tests a steady state temperature was maintained. In one test (A-11) steam flow was stopped after fission product simulants were injected; the temperature then decayed by heat loss through the insulated vessel walls.

Fission product simulants injected included cesium oxide, uranium oxide, elemental iodine, and methyl iodide. These substances were sampled by means of Maypack samplers,

* Product of the Carboline Company, St. Louis, Missouri

and analyzed by gamma ray spectroscopy.

In experiments in both vessels, gas samples were obtained at seven to fourteen spatial locations to determine whether concentration gradients existed in the bulk gas phase.

Results of the six natural transport tests carried out in the CSE facility that pertain to elemental iodine are summarized in Table 10.

TABLE 10. CSE Natural Transport Tests

Run No.	Vessel Volume ft^3	Atm. Temp. ^oF	I_2 Release Conc. mg/m^3	Initial I_2 Removal $t_{½}$ min	I_2 Deposition Velocity cm/sec
D-1	4,200	252	0.66	8.0	0.097
D-2	4,200	250	0.94	9.5	0.081
A-1	21,000	181	1.17	9.0	0.137
A-2	21,000	185	94.5	9.0	0.137
A-5	21,000	253	142	13.5	0.092
A-11	21,000	253	165	16.0	0.076

* In Run A-11, temperature decayed following fission product injection.

The measured deposition velocities varied from 0.076 cm/sec to 0.137 cm/sec depending on the thermal conditions in the vessel. These values are somewhat higher than the values obtained in ADF, and this is explanable in terms of a higher gas phase mass transfer coefficient. The deposition velocities shown in Table 10

for the large scale CSE tests are in good agreement with values obtained in CRI and CDE tests.

Several key conclusions from the CSE tests listed by Hilliard and Coleman[32] are the following.

- The experimental values of the initial removal rate for elemental iodine were in good agreement with a natural convection model in which it was assumed that all mass transfer resistance resides in the gas phase.
- The gas phase limited rate for elemental iodine persisted until the gas phase concentration decreased to about 1% of the initial value. Thereafter the concentration decreased at a slower rate.
- The concentrations of all fission product simulants were essentially uniform throughout the gas space of a single compartment.

Iodine Deposition In An Unheated Cubical Volume

Measurements of iodine deposition in an unheated cubical room, whose surface was covered by a chlorinated rubber-based paint, were reported by Croft, et al.[55]. The room was 27.4 m^3 in volume and had a surface area of 60.2 m^2. Temperature within this masonry-walled room was essentially in equilibrium with the outside space, maintained at approximately 20°C. The room atmosphere was unfiltered and was maintained in a gentle state of agitation by a small fan.

Elemental iodine was released over a time period of 10 to 20 minutes, and the airborne concentration was

followed with time by means of Maypack samples. Results from these experiments are summarized in Table 11.

TABLE 11. I_2 Deposition In An Unheated Cubical Room[55]

Test No.	Relative Humidity	I_2 Release Conc., mg/m^3	I_2 Removal Halftime, min	I_2 Deposition Velocity cm/sec
1	85%	113	130	0.004
2	85%	237	170	0.0031
3	100%	190	140	0.0037

The iodine removal process was followed for 500 minutes, and was found to be first order (constant halftime) for this entire period.

The deposition velocities obtained in these tests are one to two orders of magnitude smaller than obtained in most other tests. This lower deposition velocity is consistent with the expected low gas phase mass transfer coefficient expected for the unheated room. The small fan could be expected to mix the bulk gas phase, but would provide only a minimal flow of gas along the walls. The results obtained would not be expected to apply directly to water reactor LOCA conditions, but do demonstrate that the iodine deposition velocity is controlled by the gas phase mass transfer coefficient.

Iodine Deposition in Zenith Reactor Containment

Surface deposition of elemental iodine was studied in the secondary containment of the Zenith reactor[61]. The reactor pit area, covered by a steel bonnet, had a volume of 500 m^3 with a total surface area of 700 m^2. Some 60% of the surface was concrete painted with chlorinated rubber-based paint, 40% was painted metal and 1% was bare metal. Results of two experiments reported in detail are summarized in Table 12.

TABLE 12. Results of I_2 Deposition in Zenith Reactor Containment[61]

Test No.	I_2 Release Conc. mg/m^3	Ventilation Flow Rate m^3/min	Initial I_2 Removal Halftime min	Estimated I_2 Deposition Velocity cm/sec
1	0.00078	0	21	0.039
2	0.00074	85	3.7	0.02

The initial removal rate continued until the airborne concentration decreased by two to three orders of magnitude, and then decreased more slowly.

This experiment was similar to that carried out in the painted room[55] in that there were essentially no temperature gradients to promote a convective flow along the walls of the pit region. It is obvious that more turbulence was present than in the cubical room because

the iodine deposition velocity was higher by an order of magnitude.

These results would not be expected to apply to the post accident situation in a water reactor because of the absence of a typical wall ΔT in the experiment. The experimental results are consistent with the postulate that surface deposition is controlled by gas phase mass transfer resistance.

Iodine Release in DIDO Reactor Containment Shell

Stinchcombe and Goldsmith[62] described the results of experiments involving release of elemental iodine into the DIDO containment shell. While the details of the experimental facilities are somewhat sketchy, iodine deposition velocities can be estimated. The DIDO shell had a volume of 7000 m^3, and if equipment surfaces are ignored, a surface area of 1020 m^2. The experimental releases were done at ambient temperature and pressure. Results of the tests are summarized in Table 13.

TABLE 13. Results of Iodine Deposition in DIDO Containment Vessel[62]

Test No.	I_2 Release Conc. mg/m^3	I_2 Removal Halftime min	Estimated I_2 Deposition Velocity, cm/sec
A	0.00012	6.4	0.45
B	0.00012	8.3	0.34

The iodine deposition velocity obtained in the DIDO vessel is appreciably larger than obtained in most other natural transport tests. For example, these values are roughly 100 times larger than obtained in the cubical room tests of Croft, et al.[55]. The higher deposition velocities are attributable to the mixing of the gas phase by ventilation equipment in the DIDO vessel and to use of only wall surface area in calculating deposition velocities.

The long term elemental iodine behavior was similar to that typically obtained: the initial rapid removal rate persisted until the concentration fell by about two orders of magnitude, and then fell more slowly at longer times. The observed high deposition velocity indicates that the paint adsorption rate was not a limiting factor.

In a supporting experiment, Stinchcombe and Goldsmith[62] studied the effect of condensing steam on iodine deposition. The amount of iodine deposited on a cold, condensing surface was the same as that on a non-cooled silver surface subjected to the same gas flow. It was concluded that the deposition was entirely due to the forced convection flow, and that the condensation of steam was unimportant in I_2 deposition. This result is in agreement with Hilliard's[32] results which showed that steam sweep was small compared to diffusional mass transfer.

Conclusions From Large Vessel Iodine Experiments

The results of all reported large scale tests are

consistent with small scale results in that initial iodine deposition proceeds at a rate limited by gas phase mass transfer, and then after the concentration decays by a factor of 100 or so, the removal rate slows. There is no evidence that the properties of the surface limit the initial deposition rate. Nor is there evidence that the sweep effect of condensing steam is controlling. Therefore, ones ability to predict iodine deposition under accident conditions depends primarily on ones ability to predict gas phase mass transfer coefficients under accident conditions.

Model For Surface Deposition of Elemental Iodine In Containment Vessels

Based on the experimental evidence, a satisfactory model will be one which agrees with the following experimentally derived behavioral characteristics.

- Initial deposition rate is limited by gas phase mass transfer.
- The bulk volume of a single compartment is well mixed.
- Steam flux plays a minor role in iodine deposition.
- Effects of size scale must be included in the model.

On the several models[30,31,54,63,64] which have been proposed to describe fission product removal due to natural transport, two models[30,31] account for the effects noted above.

The Knudsen-Hilliard model[30] views deposition as a film transport process to vessel surfaces. The mass transfer coefficient across the gas film is predicted from natural convection heat transfer correlations, by using a mass transfer-heat transfer analogy. Prediction of the mass transfer coefficient requires a knowledge of the wall heat transfer rate.

The Yuill-Baston model[31] tackles the transport process using the penetration theory of mass transfer[65]. The mass transfer rate is predicted under gas exposure times predicted for natural convection flows. Thermal conditions at the wall are needed to predict the mass transfer rate.

Both of these models yield predictions which are in good agreement with measured rates of removal. Of the two, the Knudsen-Hilliard model offers several advantages, and has been adopted for use in the SPIRT Code[47]. A listing of a recent version of this code, SPIRT 10 is appended to this report. Reasons for selecting this model are as follows:

- The film model accounts for the laminar to turbulent transition boundary layer flow whereas the penetration theory model treats the boundary layer as stagnant.
- The film model is easier to visualize and use than the penetration theory model.
- The film model appears to be better able to predict scale-up effects because it accounts for turbulent flows which develop in large vessels.

For laminar flow, the heat transfer rate is described by

$$\frac{h_{nc}l}{k} = 0.59(Gr_T Pr)^{\frac{1}{4}} \tag{69}$$

where h_{nc} = heat transfer coefficient on vertical plate,
l = length of surface,
k = thermal conductivity of gas,
Gr_T = Grashov number due to wall temperature difference,
Pr = Prandtl number for gas.

The form of Eq. (69) was obtained from the theoretical work of Schmidt and Beckman[66], and the constant (0.59) obtained empirically. A relationship of similar form applies for turbulent flow (transition from laminar to turbulent flow occurs at Grashov numbers between 10^9 and 10^{12}).

$$\frac{h_{nc}l}{k} = 0.13(Gr_T Pr)^{1/3} \tag{70}$$

Eqs. (69) and (70) may be transformed through a mass transfer-heat transfer analogy to give relationships to predict mass transfer coefficients[30]. For laminar flow

$$\frac{k_c l}{D} = 0.59(Gr_c Sc)^{\frac{1}{4}} \tag{71}$$

and for turbulent flow

$$\frac{k_c l}{D} = 0.13(Gr_c Sc)^{1/3} \qquad (72)$$

where k_c = mass transfer coefficient,
Gr_c = Grashov number accounting for molecular weight difference between bulk gas and interface,
D = molecular diffusivity of I_2,
Sc = Schmidt number for iodine in gas.

These two equations allow a mass transfer coefficient to be calculated once the temperature difference at the wall is known. For typical LOCA conditions, Hilliard and Coleman[32] quote a distance of 10 feet from the top of the containment wall for the transition from laminar to turbulent boundary layer flow.

In addition to diffusional transport, Knudsen and Hilliard[30] add a second mass transport term to account for the sweep effect of condensing steam. The condensation mass transfer coefficient is given as

$$k_s = \frac{n_s R T_b}{18P} \qquad (73)$$

where k_s = steam sweep mass transfer coefficient,
n_s = steam flux toward surfaces,
R = gas constant,
T_b = bulk gas temperature,
P = total gas pressure.

The formulation of Eq. (73) is based on the concept that

iodine is transported to the wall with the steam at a velocity equal to the bulk flow velocity caused by the condensation. The enhancement predicted by Eq. (73) for bulk flow is probably an overestimate of the effect[28]. Therefore the contribution of steam sweep will not be included in the model chosen here. The net effect of disregarding Eq. (73) is small, because steam sweep predicted by Eq. (73) typically accounts for less than 10% of the overall mass transfer coefficient.

Predictions based on Eqs. (71), (72) and (73) are compared to experimental results obtained in CSE in Table 14. The results shown in Table 14 were calculated by assuming that all exposed surface areas inside the CSE vessel were iodine deposition surfaces.

TABLE 14. Comparison of Predicted Removal Rates For Elemental Iodine by Steam Sweep Effect and by Diffusion[32]

CSE Run No.	Predicted Halftime, min		Measured Half Life, min
	By Steam Sweep[a]	By Diffusion Across B.L.[b]	
D-1	36	7.7	8.0 ± 1
D-2	38	7.8	9.5 ± 0.5
A-1	130	10.0	9.0 ± 4.0
A-2	122	9.9	9.0 ± 0.5
A-5	475	16.1	13.5 ± 0.5
A-11	500	16.8	16.0 ± 0.5

(a) Calculated from Eq. (73)

(b) Calculated from Eqs. (71) and (72), using a transition from laminar to turbulent boundary layer flow at 10 feet from the top of the vessel

Two important facts evident from these results are: (1) the steam sweep effect is small, and (2) the measured and predicted removal rates are in good agreement.

Typical mass transfer coefficients predicted for turbulent flow for saturated steam-air mixtures have been calculated by Knudsen and Hilliard[30]. Examples are shown in Figure 8.

From the results pictured in Figure 8, it is obvious that the mass transfer coefficient is not highly sensitive to the bulk gas temperature. The transfer coefficient is highly dependent on the inside temperature difference for ΔT values less than 4^0F. For higher ΔT values, only a small increase in k_c results from increasing the temperature difference.

From a practical standpoint, the temperature difference in the gas boundary layer will not fall below about 1^0F for LOCA times of interest. Order of magnitude calculations for two cases show this. First, for infinite time (equilibrium) Hilliard and Coleman[32] show that a ΔT of 1^0F exists for heat transfer through 5 feet of concrete, where the internal temperature is 250^0F and the outside temperature is 80^0F. Second, a transient heat transfer calculation made under the assumption that a concrete wall 2 feet thick is heated from both sides by an initial ΔT of 100^0F, a $1\text{-}2^0F$ ΔT will continue to exist after 25 hr. Therefore, in the absence of a transient heat transfer analysis, a minimum ΔT of 1^0F can be assumed to exist in all compartments exposed to steam in the LOCA.

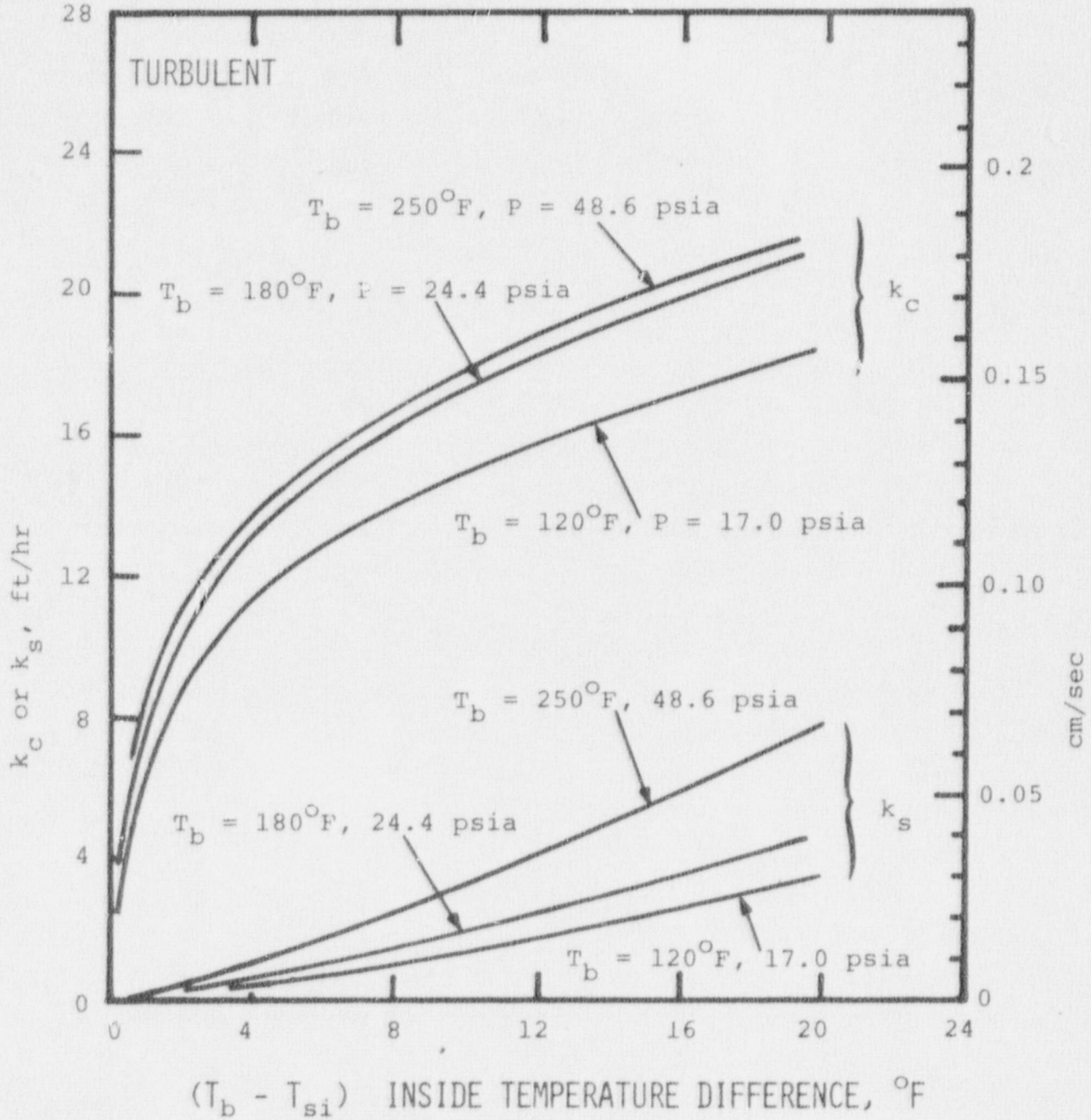

FIGURE 8. Mass Transfer Coefficients As a Function of Inside Temperature Difference for Steam-Air Atmospheres[30]

Wall Plateout During Spray Operation

Spray operation would influence surface deposition in two ways. First, the sprays would impart turbulence to the gas phase, thereby increasing the mass transfer coefficient. Second, spray operation would affect the temperature gradient at solid surfaces, and thereby affect the mass transfer rate.

Spray Induced Turbulence Promotion of Mass Transfer

While we know of no data of direct applicability to spray induced turbulence in containment vessels, an order of magnitude estimate of the effect may be obtained by examining the enhancement in wall plateout observed in CSE tests on air cleaning[67].

The CSE air cleaning tests of interest involved the operation of a cleanup loop inside the main compartment. Contaminated air was drawn into a series of filters and adsorbents, and then discharged back into the containment atmosphere. Air motion resulting from the operation of the air cleaning loop enhanced the iodine plateout rate on vessel surfaces. The enhanced wall plateout in air cleaning tests is summarized in Table 15.

TABLE 15. Enhancement of Iodine Surface Deposition In CSE Air Cleaning Experiments[67]

CSE Run Number	A-13	A-14	A-15	A-16
Air Flow Rate, CFM	1000	1000	1000	1800
Gas Temperature, ^0F	96	250	250	246
λ_0 - Observed, min^{-1}	0.095	0.141	0.115	0.182
F/V - loop, min^{-1}	0.0475	0.0475	0.0475	0.086
(λ_0-F/V) - wall deposition, min^{-1}	0.0475	0.0935	0.0675	0.096
λ (natural convection), min^{-1}	0.0266	0.0432	0.0257	0.0532
λ (enhancement), min^{-1}	0.0209	0.0503	0.0418	0.0428

In Table 15, λ_0 is the observed removal rate constant which resulted from both surface deposition and cleanup in the aircleaning components. F/V, the ratio of air-cleaning loop flow rate to vessel volume, is the removal rate constant due to the loop itself. λ (natural convection) is the removal λ which was observed due to natural convection plateout when the loop was not operated. Thus, λ (enhancement) is the observed removal rate constant minus the λ's due to loop cleanup and wall plateout due to natural convection.

As shown from Table 15, there is an appreciable enhancement in wall plateout caused by loop operation. The kinetic energy per unit volume of gas may be calculated by

$$\frac{\text{Energy/Time}}{\text{Volume}} = \frac{Mv^2}{(\text{Volume})(2g_c)} = \frac{\rho F.(\frac{F}{A})^2}{(21{,}000)(2g_c)} \quad (74)$$

where ρ = gas density,
v = gas velocity
F = loop flow rate,
A = area of discharge duct,
M = mass of air per unit time,
g_c = gravitational constant.

This is the kinetic energy carried by the exiting gas stream from the air cleaning loop per unit time. The enhanced deposition rate, expressed as a deposition velocity, is plotted Figure 9 as a function of energy dissipated per unit time per unit volume. From these data, it appears that surface deposition is greatly enhanced for low values of energy, and that an upper level or saturation value is attained at an energy dissipation rate of about 0.001 ft lb/sec ft^3.

For a PWR spray system operating at 40 psid at 3000 gpm in a containment vessel of 2×10^6 ft^3, the kinetic energy dissipated by the sprays is about 0.02 ft lb/sec ft^3. This value is about 4 times larger than the highest value shown on Figure 9; hence, a deposition velocity of at least 0.07 cm/sec would be predicted as a result of spray enhancement of surface deposition.

6.1.10 Approach to Equilibrium by Recirculated Spray

When spray water is recirculated to the spray headers,

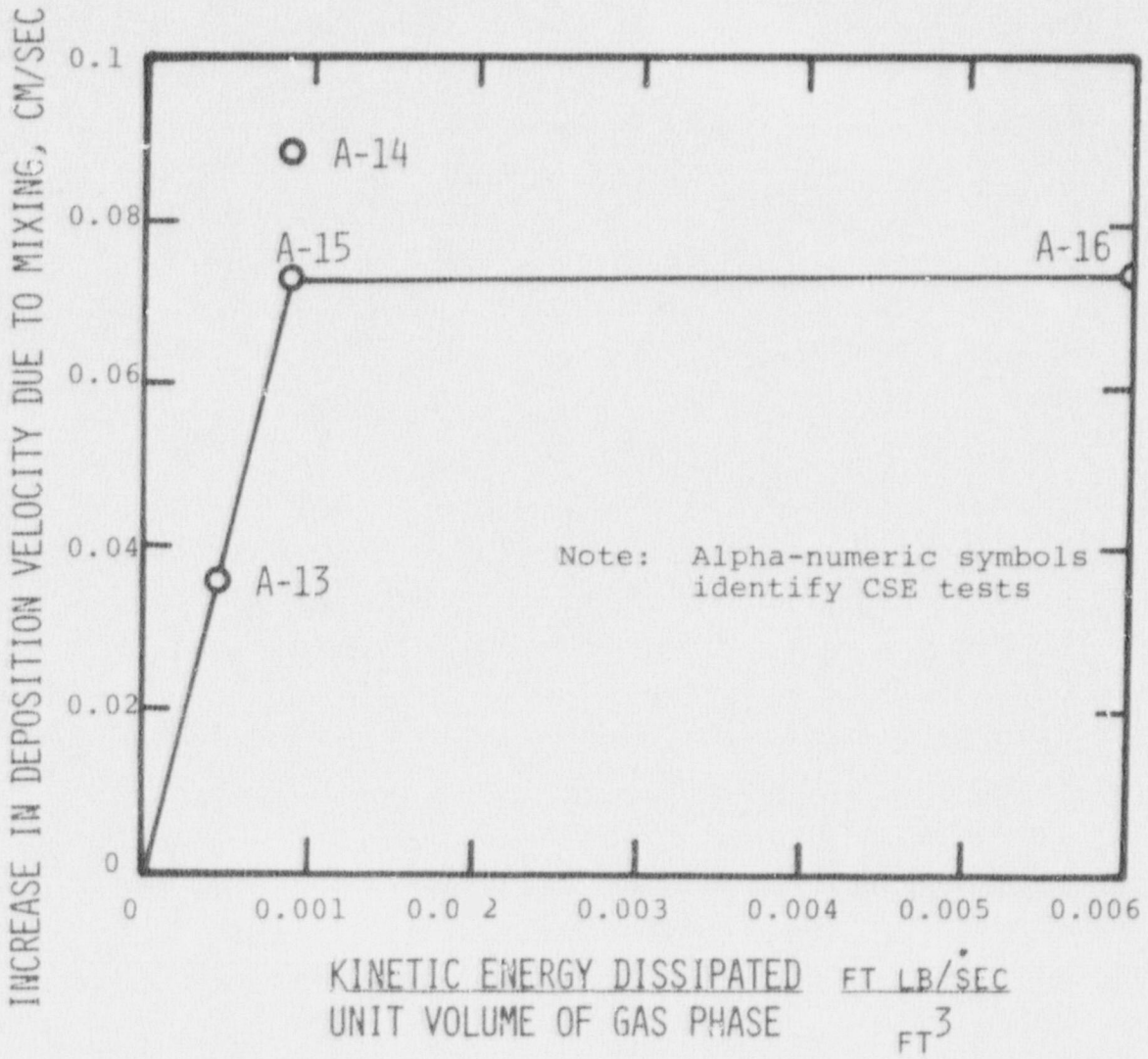

FIGURE 9. Estimated Enhancement in Surface Deposition Resulting From Operation of Air Cleaning Loop in CSE

equilibrium will eventually be approached. The removal lambda will therefore decrease in magnitude, until ultimately iodine in the spray water will be in equilibrium with iodine in the containment atmosphere. In order to simplify the washout equation, early models used by the staff[1,2] accounted for the approach to equilibrium by means of a cut-off concentration level. When the cut-off level was reached, λ was set equal to zero. Cut-off levels were applied to caustic and thiosulfate sprays when the instantaneous source was depleted by factors of 100 and 1000 respectively.

These factors are not limiting for the calculation of 2 hr doses, but they could be controlling in the calculation of doses from venting, which might be done after 30 days. If a non-removable iodine specie, like methyl iodide, makes up as much as 4% of the iodine source term, then the cut-off levels cited above have little effect.

Large scale containment spray test show that the 1% cut-off limit is conservative for caustic spray[14,48,52], for spray containing trace levels of hydrazine[17], and for boric acid without other additives[18,52]. The 0.1% cut-off limit conservatively described large spray tests in which spray water contained 1% by weight of sodium thiosulfate[34,68].

For long term spraying, the airborne iodine concentration will be in equilibrium with iodine in the spray liquid. From an iodine mass balance on the gas and liquid phases, the equilibrium airborne concentration is calculated to be

$$\frac{C_e}{C_o} = \frac{1}{1 + \frac{LH}{V}} \qquad (75)$$

where C_e = equilibrium airborne concentration,
C_o = initial airborne concentration for puff release,
H = iodine partition coefficient,
L = total volume of water in the sump,
V = total contained gas volume.

From Eq. (75) it is apparent that the equilibrium concentration depends on the partition coefficient, and on the volumes of the two phases. The attained value of H will be larger than the values used for spray washout. For a typical PWR, V = 2 x 10^6 ft^3, and L = 500,000 gal. Using H = 5000 for caustic and 10^5 for thiosulfate, one predicts equilibrium concentration ratios of 0.0059 for caustic, and 0.00030 for thiosulfate. Therefore, the cut-off limits for times beyond 2 hr should be at least as small as the equilibrium value predicted from Eq. (75) using the partition coefficients applicable to spray washout.

In summary, the cut-off concentration method is considered a conservative expedient for treating equilibrium effects for 2 hr dose calculations. The cut-off limits applicable to 2 hr dose calculations may yield overly conservative results for long term concentration of airborne iodine. Consequently long term iodine concentration in the containment atmosphere may be calculated using equilibrium iodine partition coefficients with

Eq. (75). The use of equilibrium partition coefficients is justified since experimental data consistently point to much higher concentration reduction factors. Comparisons of cut-off limits with those achieved in long term large scale tests are presented in this report under "Comparison of Model Predictions with Large Scale Experiments".

6.1.11 Comparison of Model Predictions With Large Scale Experiments

Inorganic Iodine

Boric Acid Spray

Two large scale CSE tests[18,52] have been run using boric acid. For the test which employed 1713* spray nozzles, the following parameters apply.

Injection period	F = 160 gpm, V = 21,000 ft^3
Recirculation period	F = 160 gpm, V = 26,500 ft^3

Using these data, the predicted removal rate constant for the injection period is 0.024 min^{-1} and for the recirculation phase is 0.019 min^{-1}. The predicted and measured airborne concentrations of inorganic iodine are compared in Figure 10. The stagnant film model evaluated with a partition coefficient of 50 is conservative compared to experiment. The measured removal rate is 7.8 times

*Manfd. by Spray Engineering Co., Burlington, Mass.

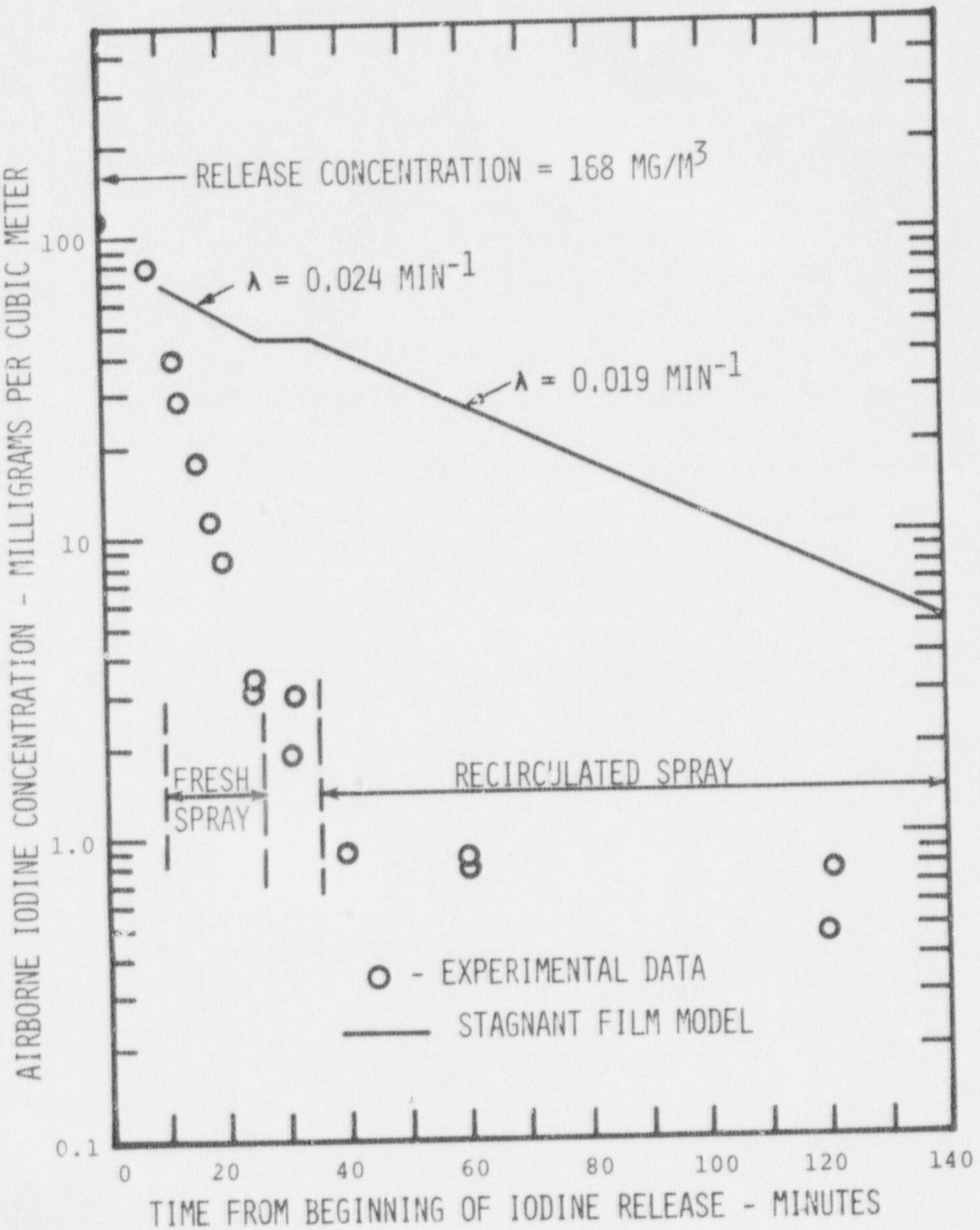

FIGURE 10. Comparison of Stagnant Film Model for Boric Acid Spray with Large Scale Test

higher than predicted.

Removal of airborne iodine by boric acid spray for longer term recirculation is compared to the 1% cut-off limit in Figure 11.

The data shown in Figure 11 demonstrate that for times longer than a few hours, a 1% cut-off limit greatly overpredicts the airborne iodine concentration. For example, after one week the data fall below the cut-off limit by a factor of 1000. As noted earlier in this report, a cut-off limit introduces little error for a 2 hr calculational period, but can lead to overly conservative predictions for longer time periods.

Spray removal of elemental iodine by boric acid spray was also measured in the Nuclear Safety Pilot Plant at ORNL[11]. Three tests, designated as Runs 79, 80, and 82, resulted in iodine decontamination factors of 45, 38, and 59 respectively after 4 hours of spraying. These concentration reduction factors can be used to calculate partition coefficients using Eq. (75). Based on a gas phase volume of 1350 ft^3 and a spray solution volume of 100 gallons, we calculated partition coefficients of 4440, 3740, and 5860 for the three tests. These results support the large scale CSE test data shown in Figures 10 and 11. The stagnant film model is thus assured of providing conservative predictions of iodine removal by boric acid spray solutions.

Sodium Hydroxide Sprays

A total of five large scale CSE spray tests used

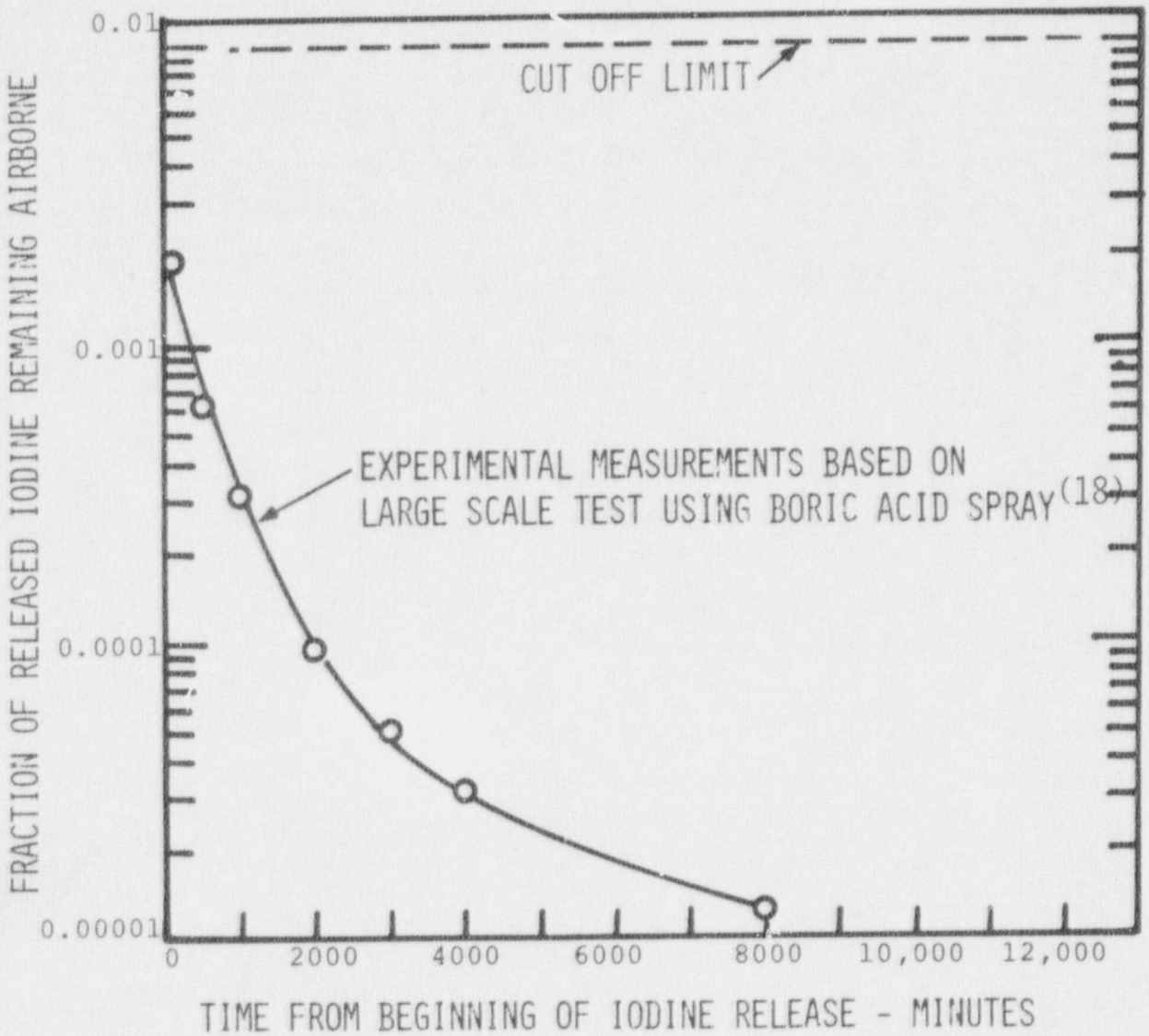

FIGURE 11. Comparison of Cut-Off Limit With Large Scale Test Results for Boric Acid Spray

basic sodium borate solution at an initial pH of 9.5.

The parameters which apply to the initial washout rate are listed in Table 16. Also listed is the measured λ spray.

TABLE 16. Spray Parameters For Caustic Spray Tests in CSE[48,52]

CSE Test	Measured λ, min^{-1}	Spray Rate, gpm	MMD*	σ_g**	Drop Fall Height, ft	Gas Volume ft^3
A-3	0.126	12.8	1210	1.5	38	21,000
A-4	0.495	48.8	1210	1.5	38	21,000
A-6	0.330	49	1210	1.5	38	21,000
A-9	1.19	145	1220	1.5	38	21,000
A-8	1.08	50.5	770	1.5	38	21,000

* MMD is the mass median drop diameter

** σ_g is the geometric standard deviation for an assumed log-normal distribution

The iodine washout rates measured in CSE tests were compared with predictions made from the stagnant drop model and the stagnant film model described in this report. In addition, a "realistic" model was also formulated and compared with the experimental measurements. In the realistic model, the drop was assumed to be well-mixed, and drop coalescence was neglected. The partition coefficient was taken as 5000 for all three models.

The predicted spray lambda's are listed in Table 17

along with the experimental values. The comparison is also shown graphically in Figure 12.

TABLE 17. Comparison of Predicted and Experimentally Measured Removal Rates of Elemental Iodine by Caustic Spray

CSE Run No.	Drop Size,* microns	Experimental λ, hr^{-1}	Realistic Model λ, hr^{-1}	Stagnant Film Model λ, hr^{-1}	Rigid Drop Model λ, hr^{-1}
A-3	1210	7.6	6.9	2.8	4.7
A-4	1210	27.5	26.4	10.8	17.9
A-6	1210	19.8	24.1	19.8	21.8
A-8	770	63	44.2	36.7	40.8
A-9	1220	71.4	72.7	58.4	65.0

*mass median diameter

The realistic model provides the best overall between agreement with the CSE spray tests. The stagnant film model yields the lowest predictions, as expected, and is conservative compared to the experiments. The largest differences between the stagnant film model and the realistic model occurs for Runs A-3 and A-4. These runs were carried out at room temperature where iodine diffusivity is too low to effectively mix the drops. For Run A-8, which used small drops (770 micron mass median diameter) the three models yield prediction which differ by less than 20 percent. The rigid drop model yields prediction which are intermediate between those

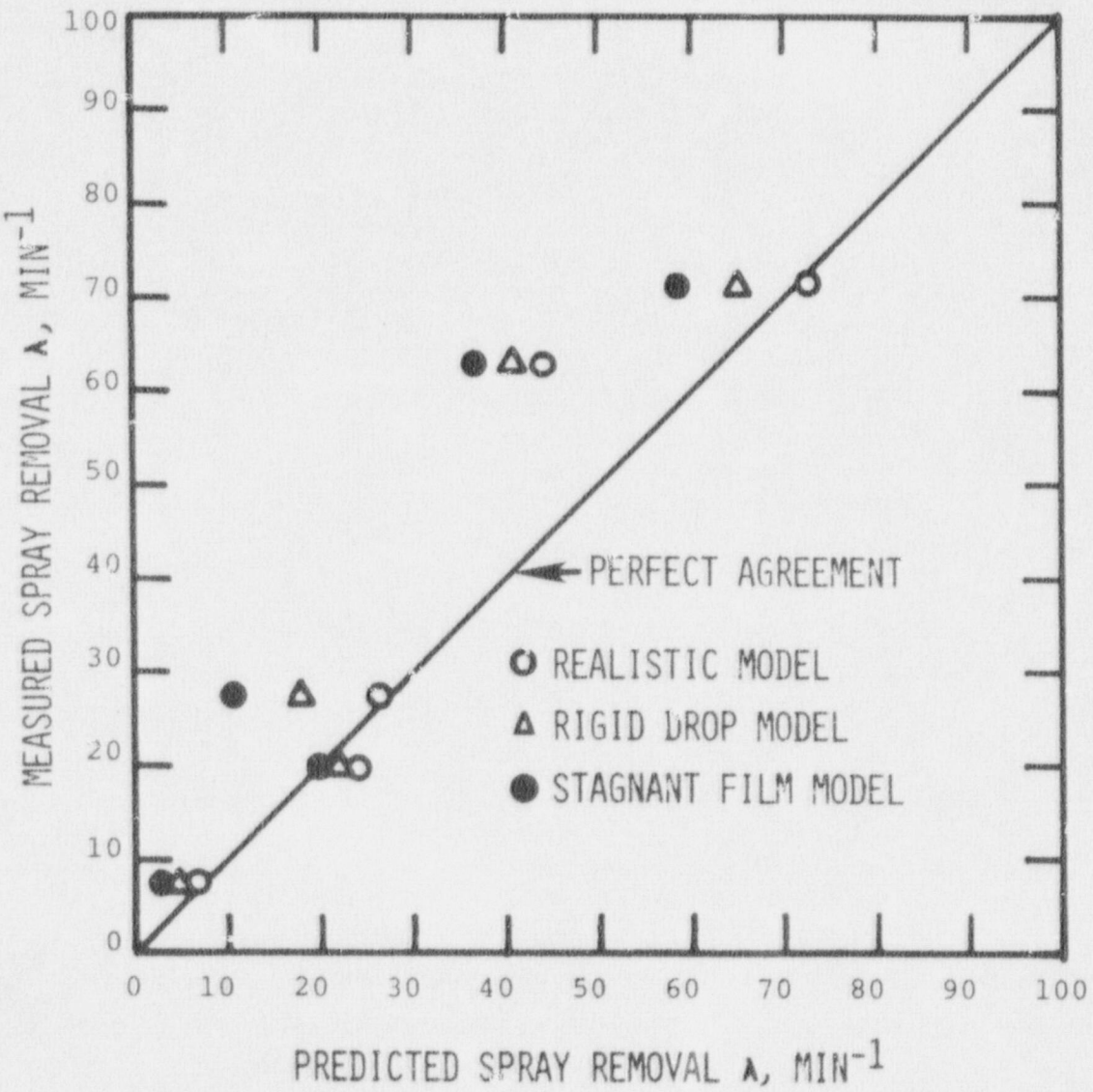

FIGURE 12. Comparison of Iodine Washout Predicted by Several Models With That Measured in CSE Using Caustic Spray

of the realistic model and the stagnant film model, as expected.

Calculations based on the stagnant film and realistic models were also made for typical PWR spray parameters. The results for a full sized containment are compared in Table 18.

TABLE 18. Comparison of Model Predictions For Typical PWR Spray Parameters*

Model	Predicted λ hr^{-1}
Stagnant Film	14.2
Realistic	17.0

* Spray Flow = 1500 gpm,
sprayed volume = 1.75×10^6 ft^3,
fall height = 90 ft,
temp. = 250^0F,
drop size histogram for 1713 spray nozzle.

The spray lambda predicted by the stagnant film model is only 16% lower than the lambda predicted from the realistic model for the typical PWR case described in Table 18. The two models yield similar predictions because for the long fall paths and high temperatures involved, molecular diffusion is quite effective in mixing dissolved iodine throughout the drop volume.

Removal of elemental iodine by the longer term recirculating spray is shown in Figure 13 where experimental

data for CSE test A-11[34] are compared to a .05% cut-off limit, the equilibrium level based on Eq. (75).

Although these test results do not cover as long a time period as did the boric acid test, the conclusions are similar. For a 2 hr period a .05% cut-off limit will introduce little error. If such a cut-off were used for long time periods the airborne iodine concentration would be appreciably overpredicted. The fact that the concentration decreased below the phase equilibrium level shows that the iodine partition coefficient increased with time beyond the value of 5000 which applies to initial spray removal.

Washout measurements made in the Nuclear Safety Pilot Plant[11] confirm the conservatism inherent in the stagnant drop model. While the smaller size of the NSPP makes spray absorption measurements more difficult to interpret, the observed washout rates were found to be appreciably higher than predicted from a rigid drop model. Four runs employing caustic spray were analyzed in reference 19, and results are summarized in Table 19.

While quantitative agreement between the predicted and measured halftimes displayed in Table 19 cannot be claimed, the results support the conservative nature of the spray models employed by the staff.

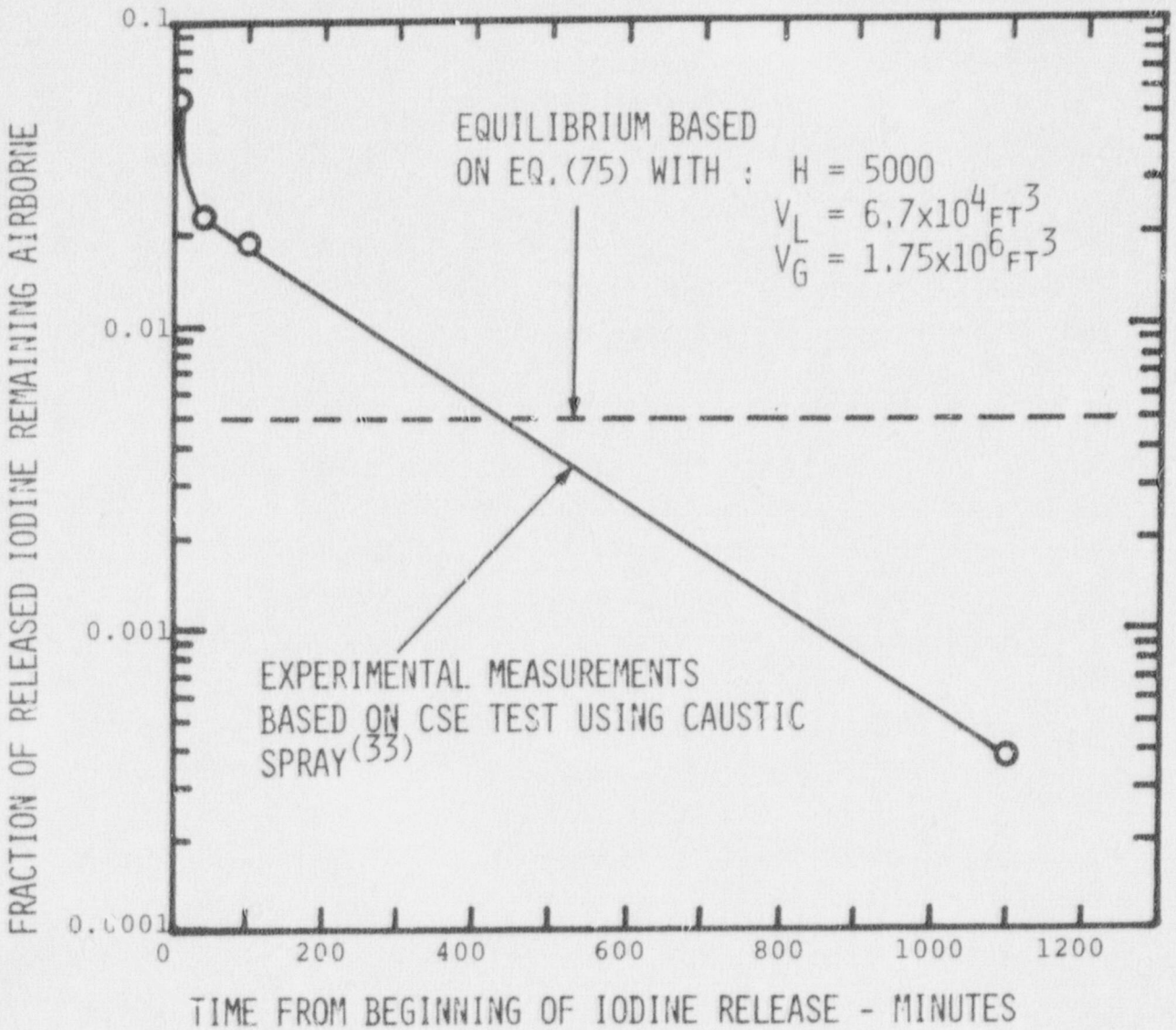

FIGURE 13. Comparison of Cut-Off Limit With Large Scale Test Results for Caustic Spray

TABLE 19. Comparison of Predicted[19] and Measured[11] Iodine Washout Halftimes for NSPP Tests Using Caustic Spray

Spray Conditions	Run Number			
	28	30	31	32
Solution Temp. ^{0}F	248	86	86	86
Mass median drop diameter, microns	1750	1080	1100	1630
Atmosphere Temp. ^{0}F	266	266	86	266
Measured half-life from gamma intensity data, sec	48	24	38	41
Measured half-life from overall removal factor, sec	35	32	30	31
Predicted halftime from rigid drop model, sec	415	49	382	173

Sodium Thiosulfate Sprays

One CSE test was conducted in which elemental iodine was scrubbed continuously with sprays containing sodium thiosulfate. In this test[34] iodine release coincided with spray operation, which precluded measurement of a spray λ. However, the results obtained agreed well with a perfect sink drop model[34]. This agreement supports the applicability of the stagnant drop model with $H = 10^5$.

Removal of elemental iodine by a recirculating thiosulfate spray is compared to a 0.05% cut-off limit in Figure 14. The 0.05% cut-off limit computed from Eq. (75)

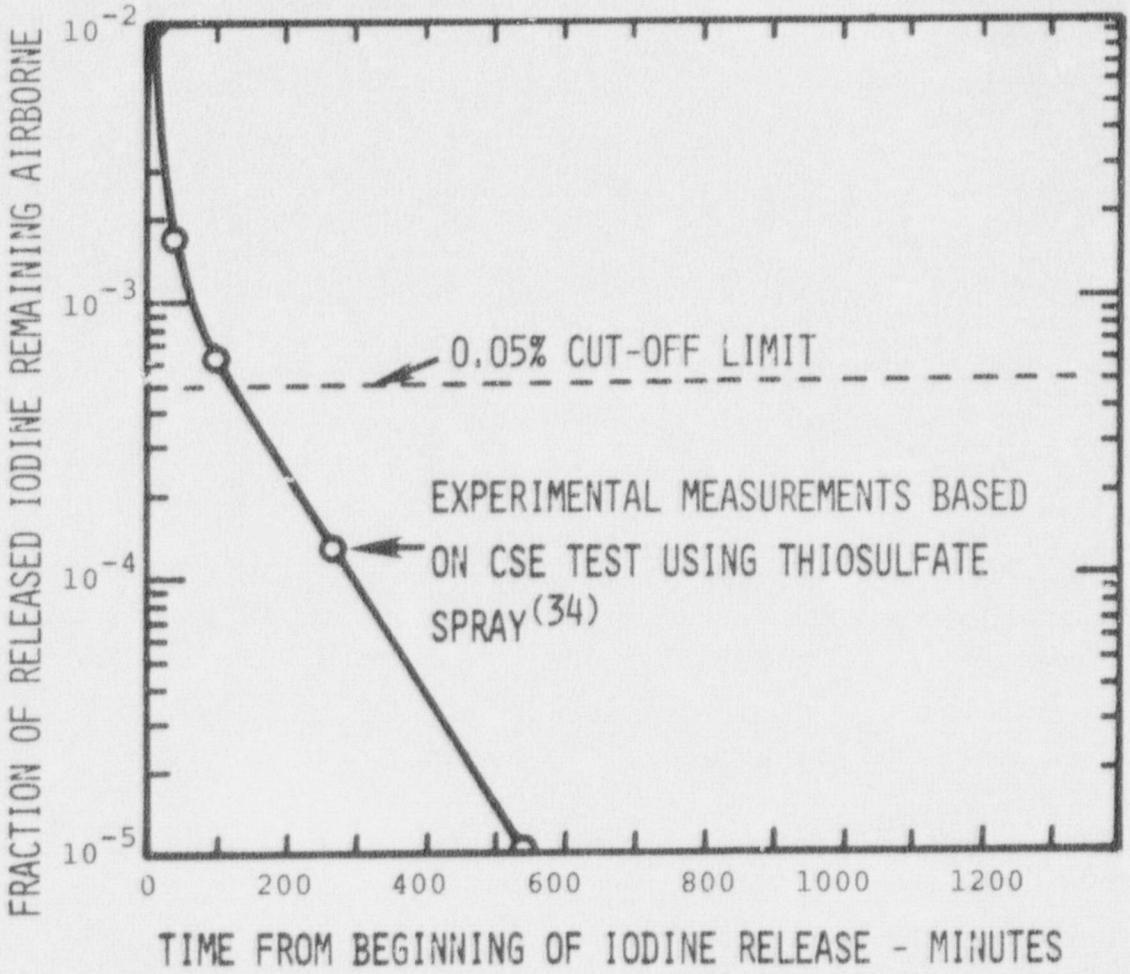

FIGURE 14. Comparison of Model Cut-Off Limit with CSE Test Results for Alkaline Borate Solution Containing 1 wt Percent Sodium Thiosulfate

using $H = 10^5$ will introduce little error for the 2 hr calculational period, but would lead to overpredictions of dose for longer time periods. As noted in Figure 14, elemental iodine concentration was reduced by 5 decades at 550 minutes. Beyond this time the gas phase concentration was too low to be detected.

Some ten spray tests using basic borax solutions containing 0.013 moles per liter of sodium thiosulfate were carried out in the NSPP[11]. Eight of these runs were short in duration and used only fresh spray. Two were longer in duration and involved recirculation of spray solution from the vessel's sump. Analysis of the NSPP tests by others[19] shows that the observed washout rate was from two to ten times faster than predicted by a rigid drop spray model. Thus the NSPP test results support the large scale CSE tests and the conservatism inherent in the stagnant film model described in this report.

6.2 Organic Iodides

6.2.1 Experimental Measurements of Methyl Iodide Absorption

Absorption of methyl iodide from steam-air atmospheres has been measured in a number of studies related to nuclear safety. These studies will be briefly reviewed in the following sections.

Absorption of Methyl Iodide by Hydrazine Sprays

Schwendiman, et al.[37] reported the results of pilot scale tests on absorption of methyl iodide by aqueous sprays containing up to ten weight percent hydrazine. Most tests were carried out in a stainless steel cylinder 4 ft in diameter and 10 ft in height. The methyl iodide removal rate was found to be dependent on the concentration of the hydrazine, on the temperature within the spray vessel, and on the spray flow rate.

Postma[39] reviewed and further analyzed the results obtained by Schwendiman, et al.[37]. Experimental results were classified in three sets. In the first set of experiments the temperatures were initially close to 100°C. No heat was added during the spray period, hence the temperature decreased with time. The second set of experiments consisted of three spray tests carried out at temperatures near 120°C. In two of these runs, once-through spray periods were employed in which the wall film liquid and the liquid collected in the bottom of the chamber were separately analyzed to permit assessment of wall film absorption. The third set of experiments was designed to differentiate between wall film and drop absorption.

Measurements in the first set of experiments were carried out in a stainless steel cylindrical tank 10 ft high and 4 ft in diameter. Spray solution was injected initially free of methyl iodide, and then recirculated for several hours. Results of these tests are summarized in Table 20. Results listed in Table 20 show that the washout rate increases with hydrazine concentration, and with spray flow rate.

TABLE 20. Results of Recirculating Spray Tests of CH_3I Absorption by Hydrazine Sprays[39]

Test No.	Drop Size MMD,* Microns	Liquid Flow Rate, cm^3/sec	Fraction of Liquid Flowing on wall	Initial Gas Temp. ^0C	Initial Hydrazine Conc., wt%	Duration of Run, Minutes	Initial Washout Half-Time Min.
1	280	56.8	0.52	95	4.3	62	82
2	280	56.8	0.52	95	4.3	327	82
3	270	33.4	0.36	93	4.3	354	125
4	280	56.8	0.52	95	16	350	22
5	280	58.0	0.52	95	17	291	21

* MMD= mass median diameter

The second set of experiments was carried out in a spray chamber 3 ft in diameter and 8 ft in height. This vessel permitted tests at higher temperatures. Results of these tests at higher temperature are summarized in Table 21.

TABLE 21. Results of High Temperature Tests on Methyl Iodide Absorption by Hydrazine Spray[39]

Test No.	Drop Size MMD, Microns	Wall Flow Rate, cm^3/sec	Drop Flow Rate, cm^3/sec	Average Temp. ^0C	Initial Hydrazine Conc., wt%	Initial Washout Half-Time Min.
6	340	10.3	26.4	120	8.5	8
8	340	17.0	43.7	119	5.2	9
8	[illegible]	10.6	27.2	123	9.9	7

Comparison of results in Table 21 with results presented in Table 20 shows that the washout rate is appreciably increased when the temperature increases from 100°C to 120°C. Measurements reported by Postma[39], but not reported in Table 21, indicated that wall films were more effective, on a unit volume of liquid basis, than were spray drops.

The third set of experiments reported by Postma[39] were once-through tests in which spray liquid exposed in the spray chamber as a liquid film was kept separate from that exposed as falling drops. These experiments were designed to provide additional information on absorption efficiencies for wall films and spray drops. Results obtained in tests 6, 7, and 8 had shown wall films to be appreciably more effective than spray drops. Results of these four tests are summarized in Table 22.

TABLE 22. Results of Single Pass Absorption Tests Reported by Postma[39]

Test No.	Solution Sprayed	Average Temp. °C	H Measured* Wall Film	H Measured* Drops
9	2.5 wt % N_2H_4	89	6.3	1.1
10	0.64 wt % $Na_2S_2O_3$	88	4.8	1.6
11	4.38 wt % N_2H_4	86	8.6	2.0
12	0.64 wt % $Na_2S_2O_3$	87	4.4	1.2

* $H = \frac{\text{Conc. of } CH_3I \text{ In Liquid}}{\text{Conc. of } CH_3I \text{ In Gas}}$

These results demonstrate the relatively higher effectiveness of absorption by wall films than by spray drops. In order to obtain the overall effectiveness, one would have to multiply the H values by the flow rates.

Postma[39] compared the experimental results with absorption theory and concluded that all 12 runs were well explained by a theory based on absorption by stagnant drops, Eq. (21), and a stagnant wall film, Eq. (29).

Absorption of Methyl Iodide by Sodium Thiosulfate Sprays

Absorption of methyl iodide by sprays containing sodium thiosulfate has been studied at several laboratories in vessels of varying size scale.

Parsly[11] reported the results of spray absorption of methyl iodide in the Nuclear Safety Pilot Plant (NSPP). The principal component of the NSPP is a 1350 ft^3 stainless steel containment vessel. Spray nozzles located near the top of the vessel permitted scrubbing of the containment atmosphere with spray containing 0.28 M H_3BO_3, 0.17 M NaOH, and 0.063 M $Na_2S_2O_3$. Results of tests involving methyl iodide are summarized in Table 23.

The results in Table 23 show several important facts. First, the rate of washout of methyl iodide is much slower than that of elemental iodine. Parsly[11] reported I_2 removal half-times in this vessel near 30 seconds. Second, the removal rate increases with spray flow rate, and with increasing temperature. This same

TABLE 23. Results of Methyl Iodide Removal Experiments in the NSPP[11]

Test Parameter	Run Number 34	35	36	43	44	46	47	49	54	58	65	66	69
Spray Flow, gpm	15	12	12	11	11	11	11	11	11	11	7.1	1.1	14.2
Nozzle Type	1713[a]	1713	1713	7G3[b]	7G3	7G3	7G3	7G3	7G3	7G3	A-8[c]	A-8	A-8
Solution Temp. ^{0}C	30	120	120	30	120	120	120	30	120	120	120	120	120
Initial Vessel Temp. ^{0}C	30	130	130	30	130	130	130	30	130	130	130	130	130
Mean Half-Time For CH_3I Removal, min	107	63	106	long	53	57	61	180	27	49	46	46	26

a - Spray Engineering Co. Cat. 1713 ramp bottom nozzle.
b - Spraying Systems Co. Cat. No. 7G3 cluster.
c - Spraying Systems Co. Cat. No. A-8 whirljet nozzle.

behavior was observed by Postma[39] for hydrazine sprays.

Postma, et al.[68,34] and Hilliard, et al.[52,48] reported results of methyl iodide absorption by sodium thiosulfate sprays in the CSE. Results of five large scale tests are summarized in Table 24. Absorption of CH_3I was predicted on the basis of a model which considered the drops to be perfectly mixed and the wall film to be laminar. Measured and predicted half-times are in good agreement, except for Run A-12(2) where a high wall flow rate was used. For this run, the wall film was highly turbulent, increasing the washout over that for a laminar film. The two most important

conclusions from these results are that wall film absorption appears to be more important than drop absorption, and that the theory predictions are in reasonable agreement with the measurements.

TABLE 24. Removal of Methyl Iodide by Thiosulfate Sprays in CSE[68]

Test Parameter	Run Number A-7	A-8	A-10	A-12(1)	A-12(2)
Spray Duration, min	50	50	240	1270	120
Drop Diameter, microns	1210	770	1210	1210	wall only
Flow Rate, gpm	49.0	50.0	50.0	50.0	50.0
Average Temp. ^{0}F	210	212	246	245	246
Wall Flow Rate, gpm	1.7	3.0	2.3	2.3	50.0
Predicted $t_{\frac{1}{2}}$ for wall film, min	200	180	83	83	382
Predicted $t_{\frac{1}{2}}$ for drops, min	520	340	180	185	---
Predicted Overall $t_{\frac{1}{2}}$, min	145	120	57	57	380
Measured $t_{\frac{1}{2}}$, minutes	130	140	85	80	100

Evaluation of Physical Properties Used In Absorption Models

Evaluation of the washout models described herein required input of several physical properties. Knudsen[42]

provides tabular data for viscosity, diffusivity and other useful properties for steam/air mixtures as functions of temperature. Hasty and Sutter[38], Hasty[69], and Schwendiman, et al.[37,70], summarize available data on the reaction rate constant, k, for methyl iodide reactions in water.

Postma[39] reported measurements of the partition coefficient, H. His results are compared with data of Schwendiman, et al.[37,70] and of Glew[71] in Figure 15.

6.3 Aerosol Particles

6.3.1 Models For Spray Washout

From Eq. (39), the first order spray removal constant, λ_s, may be related to spray and particle parameters by:

$$\lambda_s = \frac{3hFE}{2dV} \tag{76}$$

where λ_s = spray removal constant for particles,
h = drop fall height,
F = spray flow rate,
E = single drop collection efficiency,
d = spray drop diameter,
V = volume of contained gas phase.

The quantities h, F, and V are parameters of the containment system design. The drop diameter, d, is

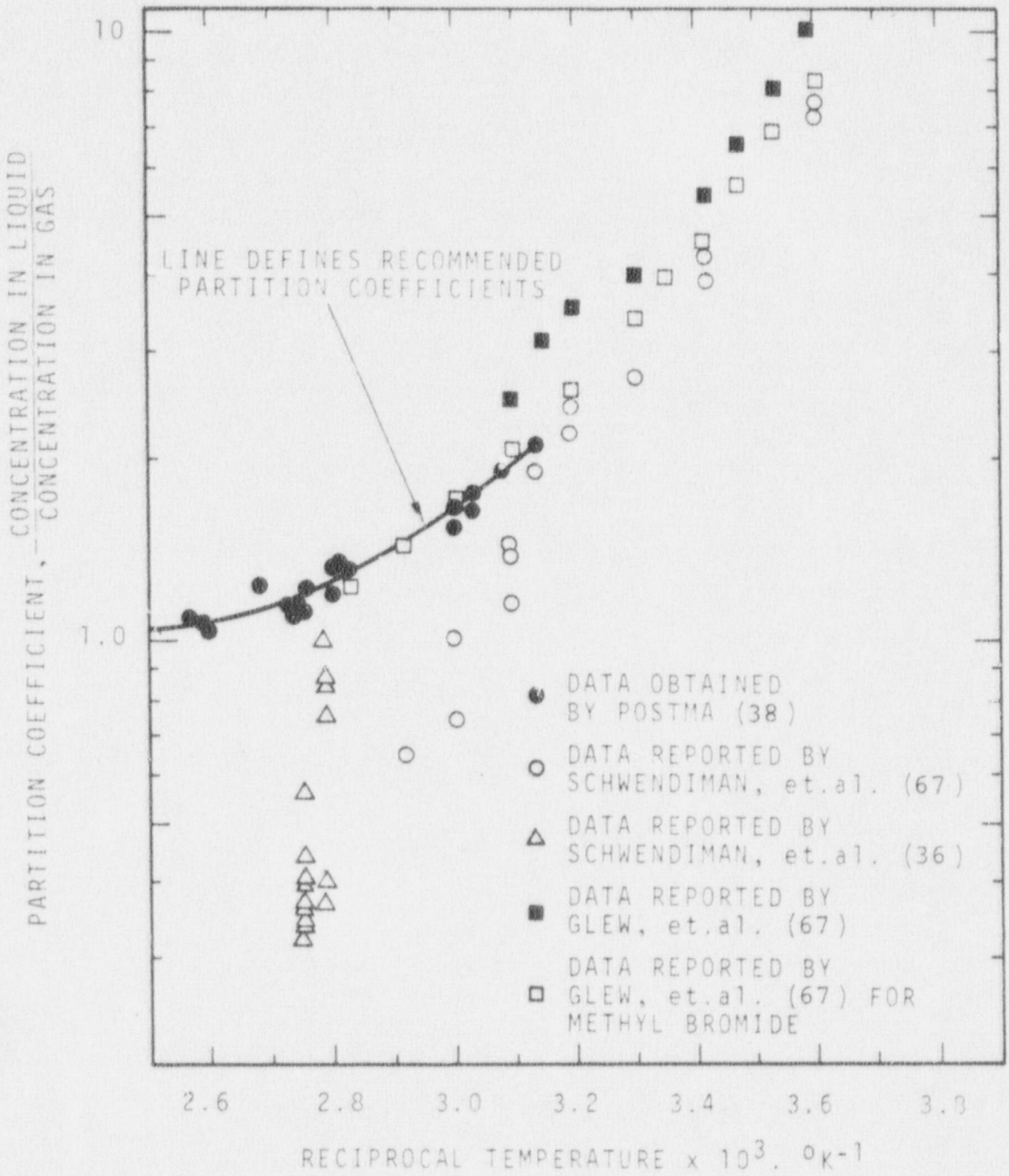

FIGURE 15. Partition Coefficients For Methyl Iodide in Water As Reported by Postma (39)

determined by the spray nozzle design and operating conditions, and is subject to direct experimental measurement. The most difficult-to-determine parameter in Eq. (76) is the single drop collection efficiency, E. Although E is subject to direct experimental measurement, available experimental data are few. Therefore, one must usually rely on numerical values of E for each mechanism operating singly as predicted from available theories. The total E is then obtained as the sum of the E's for each mechanism. Predicted[29] values of E for a 1210 micron diameter drop falling at terminal velocity are shown in Figure 16.

For an aerosol released as a puff at time zero the particle size spectrum would change with time because the particles with the highest E would be preferentially removed. Thus washout calculations must be carried out at a number of time steps, with a new value of E being calculated to account for the new particle size spectrum. E varies with drop diameter; hence one should break the drop size spectrum into a number of increments, and sum the contribution of each increment to obtain the whole spray wahsout rate. It is clear that numerically predicting spray washout of particles can become a complex and time consuming calculational exercise.

The most sophisticated calculational approach used to date, appears to be that presented by Ritzman, et al.[29] These authors modified the HAA-3 aerosol code[41] to account for washout by spray drops. It was found that the modified HAA-3 predictions were in very good agreement with the simpler model given here as Eq. (39). A comparison between Eq. (39) and the modified HAA-3 model is

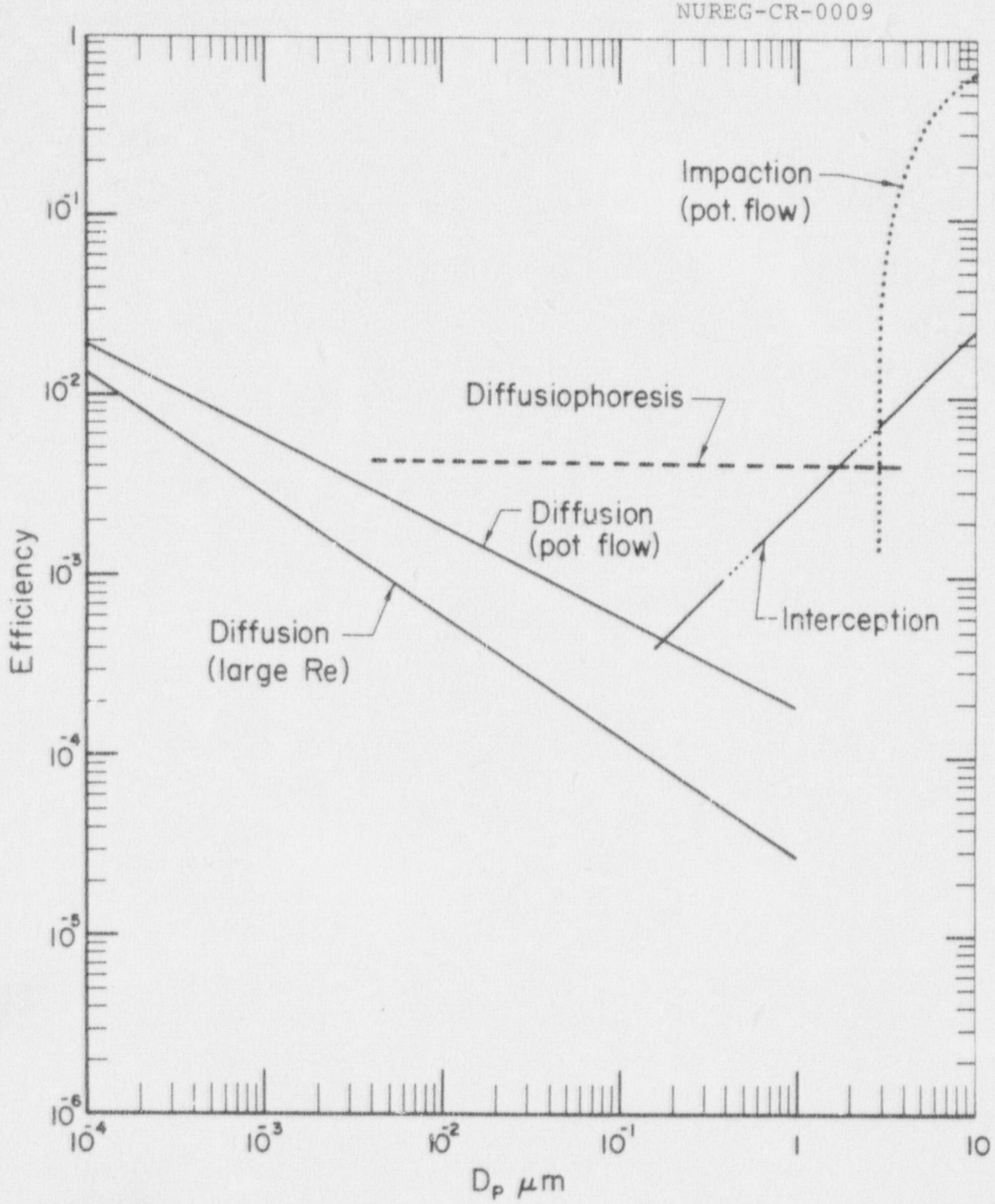

FIGURE 16. Aerosol Collection Efficiency of 1210 μm Drop[29]

shown in Figure 17. The straight lines of Figure 17 are consistent with a constant drop removal efficiency over the time period considered.

While agreement between models is a positive indication, model verification must include agreement between predicted and measured aerosol washout. Hilliard et al.[52] have pointed out that the observed washout rate in CSE tests was consistent with that for particles of 1 to 2 microns in diameter but that measured particle sizes were about 0.4 microns mass median diameter. The discrepancy was explained in terms of evaporation of water from the particles during the sampling process.

For accident conditions, Ritzman, et al.[29] predicted an initial particle size in the containment vessel by estimating the degree of agglomeration of freshly generated aerosol (0.1 μ assumed diameter) in the primary vessel. The predicted particle diameter was 1.43 microns for a case involving release of 1% of fission product mass (called TID by Ritzman[29]). For an accident case involving core meltdown, these authors estimated the initial particle diameter to be 0.8 micron. Since the particle size predicted in this way would depend on the aerosol mass release rate and on the holdup time in the primary vessel, different particle sizes would be obtained for different assumed sources.

Knowledge of the particle size which is correct for accident conditions is extremely important. If the most penetrating size were chosen, the predicted washout rate would be unrealistically low. On the other hand, if the selected particle size were too large, then the predicted spray removal rate would be too high. The importance of

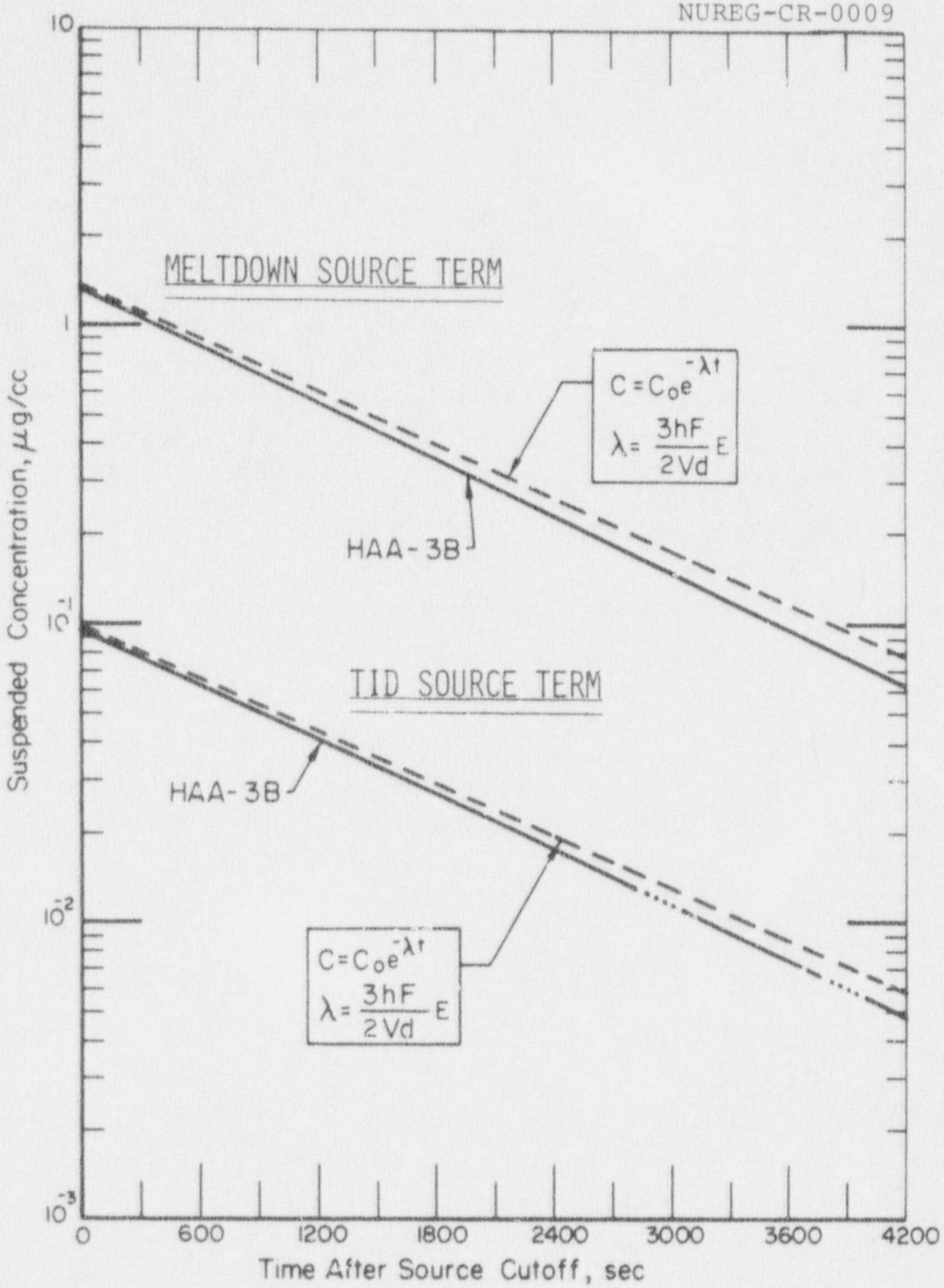

FIGURE 17. Comparison of Modified HAA-3 Model With Exponential Washout Model[29]

selecting the correct particle size is common to all washout models based on single drop collection efficiencies.

6.3.2 Approach Used to Determine Drop Capture Efficiency

After considering alternative approaches, it was determined that the use of experimental washout rate data from large scale tests would provide the firmest basis for arriving at a simple, conservative model for washout of particulate iodine. The use of large scale test data eliminates the need to resolve the following questions:

(1) To what extent is particulate iodine reversibly absorbed by fog drops?
(2) What particle size spectrum should be used for particulate iodine aerosol?
(3) How accurately can the single drop collection efficiency be computed on the basis of assumed drop and aerosol physical parameters?

Remaining factors which must be accounted for in applying test results to full scale containment vessels include the following: (1) diffusiophoretic capture of particles, (2) particle size of test aerosol compared to that in the projected accident environment, and (3) spray drop size distribution. The approach used to handle these factors in the present work is outlined in the following paragraphs.

For particles in the 0.1 micron to 1 micron size range, diffusiophoresis can be an important mechanism. Since diffusiophoresis is present when a cool spray drop enters a hot steam-saturated atmosphere, it would be reasonable to conclude that this mechanism would be as effective under the LOCA as it was in tests. However, this question was made moot in the present work by including in the analyzed data, tests carried out at room temperature and tests using recirculated (hot) spray. For these tests, negligible condensation on the drops occurred, and hence diffusiophoresis was unimportant. Since the value of E was chosen conservatively for all test data, diffusiophoretic effects have been largely neglected. Diffusiophoretic capture which occurred under accident conditions would enhance particle removal beyond that projected on the basis of test data. Thus diffusiophoretic capture is neglected in this work, a conservative simplification.

Aerosols used in CSE tests were produced by vaporizing cesium oxide, uranium oxide, and elemental iodine. The resulting airborne particles were agglomerates made up of submicron primary particles. The aerosol mass concentrations obtained in CSE tests were much lower than those predicted for a LOCA in a PWR containment vessel; thus the agglomerate particle size in CSE tests would be smaller than the size obtained under accident conditions. Since E increases with particle size, the test results would be conservative compared to the LOCA. This argument may not hold for particulate iodine if the iodine is associated with other than solid fission product aerosol. As will be seen, particulate iodine is removed

faster than cesium and uranium aerosols. A conservative estimate was obtained by including data on washout of cesium and uranium aerosols.

Spray drop size would be expected to influence the washout rate because the capture efficiency varies with drop size. Test results could be used directly provided the drop size spectrum were the same in the full sized containment as in the CSE tests. CSE tests used G-3* and A-50* nozzles, which reportedly produced drops having mass median diameters of about 1200 microns[52]. Thus the results obtained in the present study will apply directly to containment systems which use sprays of the size produced by these nozzles. The effect of drop size on aerosol washout rate, and application of the present results to sprays of different drop size are discussed in a later section of this report.

Ideally, test results would be translated to full sized containment sprays through use of the single drop collection efficiency, E. This could be done if the correct average drop size, d, were accurately known. In order to avoid difficulties in defining the correct diameter, the quantity E/d was correlated rather than E itself.

For an aerosol composed of a finite number of size groups, the fraction airborne at time t after a puff release is given by:

$$\frac{C}{C_o} = f_1 e^{-\lambda_1 t} + f_2 e^{-\lambda_2 t} + f_3 e^{-\lambda_3 t} + .. f_n e^{-\lambda_n t} \quad (77)$$

---

* Spraying Systems Co., Bellwood, Illinois

where C = aerosol concentration at time t,

C_o = aerosol concentration at time zero,

f_n = fraction of original aerosol in nth size increment,

$\lambda_n = \frac{3hF}{2V}\left(\frac{E_n}{d}\right)$ = removal rate constant for nth size increment.

The washout of a heterodispersed aerosol is depicted schematically in Figure 18. At time t, the fraction airborne may be computed from Eq. (77), or it may be computed from the average λ by:

$$\frac{C}{C_o} = \exp(-\lambda_{avg}\, t) = \exp - \frac{3hF}{2V} \cdot \left(\frac{E}{d}\right)_{avg} \cdot t \qquad (78)$$

At a particular value of C/C_o, Eq. (78) can be rearranged to give $\frac{3hF}{2V}\, t$ as a function of $(E/d)_{avg}$ and C/C_o:

$$-\frac{3hF}{2V}\, t = \frac{\ln \frac{C}{C_o}}{\left(\frac{E}{d}\right)_{avg}} \qquad (79)$$

When one substitutes Eq. (79) into Eq. (77) the result is:

$$\frac{C}{C_o} = \sum_{n=1}^{n=k} f_n \exp \frac{\ln \frac{C}{C_o}}{\left(\frac{E}{d}\right)_{avg}} \left(\frac{E_n}{d}\right) \qquad (80)$$

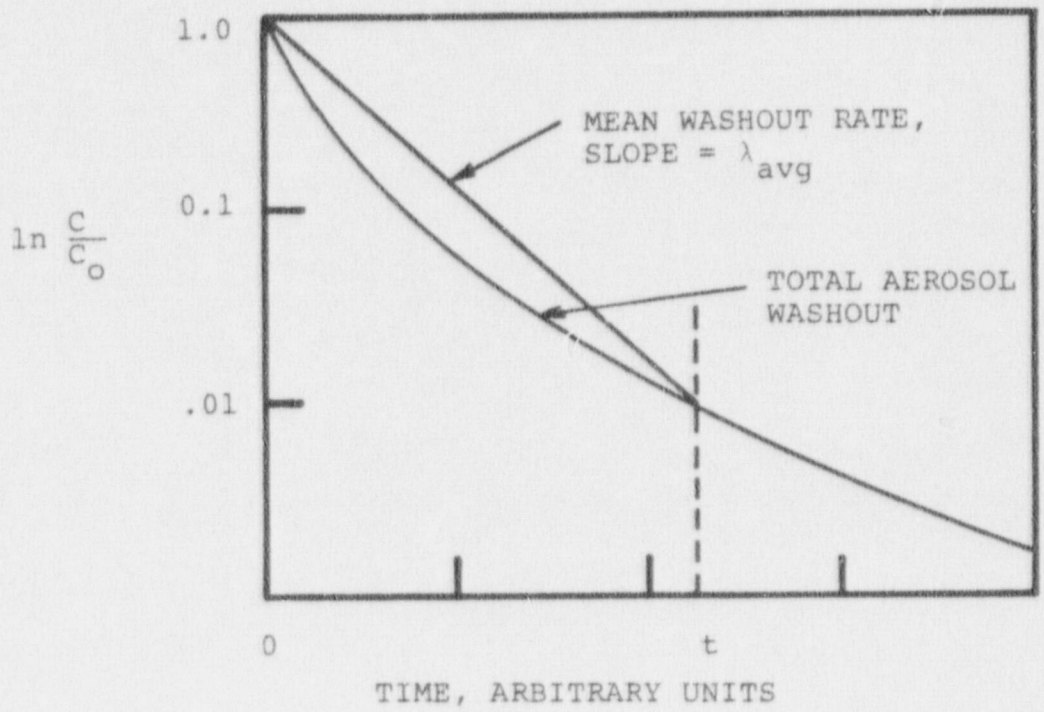

FIGURE 18. Definition of a Mean Washout Lambda

Eq. (80) defines a relationship between $(E/d)_{avg}$ and C/C_c, f_n, and E_n/d. The numerical values of f_n depend only on the particle size distribution. Therefore if it is assumed that the particle size distribution is fixed, f_n becomes a constant in Eq. (80). E_n/d is a parameter

whose numerical value depends on both the particle size distribution and on the spray drop size. If attention is limited to cases for which both the particle size and spray drop size distributions are fixed, this parameter also becomes a constant in Eq. (80). For the present study we will consider only experimental data for which both f_n and E_n/d can be considered constant. Therefore Eq. (80) defines a functional relationship between $(E/d)_{avg}$ and C/C_o. The fact that such a relationship exists is important because it shows that for a given aerosol and spray, $(E/d)_{avg}$ is a function of C/C_o only. Experimental results correlated in this way should be useful in predicting washout in containment vessels.

If one plots experimentally obtained test data as suggested above, the results will be as shown schematically in Figure 19.

Line A in Figure 19 denotes the average value of $(E/d)_{avg}$ for a spraying time corresponding to a C_o/C value of k_1. Line C represents the average $(E/d)_{avg}$ for spraying which begins at a time corresponding to $C_o/C = k_1$ and ends at a time corresponding to $C_o/C = k_2$. Line B represents the average $(E/d)_{avg}$ for spray operation beginning at time zero and ending at a time corresponding to $C_o/C = k_2$. The vertical spacing between lines A, B, and C in Figure 19 depends on the degree of polydispersity of the airborne particles. If the particles were all the same size, the three lines would be co-linear. As the standard deviation of the size distribution increases The vertical spacing between lines A, B, and C would increase because the aerosol remaining airborne at any time

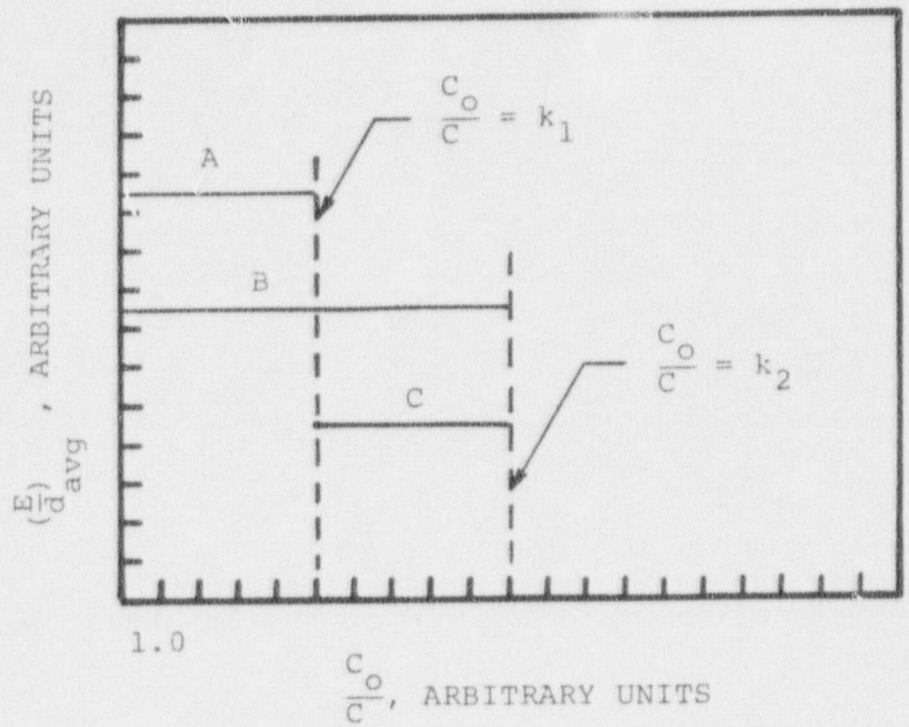

FIGURE 19. Schematic Representation of Average Drop Collection Efficiency Divided by Drop Diameter

would be smaller in size, and less easily removed than the aerosol present at earlier times.

6.3.3 Review of Available Experimental Data

For the present study, data must fulfill several characteristics to be useful. These requirements are:

(1) Spray and vessel parameters including flow rate, fall height, and vessel volume must be known.
(2) Spray drop size must be reasonably close to that generated by the 1713-A spray nozzle.
(3) The particle size distribution must be of a similar magnitude, or smaller, than the size distribution to be encountered under accident conditions.
(4) Experimental data must include spraying times, and C/C_o at the beginning of each spray period, so that an average λ can be computed.

In the search for applicable data we looked at containment research programs carried out in the U.S. and in Europe. As described below, it appears that only the USAEC Containment Systems Experiment Program reported information of direct use.

The Swedish program on spray removal of iodine conducted at Studsvik involved a model containment vessel $2.5 m^3$ in volume[21]. Unfortunately, the tests involved elemental iodine alone, and no effort was made to study either particulate iodine or other fission product aerosols. Therefore, while the iodine washout behavior observed at Studsvik generally supports spray technology it does not provide information of direct use in the present study.

The more recent Swedish study of iodine behavior at the decommissioned Marviken reactor[72] showed effective removal of elemental iodine, but the samplers used did not permit particulate iodine to be separately identified.

Japanese studies, carried out in a vessel 1.5 m diameter by 3 m high[20], were focussed on the behavior of elemental iodine and methyl iodide. No results were reported on particulate iodine or other aerosols.

Italian researchers have studied iodine washout in the PSICO-10 model containment vessel. While most tests dealt with elemental iodine, results for particulate associated iodine (iodine on the particulate filter of the Maypack train) were given for several runs[22]. Results of tests in the 95 m^3 PSICO-10 vessel which yielded data on particulate-associated iodine are summarized in Table 25.

TABLE 25. Particulate Iodine Washout In The PSICO-10 Vessel[22]

Run No.	Spray Period No.	$(\frac{C_o}{C})_{begin}$	$(\frac{C_o}{C})_{end}$	$(\frac{E}{d})_{avg}$
105	1	4.4	7.3	0.087
	2	7.3	25.	0.076
	3	25.	8730.	1.0
107	1	3170.	3.2×10^7	2.0
108	1	1430.	4600.	0.41

Note: For all of above tests, spray flow rate = 80 ℓ/m and fall height = 9 m. The spray nozzle type was described as a "pine cone".

Unfortunately, the Italian report does not include the size of drops produced by the "pine cone" spray nozzle. This lack of a drop size prevents inclusion of the PSICO-10 results with data analyzed in this report.

Work carried out in the Nuclear Safety Pilot Plant (NSPP) at Oak Ridge National Laboratory[11] was directed primarily at removal of elemental iodine and methyl iodide. The gas sampling method used in NSPP tests did not permit the behavior of particulate iodine to be isolated from that of elemental iodine, so no results of direct applicability to the present study can be obtained from NSPP iodine tests. A number of NSPP tests were conducted on spray removal of cesium and uranium aerosols[73]. For these aerosols, it was generally found that initial washout was rapid, and that for longer times, the washout rate slowed. As will be seen later, this behavior is consistent with that observed in CSE tests.

Extensive measurements of spray washout of aerosols were obtained in the CSE program. Results for washout of particulate-associated iodine and for cesium and uranium aerosols are discussed in detail in references 34, 48, and 52. Results of CSE tests on washout of particulate iodine are summarized in Table 26. The data for particulate iodine are shown graphically in Figure 20.

The data plotted in Figure 20 exhibit the anticipated decrease in drop collection efficiency with fractional collection. Based on these data, a conservative estimate of washout could be made by choosing $E/d = 0.3$ cm^{-1} for C_o/C from 1 to 20. For C_o/C values larger than 20, E/d values are larger than 0.05 cm^{-1}.

FIGURE 20. Washout Rate of Particulate Iodine In CSE Tests as Measured by $(E/d)_{avg}$

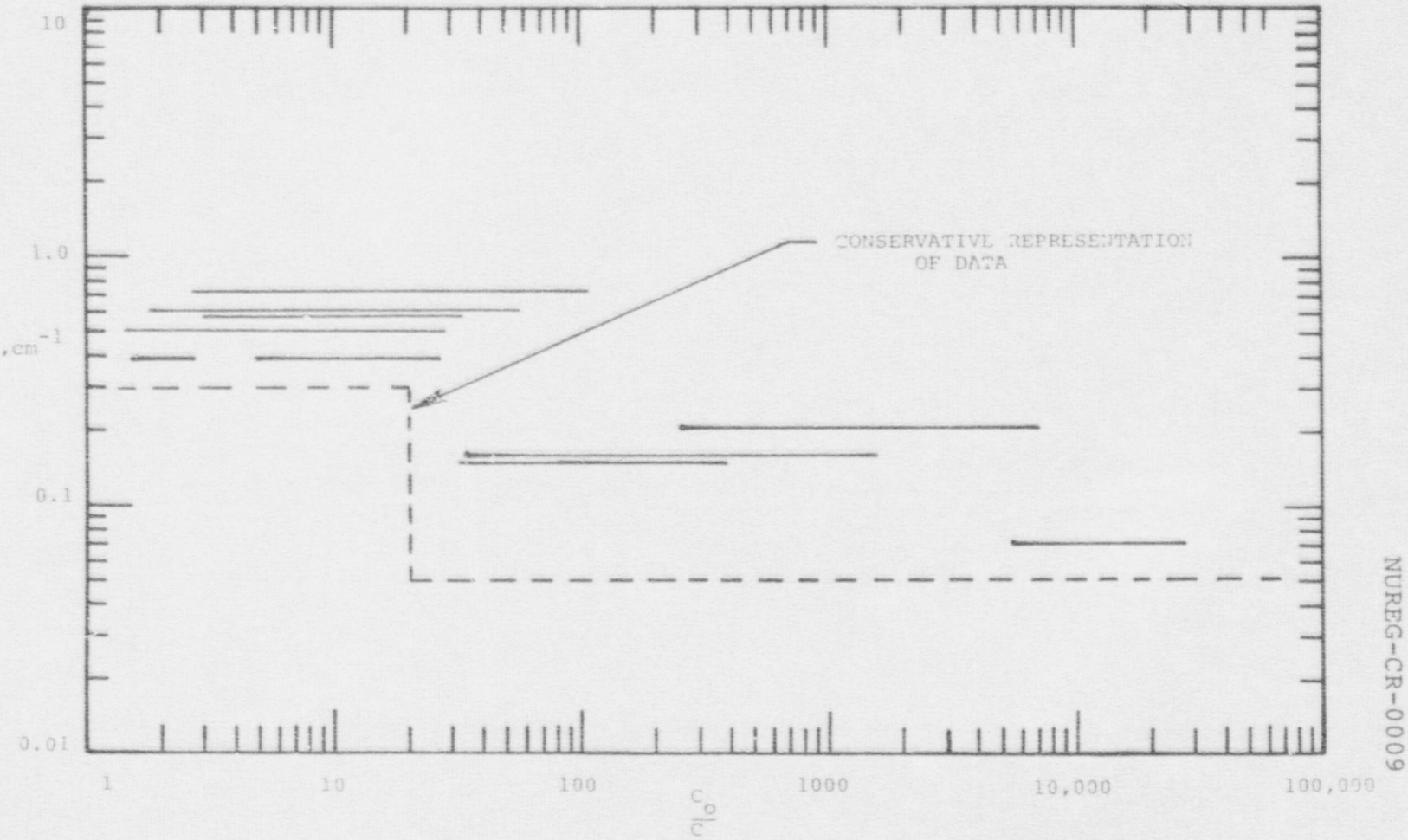

TABLE 26. Particulate Iodine Washout in CSE[48,52]

CSE Test No.	Spray Period No.	Release Conc. $\mu g/M^3$	C_o/C At Start	C_o/C At End	$(E/d)_{avg}$ cm^{-1}
A3	1	3.6×10^3	1.5	2.77	0.39
	2	3.6×10^3	4.8	27.7	0.39
A4	1	4.2×10^3	1.4	28.0	0.51
	2	4.2×10^3	32.3	382	0.15
	3	4.2×10^3	5250.	2.8×10^4	0.07
A6	1	7.0×10^3	1.75	58.3	0.61
	2	7.0×10^3	250.	7000.	0.21
A7	1	1.3×10^4	2.89	33.	0.58
	2	1.3×10^4	33.	1600.	0.16
A9	1	1.5×10^4	2.7	107	0.73

* Release conc. determined by extrapolating measured conc. to time zero.

In order to assure that a conservative estimate of $(E/d)_{avg}$ was arrived at, CSE data for cesium and uranium aerosols were also evaluated. Results of spray washout of cesium aerosols are summarized in Table 27.

The data of Table 27 are shown graphically in Figure 21. The trend toward lower $(E/d)_{avg}$ as fractional washout increases is similar to that seen for particulate iodine in Figure 20. However the drop collection efficiencies are somewhat smaller, demonstrating that the particle size for the cesium aerosol was smaller than that for particulate iodine. A conservative estimate of $(E/d)_{avg}$ based on the cesium data can be obtained by

FIGURE 21. Washout Rate of Cesium Aerosol In CSE Tests as Measured by $(E/d)_{avg}$

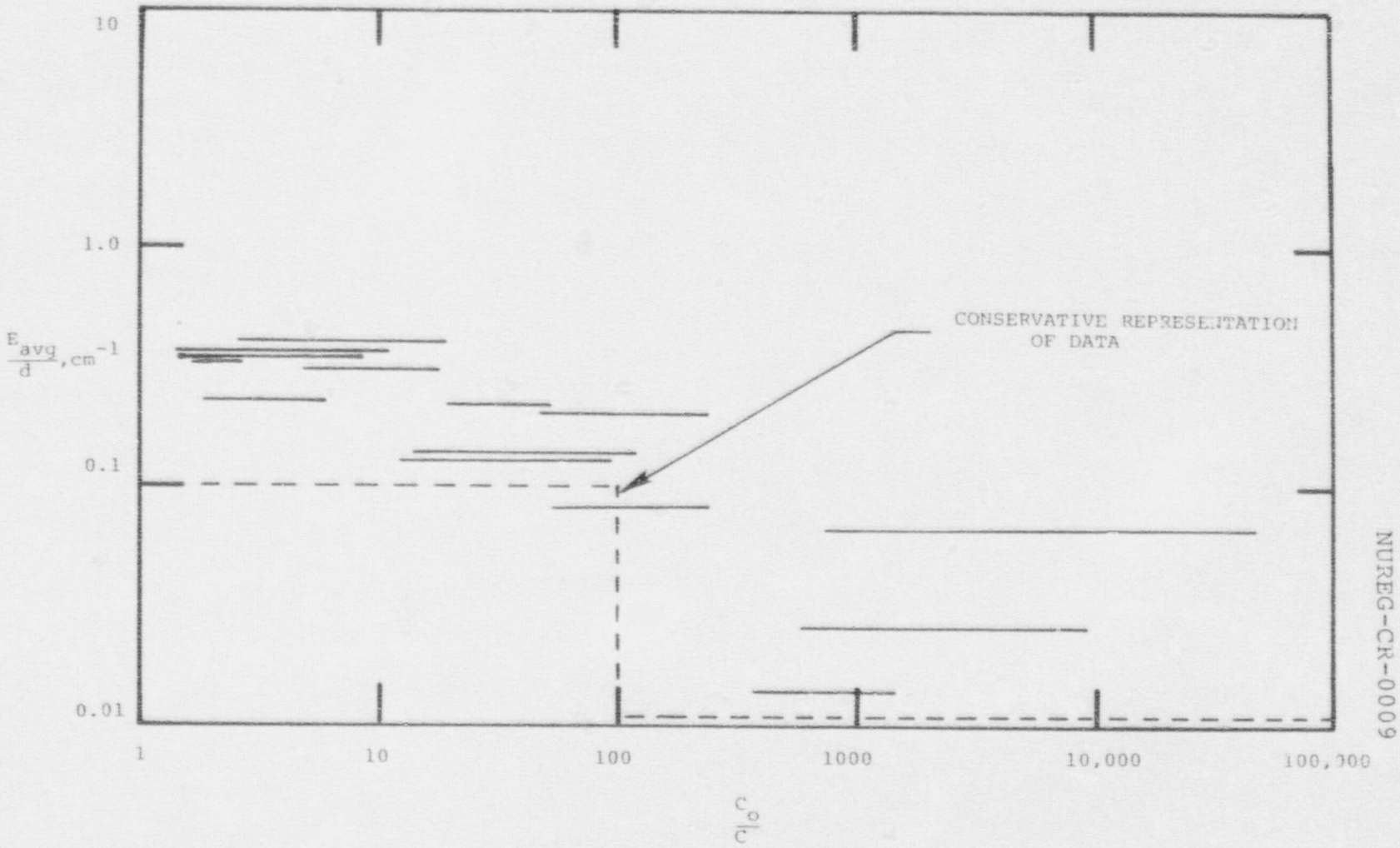

choosing $(E/d)_{avg} = 0.1\ cm^{-1}$ for C_o/C values ranging from 1 to 100. For C_o/C values larger than 100, $(E/d)_{avg}$ values are larger than $0.01\ cm^{-1}$.

TABLE 27. Cesium Aerosol Washout In CSE[48,52]

CSE Test No.	Spray Period No.	Release Conc, $\mu g/M^3$	C_o/C at Start	C_o/C at End	E_{avg}/d, cm^{-1}
A3	1	4800	1.6	2.7	0.33
	2	4800	4.8	18.	0.31
	3	4800	48.	240.	0.20
A4	1	7000	1.4	11.	0.37
	2	7000	14.	120.	0.14
	3	7000	580.	9300.	0.026
A6	1	1800	1.8	6.0	0.23
	2	1800	6.0	33.	0.098
A7	1	2600	1.3	8.7	0.34
	2	2600	12.	93.	0.13
	4	2600	740.	47000.	0.067
A9	1	3000	2.5	18.8	0.411
	2	3000	18.8	51.7	0.22
	3	3000	51.7	250.	0.083
	4	3000	366.	1500.	0.014

Washout measurements were also obtained for uranium aerosols in CSE, and the resulting data are summarized in Table 28. The data for uranium oxide aerosol washout are shown graphically in Figure 22.

FIGURE 22. Washout Rate of Uranium Oxide Aerosol in CSE Tests As Measured by $(E/d)_{avg}$

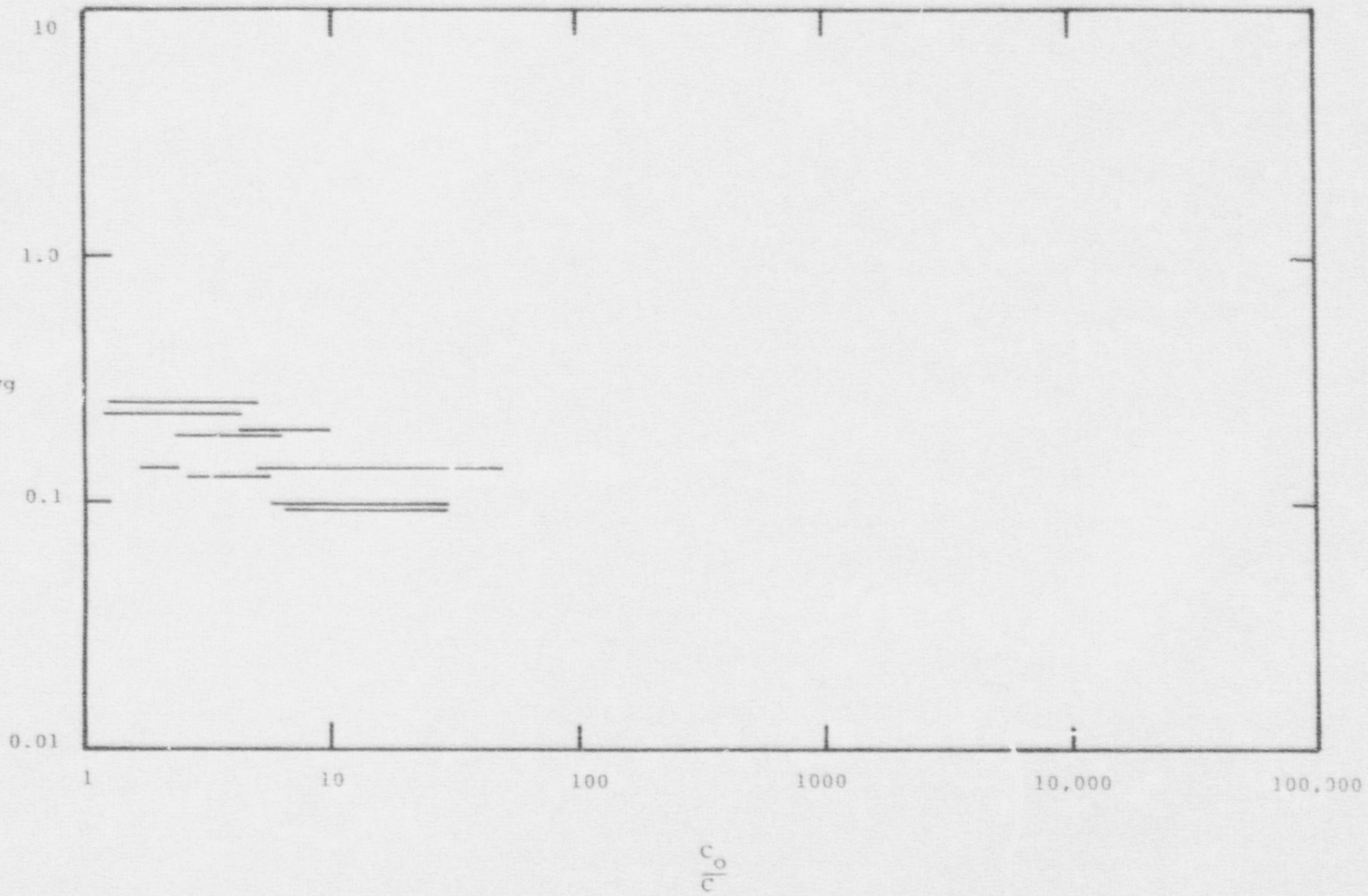

TABLE 28. Uranium Oxide Aerosol Washout in CSE[48,52]

CSE Test No.	Spray Period No.	Release Conc, $\mu g/M^3$	C_o/C at Start	C_o/C at End	E_{avg} / d, cm^{-1}
A3	1	12000	1.7	2.4	0.14
	2	12000	4.3	10.	0.20
A4	1	13000	1.2	4.3	0.23
	2	13000	6.5	28.9	0.095
A6	1	1800	2.6	5.6	0.13
	2	1800	5.6	29.	0.10
A7	1	2500	1.25	5.0	0.26
	2	2500	5.0	50.	0.14
A9	1	500	2.3	6.3	0.19

The measured $(E/d)_{avg}$ values for uranium oxide aerosol are consistent with data obtained for cesium aerosol. The detection sensitivity for uranium was much lower than for cesium and iodine, and as a result the washout of uranium could not be followed as long as for the other aerosols. The few uranium data available can be conservatively represented by the lower limit line shown on Figure 21 for cesium aerosol.

From this review of available large scale test results on aerosol washout, a conservative estimation of particulate iodine washout can be obtained by choosing $(E/d)_{avg} = 0.1$ for C/C_o values from 1 to 0.01, and 0.01 for C/C_o values smaller than 0.01.

6.3.4 Effect of Spray Drop Size

The results given above apply to spray systems which produce the same drop size distribution as was used in CSE tests. The effect of small changes in drop size distribution can be estimated using the theoretically predicted variation in E with drop size. A method for applying the present results to a different size distribution will be outlined in the following paragraphs.

The mass median diameter of containment spray drops is in the neighborhood of 0.1 cm. Therefore the E values (corresponding to $(E/d)_{avg}$ values of 0.1 and 0.01) attributed to sprays in this study fall in the approximate range of 0.01 to 0.001. From the theoretical predictions shown in Figure 16, the potentially controlling mechanisms include diffusiophoresis and interception. Diffusion is eliminated because the aerosol particle diameter in containment vessels is greater than 0.01μ. Diffusiophoresis was also eliminated as a contributing mechanism by the conservative method used to select $(E/d)_{avg}$ from the test data. As noted earlier $(E/d)_{avg}$ was chosen conservatively from data which included tests using recirculated hot spray. For such spray no condensation on drops would occur, eliminating diffusiophoresis. Therefore for the conservative $(E/d)_{avg}$ values identified here, interception is necessarily the dominant capture mechanism.

For interception, the capture efficiency varies inversely with the particle size[29]:

$$E = k \frac{D_p}{d} \qquad (82)$$

where E = target efficiency for interception,
D_p = aerosol particle diameter,
d = drop diameter,
k = a constant.

If both sides of Eq. (82) are divided by d, and if kD_p is redefined as a new k, the result is:

$$\frac{E}{d} = \frac{k}{d^2} \tag{83}$$

The overall E/d for a spray can be obtained by summing E/d for each drop size increment:

$$\left(\frac{E}{d}\right)_{avg} = k \left[\frac{f_1}{d_1^2} + \frac{f_2}{d_2^2} + \frac{f_3}{d_3^2} + \ldots \frac{f_n}{d_n^2} \right] \tag{84}$$

where f_n = fraction of spray in nth size increment,
d_n = average diameter of drops in nth size increment.

Values of k in Eq. (84) could be obtained by choosing f_n values which apply to CSE test sprays, and by setting $(E/d)_{avg}$ equal to 0.1 and 0.01. Use of these two k values with f_n values for a different spray would allow new values of $(E/d)_{avg}$ to be computed. The particle washout rate for the new spray could then be computed using Eq. (78).

Many existing PWR containments employ the 1713** nozzle which appears to produce a drop size spectrum

** Spray Engineering Co., Burlington, Massachusetts

similar to those of the G-3* and A-50* nozzles. Equivalency of drop size for iodine absorption was demonstrated in sequential tests which employed G-3 and 1713-A nozzles[17]. The removal rate was similar for the two tests[17]. Based on this evidence it is likely that the E/d values obtained from CSE tests can be used for containment vessels using 1713-A spray nozzles operating at 40 psid.

7.0 SUMMARY AND CONCLUSIONS

This report is a review of spray washout in the containment vessels of light water reactors. Spray systems may be included in containment vessels as an engineered safety feature to suppress pressure and scrub airborne contaminants in the unlikely event of a loss-of-coolant-accident. The efficacy of spray scrubbing is important in the siting of power reactors because the spray removal rate directly affects the calculated radiation dose from the design basis LOCA received by people in the plant environs.

A large body of information is available to aid in the assessment of spray performance. In this report the most relevant work is reviewed to show the technical basis for the spray models which are currently used by the NRC staff to make conservative predictions of washout under postulated accident conditions.

Specific conclusions and summary statements which are supported by this study are listed as follows.

---

* Spraying Systems Co., Bellwood, Illinois

1. Mathematical models are available to conservatively predict washout for the several physicochemical forms of iodine.
2. For elemental iodine, the most abundant airborne iodine species, a stagnant film model has been adopted by the staff. This model is a simplified form of the equation for absorption by a rigid sphere accounting for mass transfer resistance in both the gas and liquid phase.
3. Absorption of methyl iodide, the most persistant iodine form expected to be present in post-accident atmospheres, is predicted by a model in which it is assumed that both falling drops and wall films are stagnant. For most spray solutions methyl iodide absorption is too slow to appreciably affect two hour dose calculations.
4. Aerosol particle washout is predicted using a simple model in which conservative estimates of the single drop collection efficiency are obtained from large scale experiments.
5. The composition of spray solutions plays an importnat role in the absorption rate of elemental iodine because the numerical value of the partition coefficient applicable to spray washout depends on solution reactions. Experimentally derived partition coefficients are available for plain boric acid, for sodium hydroxide solutions, for trace level hydrazine solutions, and for solutions of sodium thiosulfate.
6. Methyl iodide is absorbed only slowly by spray solutions which do not contain special additives.

Of the spray solutions currently in use, only sodium thiosulfate at 1 wt. percent enhances the absorption rate to an appreciable extent. For the thiosulfate solution, absorption by wall liquid films is typically more important than that by falling spray drops.

7. Surface deposition of elemental iodine can be predicted using a model in which it is assumed that the limiting transfer resistance resides in the gas phase boundary layer. Predicted surface deposition rates are small compared to spray washout rates.
8. Spray absorption has been studied for many years in many countries. Based on the results of theoretical studies and experiments of many size scales, the models adopted by the staff are supported by firm technical bases.

8.0 LITERATURE CITED

1. Regulatory Guide 1.3, Revision 2, "Assumptions Used for Evaluating the Potential Radiological Consequences of a Loss of Coolant Accident for Boiling Water Reactors," USAEC Directorate of Regulatory Standards, June 1974.

2. Regulatory Guide 1.4, Revision 2, "Assumptions Used for Evaluating the Potential Radiological Consequences of a Loss of Coolant Accident for Pressurized Water Reactors," USAEC Directorate of Regulatory Standards, June 1974.

3. "Indian Point Nuclear Generating Station Unit No.2 Preliminary Safety Analysis Report," Consolidated Edison Company of New York, Inc., Vol. III, Docket No. 50-247, 1965.

4. "Zion Station, Preliminary Safety Analysis Report." Commonwealth Edison Company, Vols. I and II, Docket No. 50-295, June 1967.

5. "Three Mile Island Nuclear Station Unit No. I, Preliminary Safety Analysis Report," Metropolitan Edison Company, Vols, I, II and III, Docket No. 50-289, May 1967.

6. "Diablo Canyon Preliminary Safety Analysis Report," Pacific Gas and Electric Company, Vols. I and II, Docket No. 50-275, January 1967.

7. Norman, W.S., "Absorption, Distillation and Cooling Towers," Longmans, Greene and Company, London, 1961.

8. Bird, R.B., Stewart, W.E. and Lightfoot, E.N., "Transport Phenomena," John Wiley and Sons, Inc., New York, 1966.

9. Sherwood, T.K. and Pigford, R.L., "Absorption and Extraction." Second Edition, McGraw-Hill Book Company, Inc., New York, 1952.

10. Hobler, T. "Mass Transfer and Absorbers" Pergamon Press, New York, 1966.

11. Parsly, L.F. "Spray Program at the Nuclear Safety Pilot Plant" Nuclear Technology, 10, pp. 472-485 (1971).

12. Zittel, H.E. and T.H. Row "Radiation and Thermal Stability of Spray Solutions" Nuclear Technology, 10, pp. 436-443 (1971).

13. Soldano, B.A. and W.T. Ward. "A Study of the Absorption of CH_3I by Aqueous Spray Solutions" Nuclear Technology, 10, pp. 460-465 (1971).

14. Hilliard, R.K., A.K. Postma, J.D. McCormack, and L.F. Coleman. "Removal of Iodine and Particles by Sprays in the Containment Systems Experiment" Nuclear Technology, 10, pp. 499-519 (1971).

15. J.L. Gallagher, L.D. Green, and R.T. Marchese. "Design of Spray Additive Systems" Nuclear Technology, 10, pp. 406-411 (1971).

16. Joyce, W.E. "Sodium Thiosulfate Spray System for Radioiodine Removal" Nuclear Technology, 10, pp. 444-448 (1971).

17. Reid, D.L., B.M. Johnson, and A.K. Postma. "Research on Removal of Iodine by Containment Sprays Containing Trace Levels of Hydrazine" Battelle Pacific Northwest Laboratories, Richland, Washington, June 1974.

18. Postma, A.K., L.F. Coleman, and R.K. Hilliard. "Iodine Removal From Containment Atmospheres by Boric Acid Spray" Report BNP-100, Battelle Pacific Northwest Laboratories, Richland, Washington, July 1970.

19. Babcock and Wilcox Company. "Effectiveness of Sodium Thiosulfate Sprays for Iodine Removal" Topical Report BAW-10024, Babcock and Wilcox Corp., Lynchberg, Virginia 1971.

20. Nishizawa, Y., S. Oshima, and T. Maekawa. "Removal of Iodine From Atmosphere by Sprays" Nuclear Technology, 10, pp. 486-488 (1971).

21. Devell, L., R. Hesbol, and E. Bachofner "Studies on Iodine Trapping by Water Systems at Studsvik" Nuclear Technology, 10, pp. 466-473 (1971).

22. Barsali, L., et al. "Removal of Iodine by Sprays in the PSICO 10 Model Containment Vessel" Nuclear Technology, 23, pp. 146-156 (1974).

23. Eggleton, A.E.J., D.H.F. Atkins. "The Identification of Trace Quantities of Radioactive Iodine Compounds by Gas-Chromatographic and Effusion Methods," Radiochem. Acta., 3(3), pp. 151-158 (1964).

24. Ranz, W.E., and W.R. Marshall, Jr. "Evaporation from Drops, Parts I and II" Chemical Engineering Progress, 48, pp. 141-146 and pp. 173-180 (1952).

25. Frossling, N., Gerlands Beitr. Geophys., 52, p. 170 (1938), as referenced by R.B. Bird, W.E. Stewart, and E.N. Lightfoot, Transport Phenomena. John Wiley and Sons Inc., New York, 1960, p. 409.

26. Griffiths, V., "The Removal of Iodine from the Atmosphere by Sprays" AHSB(S)R 45, UKAEA, Authority and Safety Branch, Risley, Lancs, England, January, 1963.

27. Dankwerts, P.V., "Absorption by Simultaneous Diffusion and Chemical Reaction into Particles of Various Shapes and into Falling Drops", Trans. Faraday Soc., 47, pp. 1014-1023 (1951).

28. Postma, A.K., and W.F. Pasedag. "A Review of Mathematical Models for Predicting Spray Removal of Fission Products in Reactor Containment Vessels" WASH-1329, U.S. Atomic Energy Commission, Washington, D.C., 20545, June 1974.

29. Postma, A.K., R.L. Ritzman, J.A. Gieseke, and E. W. Schmidt. "Models for Predicting the Removal of Airborne Contaminants by Reactor Containment Sprays" BNWL-B-417, Battelle Pacific Northwest Laboratories, Richland, Washington, 1975.

30. Knudsen, J.G., and R.K. Hilliard. "Fission Product Transport by Natural Processes in Containment Vessels" BNWL-943, Battelle Pacific Northwest Laboratories, Richland, Washington, 1969.

31. Yuill, W.A., Jr., and V.F. Baston. "A Model for Fission Product Deposition Under Natural-Response Conditions in Containment Buildings" Nuclear Safety, 10, pp. 492-498 (1969).

32. Hilliard, R.K., and L.F. Coleman. "Natural Transport Effects on Fission Product Behavior In the Containment Systems Experiment", BNWL-1457, Battelle Pacific Northwest Laboratories, Richland, Washington, June 1973.

33. Postma, A.K., "Absorption of Iodine From Containment Vessel Atmospheres by Boric Acid Spray Containing Trace Level Chemical Additives: Final Report on Work Performed Contract 212B00621 with Consumers Power Co. Battelle Pacific Northwest Laboratory, Richland, Washington, April 1972.

34. Postma, A.K., and L.F. Coleman. "Effect of Continuous Spray Operation on the Removal of Aerosols and Gases in the Containment Systems Experiment" BNWL-1485, Battelle Pacific Northwest Laboratories, Richland, Washington, 1970.

35. Danckwerts, P.V., "Absorption by Simultaneous Diffusion and Chemical Reaction" Trans. Faraday Soc., 46, pp. 300-305 (1951).

36. Lynn, S., J.R. Straatemeier and H. Kramers. "Absorption Studies in the Light of the Penetration Theory", Chem. Engr. Sci., 4, pp. 49-57 (1955).

37. Schwendiman, L.C., R.A. Hasty, and A.K. Postma, "The Washout of Methyl Iodide by Hydrazine Sprays--Final Report" BNWL-935, Battelle Pacific Northwest Laboratories, Richland, Washington, 1968.

38. Hasty, R.A., and S.L. Sutter. "The Kinetics of the Reaction of Methyl Iodide with Sulfite and Thiosulphate in Aqueous Solutions", Canadian J. of Chem. 7, pp. 437-451 (1969).

39. Postma, A.K., "Absorption of Methyl Iodide by Aqueous Hydrazine Solttions Within Spray Chambers" Ph.D. Thesis in Chemical Engineering, Oregon State University, Corvallis, Oregon, 1970.

40. Postma, A.K., "Removal of Iodine Aerosol by Containment Sprays" BCT-101, Benton City Technology, Benton City, Washington, November, 1976.

41. Hubner, R.S., E.V. Vaughn, and L. Baurmash. "HAA-3 User Report", AI-AEC-13038, Atomics International, Canago Park, California, 1973.

42. Knudsen, J.G., "Properties of Air-Steam Mixtures Containing Small Amounts of Iodine", BNWL-1326, Battelle Pacific Northwest Laboratories, Richland, Washington, 1970.

43. Eggleton, A.E.J., "A Theoretical Examination of Iodine-Water Partition Coefficients" AERE-R-4887, Harwell, England, 1967.

44. Coleman, L.F., "Iodine Gas-Liquid Partition", Nuclear Safety Quarterly Report, February, March, April, 1970, BNWL-1315-2, Battelle-Northwest, Richland, Washington, pp. 2.12-2.19 (1970).

45. Ritzman, R.L., et al. "Release of Radioactivity in Reactor Accidents", Appendix VII of the Reactor Safety Study, WASH-1400 (DRAFT), U.S. Atomic Energy Commission, Washington, D.C., August, 1974.

46. Pasedag, W.F., and J.L. Gallagher. "Drop Size Distribution and Spray Effectiveness", Nuclear Technology, 10, p. 412, (1971).

47. "A Description of SPIRT, A Code for Calculating Fission Product Removal by Sprays", Memorandum from B.K. Grimes to J.M. Hendrie, August 30, 1973, Directorate of Licensing, USAEC, Washington, D.C.

48. Hilliard, R.K., and A.K. Postma. "The Effect of Spray Flow Rate On The Washout of Gases and Particulates In the Containment Systems Experiment", BNWL-1591, Battelle-Northwest, Richland, Washington, 1971.

49. Bird, R.B., W.E. Stewart, and E.N. Lightfoot. Transport Phenomena, Chapter 21, John Wiley and Sons, New York, (1960).

50. Perry, J.H., Chemical Engineer's Handbook, Third Edition, pp. 546, McGraw-Hill Book Co., New York, (1950).

51. Sen Gupta, K.K., and S.K. Gen Gupta, "Kinetics of Reaction Between Hydrazine and Iodine Solution" Z. fur Phys. Chemie Neue Folge, Bd. 45, S. 378-382, 1965.

52. Hilliard, R.K., et al. "Removal of Iodine and Particles from Containment Atmospheres by Sprays--Containment Systems Experiment Interium Report", BNWL-1244, Battelle Northwest, Richland, Washington, 1970.

53. Postma, A.K., and R.W. Zavadoski. "Review of Organic Iodide Formation Under Accident Conditions in Water-Cooled Reactors" WASH-1233, U.S. Atomic Energy Commission, Washington, D.C., October 1972.

54. Rosenberg, H.S., J.M. Genco, and D.L. Morrison. "Fission Product Deposition and Its Enhancement Under Reactor Accident Conditions" Deposition on Containment-System Surfaces", BMI-1865, Battelle Memorial Institute, Columbus, Ohio, May 1969.

55. Croft, S.F., R.S. Isles, and R.E. Davis. "Experiments on the Surface Deposition of Airborne Iodine of High Concentration" AEEW-R-265, UKAEA, Winfrith, England, June 1963.

56. Parker, G.W., G.E. Creek, and W.J. Marten, "Fission Product Transport and Behavior in the Stainless Steel Lined Containment Research Installation (CRI)", ORNL-4502, Oak Ridge National Laboratory, Oak Ridge, Tenn., February 1971.

57. Nebeker, R.L., et al. "Containment Behavior of Xenon and Iodine Under Simulated Loss-of-Coolant Conditions in the Contamination-Decontamination Experiment" IN-1394, Idaho Nuclear Corp, Idaho Falls, Idaho, June 1971.

58. Freeby, W.A., L.T. Lakey, and D.E. Black. "Fission Product Behavior Under Simulated Loss-of-Coolant Accident Conditions in the Contamination-Decontamination Experiment", IN-1172, Idaho Nuclear Corp. Idaho Falls, Idaho, January 1969.

59. Cottrell, W.B., "ORNL Nuclear Safety Research and Development Program Bimonthly Report for September-October 1970" ORNL-TM-3213, pp. 125-130, Oak Ridge National Laboratory, Oak Ridge, Tennessee, January 1971.

60. Hilliard, R.K. et al. "Comparisons of the Containment Behavior of a Simulant with Fission Products Released from Irradiated UO_2", BNWL-581, Battelle-Northwest, Richland, Washington, March 1968.

61. Croft, S.F., and R.S. Isles. "Experimental Release of Radioiodine in the Zenith Reactor Containment", AEEW-R-172, UKAEA Atomic Energy Establishment, Winfrith, England, September 1962.

62. Stinchcombe, R.A., and P. Goldsmith. "Removal of Iodine from the Atmosphere by Condensing Steam" J. Nuc. Energy, Parts A/B 20, pp. 261-275, 1966.

63. Ozisik, M.N., and D. Hughes. "Effects of Condensation on the Transport of Matter from Vapor and Noncondensible Gas Mixtures", Nucl. Sci. Engr., 35, pp. 384-393, 1969.

64. Watson, G.M., R.B. Perez, and M.H. Fontana. "Effects of Containment System Size on Fission Product Behavior, ORNL-4033, Oak Ridge National Laboratory, Oak Ridge, Tennessee, January 1967.

65. Bird, R.B., W.E. Stewart, and E.L. Lightfoot. Transport Phenomena, pp. 668-672, John Wiley and Sons. Inc., New York, New York, 1960.

66. Schmidt, E., and W. Beckmann. Tech. Mech. U. Thermodynam., 1, pp. 341, 391. (9130).

67. McCormack, J.D., R.K. Hilliard, and A.K. Postma, "Removal of Airborne Fission Products by Recirculating Filter Systems In the Containment Systems Experiment", BNWL-1587, Battelle Pacific Northwest Laboratories, Richland, Washington, June, 1971.

68. Postma, A.K., and R.K. Hilliard. "Absorption of Methyl Iodide by Sodium Thiosulfate Sprays", American Nuclear Soc. Trans, 12, p. 484, November 1969.

69. Hasty, R.A., "The Rate of Reaction of Methyl Iodide and Hydrazine in Aqueous Solution" Journal of Physical Chemistry, Volume 73, No. 2, February 1969.

70. Schwendiman, L.C., et al. "The Washout of Methyl Iodide by Hydrazine Spray" BNWL-530, Battelle-Northwest, Richland, Washington, 1967.

71. Glew, D.N., and E.A. Moelwyn-Hughes. "Chemical Statics of the Methyl Halides in Water" Discussions of Faraday Soc., 15, pp. 150-161, 1953.

72. "Behavior of Iodine in the Containment During the Blowdown Runs, Results" MXA-3-201, The Marviken Full Scale Containment Experiments, Sweden (1973).

73. Parsly, L.F., "Removal of Radioactive Particles by Sprays" ORNL-4671, Oak Ridge National Laboratory, Oak Ridge, Tennessee (1971).

APPENDIX A

A DESCRIPTION OF THE SPIRT COMPUTER PROGRAM

SPIRT

(A Program for the Calculation of Spray Iodine Removal Transients)

1. Purpose

The SPIRT code is intended for the calculation of iodine removal constants (lambdas) for post-LOCA containment spray systems. The code was written to permit the evaluation of the following effects encountered in the analysis of spray systems:

a. effect of the spectrum of drop sizes emitted by the spray nozzles, as opposed to the single drop size used in hand calculations.

b. effect of drop coalescence (which cannot be determined by hand calculation).

c. the precise solution of the time dependent diffusion equation.

2. Mathematical Models

The mathematical models used to achieve this purpose may be summarized as follows:

a. Drop Size Spectrum

The spectrum of drop sizes emitted from the spray nozzles is represented as a two-parameter log-normal distribution function. The parameters for this statistical distribution, i.e., geometric mean and standard deviation, are supplied as input. In the code this distribution is represented by a finite number of discrete drop size groups. All calculations involving drop size are then repeated for each drop size group.

b. Coalescence Calculations

The coalescence calculations are based on the assumption that each drop collision results in a coalescence. The number of drop collisions are derived from geometrical considerations which are based on an assumed maximum entropy spatial distribution of all drop sizes.

c. Solution of Diffusion Equation

The time-dependent diffusion equation is solved for each of the drop size groups in the distribution. The first twenty terms of the infinite series solution of Dankwerts are used.

In addition to these models several auxiliary routines are used in the program to obtain the thermodynamic and diffusion characteristics of the main constituents of interest in the post-accident containment, i.e., steam, air, water, and iodine. The two main sources for these auxiliary models are:

L. F. Parsly, ORNL-TM-1911, Oak Ridge National Lab., 1967

J. H. Perry, Ed., Chemical Engineers Handbook, 4th Ed., McGraw-Hill, 1963

3. Programming

The SPIRT code does not use any numerical routines, with the exception of a simple bisection routine used to determine the roots of a transcendental function used in the solution of the diffusion equation. Instead, explicit functions are used to describe the main variables.

The principal advantage of the SPIRT program lies in the capability it affords for repeated solution of these explicit functions for the large number of drop sizes normally present in a typical drop size distribution. The program is written in FORTRAN-IV (level G) for the IBM 360 computer. An effort was made to use only standard ANSI syntax, to facilitate the use of the program with a variety of digital computers. The FORTRAN listing is attached.

SPIRT INPUT FORMAT

Card number and format	Parameter	Unit	Remarks
1 20A4	TITLE(I)	-	-
2 6I3	NGRP	-	Numbers of groups of drop sizes to be used in calculation.
	NTYPE	-	There are two ways to read in drop size distribution. Either by reading in actual distribution, or by reading in a geometric mean and standard deviation, and ask the computer to generate a distribution. Since there are two types of drop size distribution (spatial and temporal), there are four possible numbers for this entry: 1 Computer will generate spatial drop size distribution based on input geometric mean and standard deviation. 2 Computer will generate temporal drop size distribution based on input geometric mean and standard deviation. 3 Computer reads input spatial drop size distribution. 4 Computer reads input temporal drop size distribution.
	NSTEPS	-	Number of steps from the nozzle down to the floor at which drops can interact and coalesce. If NSTEPS = 1, there is no interaction. For most calculations, the magnitude of NSTEPS is chosen such that there is 1 step/ft fall height.

Card Number and Format (cont'd.)	Parameter	Unit	Remarks
	NREAC	-	0 or 1. 0 ⇒ no methyl iodide removal 1 ⇒ methyl iodide removal
	NDATA	-	Number of data points for drop size distribution to be read in (used only if NTYPE = 3 or 4; NDATA = NGRP).
3 8E10.3	CNTVOL	ft^3	Total containment free volume
	FRCVS	-	Fraction of above volume sprayed
	FLOW	gpm	Spray flow rate
	ZMAX	ft	Fall height. One average height is used for all locations in the sprayed region.
	EFC	-	0. to 1.0. Collection efficiency of drops when they touch each other. EFC = 1.0 is most conservative.
	H	-	Elemental iodine partition coefficient
4 8E10.3	TNORM	^oF	Normal temperature at which spray water is stored.
	TEMPF	^oF	Maximum post-accident temperature
	DMEANG	cm	Geometric mean drop size: If NTYPE = 1, input is geometric mean for spatial distribution. NTYPE = 2, input is geometric mean for temporal distribution. NTYPE = 3 or 4, this parameter is not used.

Card Number and Format (cont'd.)	Parameter	Unit	Remarks
	SIGMAG	-	Geometric standard deviation for above parameter. Not used if NTYPE = 3 or 4.
	RK	sec^{-1}	methyl iodide hydrolysis rate.
	HR	-	methyl iodide partition coefficient.
5 8E10.3	AWALLR	ft^2	Interior surface over which laminar boundary layer flow occurs.
	AWALTR	ft^2	Interior surface over which turbulent boundary layer flow occurs.
	WALLFR	-	Spray water wall flow fraction.
	WALLDT	^oF	Temperature difference across wall/gas boundary.
	CNTDIA	ft	Containment diameter
	WALLSP	ft^2	Containment wall surface area impacted upon by spray.
6 8E10.3	D(I)	cm	Used only if NTYPE = 3 or 4. Drop size diameter for size group I (use as many cards as needed to describe all size groups).
7 8E10.3	F(I)	-	Used only if NTYPE = 3 or 4. Relative population for each size group I.

SAMPLE INPUT

```
//TXPSPRT1 JOB (WDC1,280,A),'P. S. TAM'
//STEP1 EXEC FORGLKGO,OPTIONS='SIZE=(172000,6144)',REGION.LOAD=180K,
//  CORE=200K
//LOAD.SYSLIN DD DSN=WDC1TXP.SPIRTPLO,VOL=SER=FILE29,UNIT=FILE,DISP=SHR
//  DD DSN=WDC1HZF.STEAMTAB,VOL=SER=FILE29,UNIT=FILE,DISP=SHR
//GO.SYSIN DD *
    SAMPLE INPUT
 50   3   1   0 50
 2.520E+06 7.400E-01 3.000E+03 1.000E+02 0.000E+00 5.000E+03
 7.000E+01 2.600E+02 1.000E+00 1.000E+00 1.000E+00 1.000E+00
 4.200E+05 1.500E+05 0.050E+00 2.000E+00 1.300E+02 1.000E+04
 3.800E-03 6.300E-03 8.800E-03 1.130E-02 1.380E-02 1.630E-02 1.880E-02 2.130E-02
 2.380E-02 2.630E-02 2.880E-02 3.130E-02 3.380E-02 3.630E-02 3.880E-02 4.130E-02
 4.380E-02 4.630E-02 4.880E-02 5.130E-02 5.380E-02 5.630E-02 5.880E-02 6.130E-02
 6.380E-02 6.630E-02 6.880E-02 7.130E-02 7.380E-02 7.630E-02 7.880E-02 8.130E-02
 8.380E-02 8.630E-02 8.880E-02 9.130E-02 9.380E-02 9.630E-02 9.880E-02 1.013E-01
 1.038E-01 1.075E-01 1.125E-01 1.175E-01 1.225E-01 1.288E-01 1.325E-01 1.425E-01
 1.613E-01 1.738E-01
 1.100E-02 2.700E-02 5.600E-02 1.500E-01 9.500E-02 8.000E-02 7.000E-02 5.100E-02
 6.600E-02 4.400E-02 2.600E-02 2.200E-02 1.700E-02 2.000E-02 2.300E-02 1.100E-02
 1.100E-02 1.500E-02 1.200E-02 1.300E-02 1.100E-02 1.600E-02 1.200E-02 8.000E-03
 8.000E-03 7.000E-03 1.100E-02 9.000E-03 1.100E-02 9.000E-03 8.000E-03 7.000E-03
 5.000E-03 5.000E-03 7.000E-03 6.000E-03 5.000E-03 5.000E-03 5.000E-03 4.000E-03
 5.000E-03 4.000E-03 5.000E-03 4.000E-03 6.000E-03 5.000E-03 2.000E-03 1.000E-03
 1.000E-03 2.000E-03
/*
```

```
//TXPSPIRT JOB (WDC1,280,A),'P. S. TAM'
//STEP1 EXEC FORGOMJ,STATUS=OLD,NAME='WDC1TXP.SPIRTPLO',DISK=FILE29
//COMP.SYSIN DD *
C   SPIRTPLS     (AUGUST 1978 VERSION)
C
C   SPRAY IODINE REMOVAL TRANSIENTS
C
      COMMON /CNTRL / NIN, NOUT, NGRP, NTYPE, MODEL, NREAC, NDATA
      COMMON /INPUT/CNTV, CNTVT, CNTD, FLO, FALLH, EFC, TNORM, TEMPF, H,
     1              DMEANG, SIGMAG, RK, HR, WALLFR,WALL,WALLLR,WALLTR,
     2              WALLDT,WALLSP
      COMMON /PROPS / PAIR, PSTM, FRAIR, FRSTM, VF, SMITNO, ETALIQ,
     1              RHOLIQ, RHOAIR, RHOSTM, RHOATM, HG, HF, HLIQ,
     2              ETAAIR, ETASTM, ETAMIX, DIAIR, DISTM, DIMIX, DSUBL
     3              ,DMCH3, DLCH3
      COMMON /DROPS / D(50), DSAVE(50), F(50), FTEMP(50),
     1              VTER(50), REYND(50), TFALL(50)
      COMMON /MASTR / KSUBG(50), KSUBL(50), EMIXD(50), EFILM(50),
     1              ERIGD(50), LAM1(50), LAM2(50), LAM3(50)
      COMMON /REACT / EMIXR(50), ERGDR(50), LAM4(50),
     1              LAM5(50), LAM6(50), WLAM
      COMMON /DATA1 / DELTAP(4),DM(4),SIGMA1(4)
      COMMON/ARRAYS/X(50),Y(50),NPOINT
      DIMENSION TITLE(20), FF(50)
      REAL KSUBG, KSUBL, LAM1, LAM2, LAM3, LAMS1, LAMS2, LAMS3
      REAL LAM4, LAM5, LAM6, LAMS4, LAMS5, LAMS6
      REAL LNDG
C
      NIN = 1
      NOUT = 6
      PI = 3.14159265
      NTITL = 20
      MODEL = 4
C
C   READ INPUT
    1 READ (NIN, 100, END=999) (TITLE(I), I = 1, NTITL)
      WRITE(NOUT,101)
      WRITE(NOUT,200) (TITLE(I), I = 1, NTITL)
      WRITE(NOUT,210)
      READ (NIN, 110) NGRP, NTYPE, NSTEPS, NREAC, NDATA
      WRITE(NOUT,201) NGRP, NTYPE, NSTEPS, NREAC, NDATA
      WRITE(NOUT,220)
      READ (NIN, 120) CNTVOL, FRCVS, FLOW, ZMAX, EFC, H
      WRITE(NOUT,202) CNTVOL, FRCVS, FLOW, ZMAX, EFC, H
      WRITE(NOUT,230)
      READ (NIN, 120) TNORM, TEMPF, DMEANG, SIGMAG, RK, HR
      WRITE(NOUT,202) TNORM, TEMPF, DMEANG, SIGMAG, RK, HR
      WRITE(NOUT,240)
      READ (NIN, 120) AWALLR, AWALTR, WALLFR, WALLDT, CNTDIA, WALLSP
      WRITE(NOUT,202) AWALLR, AWALTR, WALLFR, WALLDT, CNTDIA, WALLSP
C
C   READ TABLE OF DROP SIZE DATA IF NTYPE = 3 OR 4
      IF (NTYPE .LT. 3) GO TO 2
      IF (NDATA .LT. 4) GO TO 991
      WRITE(NOUT,250)
      WRITE(NOUT,251)
      READ (NIN, 120) (D(I),I=1,NDATA)
      WRITE(NOUT,202) (D(I),I=1,NDATA)
      WRITE(NOUT,252)
      READ (NIN, 120) (F(I),I=1,NDATA)
      WRITE(NOUT,202) (F(I),I=1,NDATA)
C
C   CONVERT INPUT PARAMETERS TO METRIC UNITS
    2 CNTVT = 28317. * CNTVOL
      CNTV = CNTVT * FRCVS
      CNTD = 30.48 * CNTDIA
      FLO = (1.0 - WALLFR) * 28317. * FLOW / (7.48*60.)
      FALLH = 30.48 * ZMAX
      WALLLR=AWALLR*929.03
      WALLTR=AWALTR*929.03
      WALL=WALLLR+WALLTR
      WALLSP=WALLSP * 929.03
C
```

```
C   CALCULATE PROPERTIES
      CALL PROPER
      WRITE(NOUT,1100)
      WRITE(NOUT,1110)
      WRITE(NOUT,1101) RHOLIQ, RHOAIR, RHOSTM, RHOATM
      WRITE(NOUT,1120)
      WRITE(NOUT,1101) ETALIQ, ETAAIR, ETASTM, ETAMIX
      WRITE(NOUT,1130)
      WRITE(NOUT,1101) DSUBL, DIAIR, DISTM, DIMIX, SMITNO
C
C   ESTABLISH DROP SIZE DISTRIBUTION
      CALL DIST
C
C   WRITE INITIAL DISTRIBUTION
      WRITE(NOUT,1200)
      WRITE(NOUT,1210)
      DO 10 I = 1, NGRP
      WRITE(NOUT,1201) I, D(I), F(I), FTEMP(I), VTER(I), REYNO(I)
   10 CONTINUE
      WRITE (NOUT,901)
      DO 701 I = 1,50
      X(I) = 0.
      Y(I) = 0.
  701 CONTINUE
      DO 702 I = 1,NGRP
      X(I) = D(I)
      Y(I) = F(I)
  702 CONTINUE
      NPOINT = NGRP
      CALL XYPLOT
      DO 705 I = 1,NGRP
      Y(I) = FTEMP(I)
  705 CONTINUE
      CALL XYPLOT
C
C   INITIAL DROP SIZE STATISTICS
      SUMN = 0.
      SUMD = 0.
      SUMF = 0.
      SURF = 0.
      SVOL = 0.
      SLND = 0.
      SLNSQ = 0.
      DRPV = 0.
      XX = 0.
      Z = 0.
      DO 20 I = 1, NGRP
      DI = D(I)
      SUMN = SUMN + FTEMP(I)
      SUMF = SUMF + F(I)
      SUMD = SUMD + FTEMP(I)*D(I)
      SURF = SURF + FTEMP(I)*PI*D(I)**2
      SVOL = SVOL + FTEMP(I) * D(I)**3
      DRPV = DRPV + FTEMP(I)*PI*D(I)**3 / 6.0
      SLND = SLND + F(I)*ALOG(DI)
      XX = XX + FTEMP(I)*ALOG(DI)
   20 CONTINUE
      DNM = SUMD / SUMN
      DSM = SQRT(SURF/(PI*SUMN))
      DVM = (SVOL/SUMN)**(1./3.)
      LNDG = SLND / SUMF
      YY = XX/SUMN
      DMEANG = EXP(LNDG)
      V = EXP(YY)
      DO 25 I = 1, NGRP
      DI = D(I)
      SLNSQ = SLNSQ + F(I)*(ALOG(DI) - LNDG)**2
      Z = Z + FTEMP(I)*(ALOG(DI) - YY)**2
   25 CONTINUE
```

```
      SIGS = SQRT(SLNSQ/SUMF)
      SIGT = SQRT(Z/SUMN)
      SIGMAG = EXP(SIGS)
      W = EXP(SIGT)
      WRITE(NOUT,1040) DRPV
      WRITE(NOUT,1070) DNM, DSM, DVM
      WRITE(NOUT,1080) DMEANG, SIGMAG
      WRITE(NOUT,1081) V, W
C
C   CALCULATE COALESCENSE EFFECT
      DZ = FALLH / NSTEPS
      DO 50 ISTEP = 1, NSTEPS
      CALL COALS(DZ)
   50 CONTINUE
C
C   FINAL DISTRIBUTION
      CALL VSUBT
      DO 55 I = 1, NGRP
      TFALL(I) = ZMAX*30.48 / VTER(I)
      FTEMP(I) = F(I) / TFALL(I)
   55 CONTINUE
C
C   WRITE FINAL DISTRIBUTION
      WRITE(NOUT,1220)
      WRITE(NOUT,1210)
      DO 60 I = 1, NGRP
      WRITE(NOUT,1201) I, D(I), F(I), FTEMP(I), VTER(I), REYNO(I)
   60 CONTINUE
      WRITE (NOUT,901)
      DO 703 I = 1,50
      X(I) = 0.
      Y(I) = 0.
  703 CONTINUE
      DO 704 I = 1,NGRP
      X(I) = D(I)
      Y(I) = F(I)
  704 CONTINUE
      CALL XYPLOT
      DO 706 I = 1,NGRP
      Y(I) = FTEMP(I)
  706 CONTINUE
      CALL XYPLOT
C
C   FINAL DROP SIZE STATISTICS
      SUMN = 0.
      SUMF = 0.
      SUMD = 0.
      SURF = 0.
      SVOL = 0.
      SLND = 0.
      SLNSQ = 0.
      DRPV = 0.
      XX = 0.
      Z = 0.
      DO 70 I = 1, NGRP
      DI = D(I)
      SUMN = SUMN + FTEMP(I)
      SUMF = SUMF + F(I)
      SUMD = SUMD + FTEMP(I)*D(I)
      SURF = SURF + FTEMP(I)*PI*D(I)**2
      SVOL = SVOL + FTEMP(I) * D(I)**3
      DRPV = DRPV + FTEMP(I)*PI*D(I)**3 / 6.0
      SLND = SLND + F(I)*ALOG(DI)
      XX = XX + FTEMP(I)*ALOG(DI)
   70 CONTINUE
      DNM = SUMD / SUMN
      DSM = SQRT(SURF/(PI*SUMN))
      DVM = (SVOL/SUMN)**(1./3.)
      LNDG = SLND / SUMF
      YY = XX/SUMN
      DMEANG = EXP(LNDG)
      DO 75 I = 1, NGRP
      DI = D(I)
      SLNSQ = SLNSQ + F(I)*(ALOG(DI) - LNDG)**2
      Z = Z + FTEMP(I)*(ALOG(DI) - YY)**2
   75 CONTINUE
```

```
      SIGS = SQRT(SLNSQ/SUMF)
      SIGT = SQRT(7/SUMN)
      SIGMAG = EXP(SIGS)
      W = EXP(SIGT)
      WRITE(NOUT,1070) DRPV
      WRITE(NOUT,1070) DNM, DSM, DVM
      WRITE(NOUT,1080) DMEANG, SIGMAG
      WRITE(NOUT,1081) V, W
C
C   MASS TRANSFER CALCULATION
      IF (MODEL .EQ. 0) GO TO 99
      CALL MASTRN
      LAMS1 = 0.
      LAMS2 = 0.
      LAMS3 = 0.
      LAMS4 = 0.
      LAMS5 = 0.
      LAMS6 = 0.
      WRITE(NOUT,1300)
      DO 80 I = 1, NGRP
      WRITE(NOUT,1201) I, KSUBG(I), ERIGD(I), LAM1(I),
     1                 LAM2(I), LAM3(I)
      LAMS1 = LAMS1 + LAM1(I)
      LAMS2 = LAMS2 + LAM2(I)
      LAMS3 = LAMS3 + LAM3(I)
   80 CONTINUE
      WRITE(NOUT,1310) LAMS1, LAMS2, LAMS3
C
C   CALCULATE MASS TRANSFER WITH CHEM. REACTION FOR METHYL IODIDE
      IF (NREAC .NE. 1) GO TO 98
      CALL REACTN
      WRITE(NOUT,1400)
      DO 90 I = 1, NGRP
      WRITE(NOUT,1201) I, EMIXR(I), LAM5(I), ERGDR(I), LAM4(I), LAM6(I)
      LAMS4 = LAMS4 + LAM4(I)
      LAMS6 = LAMS6 + LAM6(I)
   90 CONTINUE
      WRITE(NOUT,1410) LAMS4, LAMS6
      WRITE(NOUT,1420) WLAM
C
C   CALCULATE ELEMENTAL IODINE PLATEOUT
   98 CALL PLATO (LAMPL)
      WRITE(NOUT,1500)LAMPL
 1500 FORMAT(1HO,10X,'ELEMENTAL IODINE PLATEOUT RATE CONSTANT IS',
     1       1X,E10.3,' PER HOUR')
   99 CONTINUE
      GO TO 1
C
C
C   ERROR MESSAGES
  991 WRITE (NOUT,9001)
  999 STOP
C
C
  100 FORMAT(20A4)
  101 FORMAT(1H1,41X,'S P I R T',//,32X,'SPRAY IODINE REMOVAL TRANSIENT'
     1       /,15X,'ACCIDENT ANALYSIS BRANCH - ',
     2       'DIV OF SITE SAFETY AND ENVIR ANALYSIS',/,44X,'USNRC',//)
  110 FORMAT(6I3)
  120 FORMAT(8E10.3)
  200 FORMAT(1HO,41X,'I N P U T',//,1X,20A4)
  201 FORMAT(4X,6(I3,12X))
  202 FORMAT(8(1X,1PE10.3,4X))
  210 FORMAT(1HO,'NO. OF GROUPS',3X,'DISTR.TYPE',4X,'NO. OF STEPS',
     1       3X,'METHYL REMVL',2X,'TBL.DATA PTS.')
  220 FORMAT(1HO,'CONT.VOLUME ',3X,'FRACT.SPRAY',2X,' SPRAY FLOW ',
     1       3X, 'FALL HEIGHT ',3X,' COLLECTION ',3X,'I2 PARTN.COEF',/,
     2       1X, ' (CU.FT)    ',3X,'             ',3X,'    (GPM)   ',
     3       3X, '    (FT)    ',3X,' EFFICIENCY',3X,'(C-LIQ/C-GAS)')
  230 FORMAT(1HO,'NORM.AIR TEMP',2X,'MAX.ATM.TEMP',3X,'DROP SIZE,CM',
     1       3X,'STD.DEVIATN.',3X,'REACTN RATE K',2X,'METHYL PARTN.',/,
     2       1X,'  (DEG F)   ',3X,'  (DEG F)   ',3X,'(GEOM. MEAN)',
     3       3X,'(GEOMETRIC) ',3X,'  (1/SEC.)  ',3X,'(C-LIQ/C-GAS)')
```

```
 240 FORMAT(1HO,'LAM.B.L.AREA  ',2X,'TUR.B.L.AREA',1X,' WALL FLOW ',3X,
    1       'WALL DELTA T', 3X,'CONT. DIA.',3X,'WALL FLOW AREA',/,
    1       1X,' (SQ.FT.)  ',3X,' (SQ.FT.)  ',3X,'   FRACTION  ',3X,
    2       '  (DEG F)   ', 3X,'  ( FT. )   ',2X,'  (SQ.FT)    ')
 250 FORMAT(1HO,'TABLE OF DROP SIZE DISTRIBUTION',/,
    1       1X,'(DISTRIBUTION IS SPATIAL IF NTYPE = 3, ',
    2       'TEMPORAL IF NTYPE = 4)')
 251 FORMAT(1HO,'DROP SIZE (MICRONS)')
 252 FORMAT(1HO,'FREQUENCY (DROPS/CC OR DROPS/CC/SEC)')
1001 FORMAT(3X,I3,6(1PE12.3,3X))
1040 FORMAT(1HO,'INITIAL LIQUID VOLUME (CC OF LIQ)/(CC GAS)',
    1       14X,1PE10.3)
1050 FORMAT(1HO,'FINAL LIQUID VOLUME (CC OF LIQ)/(CC GAS)',16X,1PE10.3)
1070 FORMAT(1HO,'THE NUMBER, SURFACE, AND VOLUME MEANS (CM)',/,
    1       1X,'OF THE TEMPORAL DISTRIBUTION ARE',9X,3(1PE10.3,5X))
1080 FORMAT(1HO,'THE GEOMETRIC MEAN (CM) AND GEOM. STD.',/,
    1       1X,'DEVIATION FOR THE SPATIAL DISTRIBUTION ARE',14X,
    2       2(1PE10.3,5X))
1081 FORMAT(1HO,'THE GEOMETRIC MEAN (CM) AND GEOM. STD.',/,
    1       1X,'DEVIATION FOR THE TEMPORAL DISTRIBUTION ARE',13X,
    2       2(1PE10.3,5X))
1100 FORMAT(1HO,/,36X,'CALCULATED PROPERTIES')
1101 FORMAT(1X,8(1PE10.3,5X))
1110 FORMAT(1HO,'LIQ. DENSITY',3X,'AIR DENSITY ',2X,'STEAM DENSITY',
    1       3X,'ATM.DENSITY',/,
    1       2X,4('(LBS/CU.FT)',3X))
1120 FORMAT(1HO,'LIQ.VISCOSITY',2X,'AIR VISCOSITY',2X,'STM.VISCOSITY',
    1       2X,'ATM.VISCOSITY',/,
    1       1X,4('   (POISE)   ',2X))
1130 FORMAT(1HO,'LIQ.DIFFUSIV.',2X,'AIR DIFFUSIV.',2X,'STM.DIFFUSIV.',
    1       2X,'ATM.DIFFUSIV.',3X,'SCHMIDT NO.',/,
    2       1X,4(' (CM2/SEC)  ',3X))
1200 FORMAT(1H1,36X,'DROP SIZE CALCULATION',//,
    1       1X,'INITIAL DROP SIZE DISTRIBUTION',/)
1201 FORMAT(2X,I3,7X,5(1PE10.3,5X))
1210 FORMAT(1X,'GRP.NO.',3X,'DROP SIZE,CM',3X,' DROPS / CC ',
    1       3X,'DROPS/CC/SEC',3X,'TERM.VEL.,CM/S',2X,'REYNOLDS NO.')
1220 FORMAT(1H1,36X,'DROP SIZE CALCULATION',//,
    1       1X,'DISTRIBUTION AFTER CONDENSATION AND COALESCENSE')
1300 FORMAT(1H1,34X,'MASS TRANSFER CALCULATION',//,
    1       1X,'GRP.NO.',3X,'GAS FILM COEF',
    2       2X,'E RIGID DROP',3X,'LAMBDA MIXED ',3X,'LAMBDA FILM',
    3       3X,'LAMBDA RIGID')
1310 FORMAT(1HO,3X,'TOTAL LAMBDA (1/HR)', 19X, 3(1PE10.3,5X))
1400 FORMAT(1H1,22X,'MASS TRANSFER WITH SIMULTANEOUS CHEMICAL REACTION'
    1       ,/,25X,'(METHYL IODIDE REMOVAL BY THIOSULFATE SPRAYS)',//,
    2       1X,'GRP.NO.',
    3       3X,'E MIXED DROP',3X,'QDROP (RIGID)',2X,'E RIGID DROP',
    4       3X,'LAMBDA MIXED',3X,'LAMBDA RIGID')
1410 FORMAT(1HO,3X,'TOTAL SPRAY LAMBDA WITH CHEM. REACTION (1/HR)',18X,
    1       2(1PE10.3,5X))
1420 FORMAT(1HO,3X,'LAMBDA FOR WALL FILM EFFECT (1/HR)',4X,1PE10.3)
 901 FORMAT(1HO,'FOLLOWING ARE TWO PLOTS OF DROP SIZE VS. ',
    1       'SPATIAL THEN TEMPORAL DISTRIBUTION',/,5X,'X-AXIS =',
    2       ' DROP SIZE IN CM',/,5X,'Y-AXIS = RELATIVE DIST.')
9001 FORMAT(1H1,' I N P U T  E R R O R',//,
    1       1X,'INSUFFICIENT DROP SIZE DATA')
      END
      SUBROUTINE PROPER
C
C   THIS SUBROUTINE CALCULATES THE DENSITIES, VISCOSITIES, AND
C   DIFFUSIVITIES REQUIRED FOR THE SPRAY ANALYSIS
C   THE CALCULATION OF GAS VISCOSITIES AND DIFFUSIVITIES ARE
C   ADAPTED FROM L.F.PARSLY, ORNL-TM-1911
C
      COMMON /INPUT/CNTV, CNTVT, CNTD, FLO, FALLH, EFC, TNORM, TEMPF, H,
     1               DMEANG, SIGMAG, RK, HR, WALLFR,WALL,WALLLR,WALLTR,
     2               WALLDT,WALLSP
      COMMON /PROPS / PAIR, PSTM, FRAIR, FRSTM, VF, SMITWO, ETALIQ,
```

```
     1               RHOLIQ, RHOAIR, RHOSTM, RHOATM, HG, HF, HLIQ,
     2               ETAAIR, ETASTM, ETAMIX, DIAIR, DISTM, DIMIX, DSUBL
     3               ,DMCH3, DLCH3
      REAL NUM, MOLW
      TEMPC = (TEMPF-32.0) * 5./9.
      TEMPK = TEMPC + 273.1
      PAIR = 14.7 * (TEMPF+460.)/(TNORM+460.)
      PSTM = PSL(TEMPF)
      PATM = PAIR + PSTM
      FRAIR = PAIR / PATM
      FRSTM = PSTM / PATM
C   LIQUID DENSITY
      RHOLIQ = 1.0/VSL(TEMPF)
C
C   DENSITY OF AIR-STEAM MIXTURE (SATURATED CONDITIONS ASSUMED)
      RHOAIR = 0.0808 * 460./(TNORM+460.)
      HG = HSV(PSTM,T,S,VG)
      RHOSTM = 1.0/VG
      RHOATM = RHOAIR + RHOSTM
C
C   CALCULATE VISCOSITY OF STEAM
C  REF. KEENAN AND KEYES, P. 23
      PSTMKG =  1.0332 * (PSTM/14.696)
      NUM = 1.5D1E-05 * SQRT(TEMPK)
      DENOM = 1.0+ 446.8*(1./TEMPK)
      ETA0 = NUM / DENOM
      TEXP = -1340./TEMPK
      F1OFP = 1.0E-4*(1./TEMPK)*PSTMKG*(6.36-2.31E-03*10.0**TEXP)
      F2OFP = 1.0E-4*.0389*10.0**(-0.005476*TEMPK)*(PSTMKG**2)
      ETA = ETA0 + F1OFP + F2OFP
      ETASTM = ETA
C
C   CALCULATE VISCOSITY OF AIR FROM PERRY (3RD ED.),PAGE 370
      ETAAIR = (1.709E-04)*((TEMPK/273.1)**.768)
C
C   CALCULATE MIXTURE VISCOSITY
      NUM = (1.+((ETAAIR/ETA)**.5)*((18./29.)**.25))**2
      DENOM =(4./SQRT(2.))*(1.+(29./18.)**.5)
      PHI12 = NUM/DENOM
      NUM   = (1.+((ETA/ETAAIR)**.5)*((29./18.)**.25))**2
      DENOM =(4./SQRT(2.))*(1.+(18./29.)**.5)
      PHI21 = NUM/DENOM
      DENOM = 1.+(FRSTM/FRAIR)*PHI12
      TERM1 = ETAAIR / DENOM
      DENOM = 1.+(FRAIR/FRSTM)*PHI21
      TERM2 = ETA / DENOM
      ETAMIX= TERM1 + TERM2
C
C  CALCULATE THE DIFFUSIVITY OF IODINE IN AIR AND STEAM
      EPS1K = 550.
      EPS2K = 97.
      EPS3K = 363.
      EPS12K = SQRT(EPS1K*EPS2K)
      EPS13K = SQRT(EPS1K*EPS3K)
      COLINT = 0.3674 + 0.3478*(EPS12K/TEMPK)
      RAIR = 3.617
      RI = 4.982
      RIAIR = 0.5*(RAIR+RI)
      FOFM = SQRT((1./254.)+(1./29.))
      B    = (10.7 - 2.46*FOFM)*1.0E-04
      PFUNT= TEMPK**1.5
      NUM  = B*PFUNT*FOFM
      PTOTL= (PAIR+PSTM)/14.696
      DENOM= PTOTL* RIAIR*RIAIR*COLINT
      DIAIR= NUM / DENUM
C     STEAM AND MIXTURE
      COLINT = 0.3674 + 0.3478*(EPS13K/TEMPK)
      RW   = 2.655
      RIW  = 0.5*(RW+RI)
      FOFM = SQRT((1./254.) + (1./18.))
      B    = (10.7 - 2.46*FOFM)*1.0E-04
      NUM = B*PFUNT*FOFM
      DENOM = PTOTL*RIW*RIW*COLINT
      DISTM = NUM/DENOM
      DIMIX = 1.0/(FRAIR/DIAIR + FRSTM/DISTM)
```

```
C
C   REPEAT CALC. OF GAS DIFFUSIVITIES FOR METHYL IODIDE
      EPS1K = 363.
      EPS12K = SQRT(EPS1K*EPS2K)
      EPS13K = SQRT(EPS1K*EPS3K)
      COLINT = 0.3674 + 0.3478*(EPS12K/TEMPK)
      VO = 62.1
      RI = 1.18 * VO**(1./3.)
      RIAIR = 0.5*(RAIR+RI)
      FOFM = SQRT(1./142. + 1./29.)
      B    = (10.7 - 2.46*FOFM)*1.0E-04
      NUM  = B*PFUNT*FOFM
      DENOM= PIOTL* RIAIR*RIAIR*COLINT
      DIACH= NUM / DENOM
      COLINT = 0.3674 + 0.3478*(EPS13K/TEMPK)
      RIW = 0.5*(RW+RI)
      FOFM = SQRT((1./142.) + (1./18.))
      B    = (10.7 - 2.46*FOFM)*1.0E-04
      NUM = B*PFUNT*FOFM
      DENOM = PIOTL*RIW*RIW*COLINT
      DISCH = NUM/DENOM
      DMCH3 = 1.0/(FRAIR/DIACH + FRSTM/DISCH)
C
C   CALCULATE VISCOSITY OF WATER FROM PERRY'S HANDBOOK (4TH ED),
C   PAGE 3-201
      TCM8 = TEMPC - 8.453
      VSCINV= 2.1482*((TCM8+SQRT(8078.4+TCM8*TCM8)) - 120.
      ETALIQ = 1.0/VSCINV
C
C   CALCULATE DIFFUSIVITY OF IODINE IN WATER FROM
C   PERRY'S HANDBK.(4TH ED.), PAGE 14-21
      VO = 71.5
      X = 2.6
      MOLW = 18.
      DMUT = 7.4E-08 * SQRT(X*MOLW)/VO**0.6
      DSUBL = DMUT * TEMPK * VSCINV /100.
C
C   REPEAT CALC. OF LIQUID DIFFUSIVITY FOR METHYL IODIDE
      VO = 62.1
      DMUT = 7.4E-08 * SQRT(X*MOLW)/VO**0.6
      DLCH3 = DMUT * TEMPK * VSCINV /100.
C
C   CALCULATE SCHMIDT NUMBER
      SMINO = ETAMIX/(RHOATM*0.016018*DIMIX)
      RETURN
      END
      SUBROUTINE DIST
C   THIS ROUTINE SETS UP THE INITIAL DISTRIBUTION
      COMMON /CNTRL / NIN, NOUT, NGRP, NTYPE, MODEL, NREAC, NDATA
      COMMON /INPUT/CNTV, CNTVT, CNTD, FLO, FALLH, EFC, TNORM, TEMPF, H,
     1              DMEANG, SIGMAG, RK, HR, WALLFR,WALL,WALLLR,WALLTR,
     2              WALLDT,WALLSP
      COMMON /DROPS / D(50), DSAVE(50), F(50), FTEMP(50),
     1              VTER(50), RENO(50), TFALL(50)
      DIMENSION FF(50)
      REAL LNX2
      PI = 3.14159265
      FTOT = 0.
      X1 = DMEANG
      GRP = NGRP
      LNX2 = ALOG(SIGMAG)
      DMAX = 0.18
C
C   ESTABLISH DROP SIZE INCREMENTS FOR LOGNORMAL DISTRIBUTION
      IF (NTYPE .GT. 2) GO TO 5
      DELLOG = (ALOG(DMAX) - ALOG(X1))/((GRP - 1.0)/2.)
      DMINLN = ALOG(X1) - DELLOG*((GRP - 1.)/2.)
    1 DO 3 I = 1, NGRP
      XI = I
      D(I) = EXP(DMINLN + (XI-1.0)*DELLOG)
    3 CONTINUE
      CALL VSUBT
C
```

```
      5 GO TO (10,15,20,25), NTYPE
C
C     ASSUME LOGNORMAL SPATIAL DISTRIBUTION DERIVED FROM INPUT VALUES FOR
C     LOG MEAN AND LOG STD. DEVIATION.
     10 DO 11 I = 1, NGRP
        TFALL(I) = FALLH / VTER(I)
        X = D(I)
        F(I) = EXP(-0.5*((ALOG(X/X1)/LNX2)**2))
        FF(I) = F(I) * PI * D(I)**3 / (6.0 * TFALL(I))
        FTOT = FTOT + FF(I)
     11 CONTINUE
        GO TO 30
C
C     ASSUME LOGNORMAL TEMPORAL DISTRIBUTION DERIVED FROM INPUT VALUES
C     FOR LOG MEAN AND LOG STD. DEVIATION.
     15 DO 16 I = 1, NGRP
        X = D(I)
        TFALL(I) = FALLH / VTER(I)
        F(I) = EXP(-0.5*((ALOG(X/X1)/LNX2)**2))
        FF(I) = F(I) * PI * D(I)**3/6.0
        FTOT = FTOT + FF(I)
     16 CONTINUE
        GO TO 30
C
C     USE TABULAR INPUT FOR DROP SIZE DISTRIBUTION
C     ASSUME INPUT DATA IS SPATIAL DISTRIBUTION
     20 NGRP = NDATA
        CALL VSUBT
        DO 22 I = 1, NDATA
        TFALL(I) = FALLH / VTER(I)
        FF(I) = F(I) * PI * D(I)**3 / (6.0 * TFALL(I))
        FTOT = FTOT + FF(I)
     22 CONTINUE
        GO TO 30
C
C     INPUT DATA IS TEMPORAL DISTRIBUTION
     25 NGRP = NDATA
        CALL VSUBT
        DO 26 I = 1, NDATA
        TFALL(I)=FALLH/VTER(I)
        FF(I) = F(I) * PI * D(I)**3 / 6.0
        FTOT = FTOT + FF(I)
     26 CONTINUE
        GO TO 30
C
C     NORMALIZE DROP SIZE DIST, TO TOTAL SPRAY FLOW
     30 DO 35 I = 1, NGRP
        DSAVE(I) = D(I)
        FTEMP(I) = (FF(I)/FTOT) * FLO * 6.0 / (CNTV * PI * D(I)**3)
        F(I) = FTEMP(I) * TFALL(I)
     35 CONTINUE
        RETURN
        END
        SUBROUTINE VSUBT
C     THIS SUBROUTINE CALCULATES TERMINAL VELOCITIES. IT IS ADAPTED
C     WITH MINOR CHANGES FROM L.F.PARSLY, ORNL-TM-1911
C     (VARIABLES USED IN THIS ROUTINE ARE IN METRIC UNITS)
        COMMON /CNTRL / NIN, NOUT, NGRP, NTYPE, MODEL, NREAC, NDATA
        COMMON /PROPS / PAIR, PSTM, FRAIR, FRSTM, VF, SMITND, ETALIQ,
       1                RHOLIQ, RHOAIR, RHOSTM, RHOATM, HG, HF, HLIQ,
       2                ETAAIR, ETASTM, ETAMIX, DIAIR, DISTM, DIMIX, DSUBL
       3                ,DMCH3, DLCH3
        COMMON /DROPS / D(50), DSAVE(50), F(50), FTEMP(50),
       1                VTER(50), REYND(50), TFALL(50)
        GSUBC = 980.
        XPGC = GSUBC**0.714
        RHOMET = RHOATM * 0.016018
        XPRHOA = RHOMET**0.286
        DELRHO = (RHOLIQ - RHOATM)*0.016018
        XPDRHO = DELRHO**0.714
        XPETA = ETAMIX**0.428
        DRAG = 0.44
```

```
C   NOTE, DRAG COEFFICIENT APPLIES FOR REYNOLDS NOS. ABOVE
C   APPROX. 800. TO SMOOTH THE CHANGE, START COMPARISON AT RE=600.
      DO 10 I = 1, NGRP
       XPDP = D(I)**1.142
      VTER1    = 0.153*XPGC*XPDP*XPDRHO/(XPRHOA*XPETA)
      REYNO1   = D(I)*VTER1*RHOMET/ETAMIX
      VTER(I) = VTER1
      REYNO(I) = REYNO1
      IF (REYNO1 .LE. 600.) GO TO 10
      VTER2    = SQRT(4.0*GSUBC*D(I)*DELRHO / (3.0*RHOMET*DRAG))
      VTER(I) = AMIN1 (VTER1,VTER2)
      REYNO(I) = D(I)*VTER(I)*RHOMET/ETAMIX
   10 CONTINUE
      RETURN
      END
      SUBROUTINE COALS(DZ)
C
C   THIS SUBROUTINE CALCULATES THE MAX. POSSIBLE EFFECT OF DROP
C   COALESCENCE ON THE DROP SIZE DISTRIBUTION.
C   REF. - PASEDAG AND GALLAGHER, NUCLEAR TECHNOLOGY, X, 4, 1971
      COMMON /CNTRL / NIN, NOUT, NGRP, NTYPE, MODEL, NREAC, NDATA
      COMMON /INPUT/CNTV, CNTVT, CNTD, FLO, FALLH, EFC, TNORM, TEMPF, H,
     1              DMEANG, SIGMAG, RK, HR, WALLFR,WALL,WALLLR,WALLTR,
     2              WALLDT,WALLSP
      COMMON /DROPS / D(50), DSAVE(50), F(50), FTEMP(50),
     1              VTER(50), REYNO(50), TFALL(50)
      DIMENSION COLL(50,50), COLLS(50)
      PI = 3.14159265
C
C   CALCULATE NO. OF COLLISIONS
      DO 60 N = 1,NGRP
      I = NGRP - N + 1
      COLLS(I) = 0.
      DO 40 J = 1,I
      DELTAV = ABS(VTER(I) - VTER(J))
      DIAM = (D(I)/2.00 + D(J)/2.0)**2
      COLL(I,J) =EFC* PI*DIAM*(DELTAV/VTER(I))*F(I)*F(J)*DZ
      IF (COLL(I,J) .LE. 0.) GO TO 40
      FADD = COLL(I,J)
C
C  CALCULATE SIZE OF COALESCED DROPS AND REDISTRIBUTE THEM
      DCOAL = (D(I)**3 + D(J)**3)**(1./3.)
      II = I
      NM1 = NGRP - 1
   20 CONTINUE
      DO 30 L = II, NM1
      IL = L
      IF(DCOAL .LE. (DSAVE(L)+DSAVE(L+1))/2.) GO TO 31
   30 CONTINUE
      DCOAL = ((DCOAL**3)/2.0)**(1./3.)
      FADD = 2. * COLL(I,J)
      II = 1
      GO TO 20
   31 CONTINUE
C
C   ADJUST (VOLUME) MEAN DROP SIZE OF THE GROUP RECIEVING
      D(IL) = ((F(IL)*D(IL)**3 + FADD*DCOAL**3)/(F(IL)+FADD))
     1                                                    **(1./3.)
      F(IL) = F(IL) + FADD
C
C   ADJUST SIZE DISTRIBUTION OF THE SMALLER DROPS
      F(J) = F(J) - COLL(I,J)
C
C  CALCULATE NO. OF COLLISIONS OF GROUP I
      COLLS(I) = COLLS(I) + COLL(I,J)
   40 CONTINUE
C
C   ADJUST SIZE DISTRIBUTION OF THE LARGER DROPS FOR
C   THE COALESCED DROPS
      F(I) = F(I) - COLLS(I)
      IF(F(I).LT.0.0) F(I) = 0.0
   60 CONTINUE
      RETURN
      END
```

```
      SUBROUTINE MASTRN
C     THIS SUBROUTINE CALCULATES MASS TRANSFER EFFICIENCIES AND
C     LAMBDAS FOR EACH DROP SIZE. THE FOLLOWING OPTIONS ARE AVAILABLE
C        MODEL = 1, GRIFFITHS' MODEL
C        MODEL = 2, STAGNANT FILM MODEL
C        MODEL = 3, RIGID DROP MODEL
C        MODEL = 4  ALL THREE MODELS
C     REF. - PORTMA AND PASEDAG, WASH-1329
C
C     THE LAMBDA RESULTING FROM MASS TRANSFER WITH SIMULTANEOUS CHEMICAL
C     REACTION (I.E.METHYL IODIDE REMOVAL BY SODIUM THIOSULFATE SPRAYS,
C     ARE CALCULATED WHEN NREAC = 1
C     REF. - DANCKWERTS, TRANS. FARADAY SOC., 47, 1014, 1951
      COMMON /CNTRL / NIN, NOUT, NGRP, NTYPE, MODEL, NREAC, NDATA
      COMMON /INPUT/ CNTV, CNTVT, CNTD, FLO, FALLH, EFC, TNORM, TEMPF, H,
     1               DMEANG, SIGMAG, RK, HR, WALLFR,WALL,WALLLR,WALLTR,
     2               WALLDT,WALLSP
      COMMON /PROPS / PAIR, PSTM, FRAIR, FRSTM, VF, SMITNO, ETALIQ,
     1               RHOLIQ, RHOAIR, RHOSTM, RHOATM, HG, HFG, HLIQ,
     2               ETAAIR, ETASTM, ETAMIX, DIAIR, DISTM, DIMIX, DSUBL
     3               ,DMCH3, DLCH3
      COMMON /DROPS / D(50), DSAVE(50), F(50), FTEMP(50),
     1               VTER(50), REYNO(50), TFALL(50)
      COMMON /MASTR / KSUBG(50), KSUBL(50), EMIXD(50), EFILM(50),
     1               ERIGD(50), LAM1(50), LAM2(50), LAM3(50)
      COMMON /REACT / EMIXR(50), ERGDR(50), LAM4(50),
     1               LAM5(50), LAM6(50), WLAM
      REAL KSUBG, KSUBL, LAM1, LAM2, LAM3
      REAL LAM4, LAM5, LAM6, KGCH3, KLCH3
      DIMENSION FV(50)
      DIMENSION ALPH(50), BETA(50), QDROP(50)
      DOUBLE PRECISION SH,THETA,ASQ
      PI = 3.14159265
      SMI3 = SMITNO**(1./3.)
      DO 10 I = 1, NGRP
      LAM1(I) = 0.
      LAM2(I) = 0.
      LAM3(I) = 0.
      LAM4(I) = 0.
      LAM5(I) = 0.
      LAM6(I) = 0.
      ERIGD(I) = 0.
      EMIXR(I) = 0.
      ERGDR(I) = 0.
C
C     CALCULATE VOLUME FRACTION OF FLOW FOR EACH GROUP
      TFALL(I) = FALLH / VTER(I)
      FV(I) = F(I)*PI*D(I)**3/(6.0*TFALL(I))
C
C     CALCULATE LIQUID AND GAS AND LIQUID FILM DEPOSITION VELOCITIES
      KSUBG(I) = (DIMIX/D(I))*(2.0+0.55*SQRT(REYNO(I))*SMI3)
      KSUBL(I) = 2.0*PI*PI*DSUBL/(3.0*D(I))
   10 CONTINUE
      GO TO (100,200,300,100),MODEL
C
C     WELL MIXED MODEL
  100 DO 150 I = 1, NGRP
      EMIXD(I) = 1.0
      EXPO = 6.0 * KSUBG(I) * TFALL(I) / (D(I)*H)
      IF (EXPO .GT. 70.) GO TO 130
      EMIXD(I) = 1.0 - EXP(-EXPO)
  130 LAM1(I) = 3600.*FV(I)*H*EMIXD(I)
  150 CONTINUE
      IF (MODEL .NE. 4) GO TO 399
C
C     STAGNANT FILM MODEL
```

```
  200 DO 250 I = 1, NGRP
      EFILM(I) = 1.0
      EXPO = 6.0*KSUBG(I)*TFALL(I)/(D(I)*(H + KSUBG(I)/KSUBL(I)))
      IF (EXPO .GT. 70.) GO TO 220
      EFILM(I) = 1.0 - EXP(-EXPO)
  220 LAM2(I) = 3600.*FV(I)*H*EFILM(I)
  250 CONTINUE
      IF (MODEL .NE. 4) GO TO 399
C
C   RIGID DROP MODEL
  300 DO 350 I = 1, NGRP
      SH = KSUBG(I)*D(I)/(2.*H*DSUBL)
      SUMATN = 0.
      DO 330 J = 1, 20
      ASQ = ALPHA(SH,J)**2
      THETA = 4.0*DSUBL*TFALL(I)/(D(I)*D(I))
      IF(ASQ*THETA .GT. 150.) GO TO 330
      SUMATN=SUMATN+6.0*SH*SH*DEXP(-ASQ*THETA )/(ASQ*ASQ+ASQ*SH*(SH-1.))
  330 CONTINUE
      ERIGD(I)= 1.0 - SUMATN
      LAM3(I) = 3600.*FV(I)*H*ERIGD(I)
  350 CONTINUE
  399 RETURN
C
C
C   MASS TRANSFER WITH SIMULTANEOUS CHEMICAL REACTION
C
      ENTRY REACTN
      GO TO (400,600,600,400), MODEL
C
C   WELL MIXED DROP MODEL
C   REF. - POSTMA AND HILLIARD, ANS TRANSACTIONS, 12, P.898, 1969
  400 DO 450 I = 1, NGRP
      EMIXR(I) = 1.0 + RK*TFALL(I)
      LAM4(I) = 3600. * FV(I)*HR*EMIXR(I)
  450 CONTINUE
      IF (MODEL .NE. 4) GO TO 900
C
C   STAGNANT FILM MODEL WITH CHEM. REALTION DELETED.
C
C   RIGID DROP MODEL
C   REF.- POSTMA, PNWL-B-417, 1975
  600 DO 650 I = 1, NGRP
      ALPH(I) = RK * TFALL(I)
      BETA(I) = 4.0 * DLCH3 * TFALL(I)/(D(I)*D(I))
       AN = 0.0
       SUM = 0.0
  620  AN = AN + 1.
       EXPON=0.
       IF((ALPH(I)+BETA(I)*(AN*PI)**2).LT.150.)EXPON=EXP(-(ALPH(I)+BETA(
     1 I))*(AN*PI)**2))
       ANUM=ALPH(I)+(BETA(I)*(AN*PI)**2/(ALPH(I)+BETA(I)*(AN*PI)**2
     1  ))*(1.-EXPON)
       DENOM=ALPH(I)+BETA(I)*(AN*PI)**2
       TERM=ANUM/DENOM
       SUM=SUM+TERM
       ERROR=(ALPH(I)+1.)/(BETA(I)*AN*PI*PI)
       IF (ERROR/SUM .GT. 0.01) GO TO 620
       QDROP(I)=6.*PI*SUM
       ERGDR(I)=3.*QDROP(I)*BETA(I)/(4.*PI)
       LAM6(I) = 3600. * FV(I) * HR * ERGDR(I)
       LAM5(I) = QDROP(I)
  650 CONTINUE
C
C   CALCULATE WALL FILM EFFECT
  900 WLAM = 0.
      IF ((WALLFR*CNTD) .LE. 0.) GO TO 999
      WALFLO = WALLFR * FLO
      DELTA = ((3.*ETALIQ*WALFLO)/(RHOLIQ*PI*CNTD))**0.333
      RKDL = SQRT(RK*DLCH3)
      WLAM = 3600.*WALLSP*HR*RKDL*TANH(SQRT(RK/DLCH3)*DELTA)/CNTVT
  999 RETURN
      END
```

```
      SUBROUTINE PLATO (LAMPL)
C   THIS SUBROUTINE CALCULATES A REMOVAL COEFFICIENT (LAMBDA) FOR
C   PLATEOUT OF ELEMENTAL IODINE ON THE CONTAINMENT LINER.
      COMMON /CNTRL / NIN, NOUT, NGRP, NTYPE, MODEL, NREAC, NDATA
      COMMON /INPUT/CNTV, CNTVT, CNTD, FLO, FALLH, EFC, TNORM, TEMPF, H,
     1               OMEANG, SIGMAG, RK, HR, WALLFR,WALL,WALLLR,WALLTR,
     2               WALLDT,WALLSP
      COMMON /PROPS / PAIR, PSTM, FRAIR, FRSTM, VF, SMITNO, ETALIQ,
     1               RHOLIQ, RHOAIR, RHOSTM, RHOATM, HG, HF, HLIQ,
     2               ETAAIR, ETASTM, ETAMIX, DIAIR, DISTM, DIMIX, DSUBL
     3               ,DMCH3, DLCH3
      COMMON /REACT / EMIXR(50), ERGDR(50), LAM4(50),
     1               LAM5(50), LAM6(50), WLAM
      REAL L, LAMPL,KSUBCL,KSUBCT
      LAMPL = 0.
      PLATLM = 0.
      PLATTR = 0.
      IF (WALL*CNTD*WALLDT .LE. 0.) GO TO 99
      PI = 3.14159265
      G = 980.
      DELT = (WALLDT)*5./9.
      BETA = 1.0/((TEMPF-32.)*5./9. + 273.)
      RHO = 0.016018 * RHOATM
      GROL3 = RHO*RHO*G*BETA*DELT/(ETAMIX*ETAMIX)
      L = 305.
C
C   LAMINAR FLOW (L ASSUMED  EQUAL TO 305CM.)
      XLAM=L
      GRASNO = GROL3 * L*L*L
      KSUBCL = (0.59*DIMIX/L)*(GRASNO*SMITNO)**0.25
      PLATLM = 3600.*KSUBCL*WALLLR/CNTVT
C
C   TURBULENT FLOW REGION
      GRASNO = GROL3 * L*L*L
      KSUBCT = (0.13*DIMIX/L)*(GRASNO*SMITNO)**(1.0/3.0)
      PLATTR = 3600.*KSUBCT*WALLTR/CNTVT
      WRITE (NOUT,97) PLATLM,PLATTR,RHOATM,RHO,GROL3,GRASNO,KSUBCL,
     1                KSUBCT,WALLLR,WALLTR
   97 FORMAT('1H1,' PLATLM    ',' PLATTR    ',' RHOATM  ',' RHO    ',
     1       '  GROL3   ',' GRASNO  ',' KSUBCL  ',
     2       '  KSUBCT  ',' WALLLR  ',' WALLTR  ',/,10(1PE10.3))
C
C   TOTAL LAMBDA FOR PLATEOUT
    9 LAMPL = PLATLM+PLATTR
      RETURN
   99 WRITE (NOUT,100)
  100 FORMAT(1H1,3X,'WALL PLATEOUT CALCULATION ABORTED DUE TO ',
     1       'IMPROPER INPUT')
      RETURN
      END
      DOUBLE PRECISION FUNCTION ALPHA (SH,J)
C
C   THIS FUNCTION CALCULATES THE FIRST 20 ROOTS OF THE
C   FUNCTION ALPHA/TAN(ALPHA) + SH - 1 = 0.
C
      DOUBLE PRECISION ZERO,DELT,PI,X,X1,F,SH
      DIMENSION F(100)
      PI =0.31415926535897930+01
      ZERO = 1.0D-11
      ITER = 1
C
C   USE BISECTION METHOD TO FIND ZEROS
      DELT = PI
      X = J * PI
      X1 = X - PI
      F(1) = X1*DCOS(X1) + (SH-1.0)*DSIN(X1)
    1 ITER = ITER + 1
      F(ITER) = X*DCOS(X) + (SH-1.0)*DSIN(X)
      IF (F(ITER)*F(ITER-1) .GT. 0.) GO TO 2
      DELT = -DELT
    2 DELT = 0.5*DELT
      IF (F(ITER) .GT. -ZERO .AND. F(ITER) .LT. ZERO) GO TO 3
```

```
      X = X + DELT
      IF (ITER .LT. 50) GO TO 1
C
C   ERROR MESSAGE
      WRITE(NOUT,100)
      WRITE(NOUT,200) J,SH,X,F(ITER),DELT
C
    3 ALPHA = X
      RETURN
  100 FORMAT(1H1,30X,'...ERROR...'//' AFTER 50 ITERATIONS FUNCTION',
     1       ' ALPHA HAS NOT CONVERGED.'//,' THE VALUES FOR J, SH, X, ',
     2       'F(ITER), AND DELT ARE')
  200 FORMAT(1H0,I3,3X,4E15.4)
      END
      SUBROUTINE XYPLOT
C
C  THIS SUBROUTINE PLOTS ONE DEPENDENT VARIABLE AGAINST AN
C    INDEPENDENT VARIABLE. THESE ARE NAMED, RESPECTIVELY,
C    X(I) AND Y(I).
C
C  UP TO FIFTY (50) DATA POINTS MAY BE USED.
C
      COMMON /CNTRL / NIN, NOUT, NGRP, NTYPE, MODEL, NREAC, NDATA
      COMMON/ARRAYS/X(50),Y(50),NPOINT
      DIMENSION IX(50),IY(50)
C  SCALING:
      XMAX=AMAX1(X(1),X(2),X(3),X(4),X(5),X(6),X(7),X(8),X(9),
     1           X(10),X(11),X(12),X(13),X(14),X(15),X(16),X(17),
     2           X(18),X(19),X(20),X(21),X(22),X(23),X(24),X(25),
     3           X(26),X(27),X(28),X(29),X(28),X(29),X(30),X(31),
     4           X(32),X(33),X(34),X(35),X(36),X(37),X(38),X(39),
     5           X(40),X(41),X(42),X(43),X(44),X(45),X(46),X(47),
     6           X(48),X(49),X(50))
      YMAX=AMAX1(Y(1),Y(2),Y(3),Y(4),Y(5),Y(6),Y(7),Y(8),Y(9),
     1           Y(10),Y(11),Y(12),Y(13),Y(14),Y(15),Y(16),Y(17),
     2           Y(18),Y(19),Y(20),Y(21),Y(22),Y(23),Y(24),Y(25),
     3           Y(26),Y(27),Y(28),Y(29),Y(28),Y(29),Y(30),Y(31),
     4           Y(32),Y(33),Y(34),Y(35),Y(36),Y(37),Y(38),Y(39),
     5           Y(40),Y(41),Y(42),Y(43),Y(44),Y(45),Y(46),Y(47),
     6           Y(48),Y(49),Y(50))
      YSCALE = YMAX/50.
      XSCALE = XMAX/50.
      DO 11 I = 1,50
      XXX = X(I)/XSCALE
      YYY = Y(I)/YSCALE
      IX(I) = XXX
      IY(I) = YYY
   11 CONTINUE
C
C  LABEL Y-AXIS:
      WRITE (NOUT,501) YSCALE
      WRITE (NOUT,502)
C
C  PLOTTING AND LABELING OF X-AXIS:
      DO 18 I = 1,50
      IF (I-NPOINT) 17,17,18
   17 IF (IX(I) .EQ. 0) GO TO 13
      IF (IX(I) .EQ. IX(I+1)) GO TO 18
      IF (IY(I) .EQ. 0) GO TO 200
      IRS = IY(I)
      GO TO (201,202,203,204,205,206,207,208,209,210,
     1       211,212,213,214,215,216,217,218,219,220,
     2       221,222,223,224,225,226,227,228,229,230,
     3       231,232,233,234,235,236,237,238,239,240,
     4       241,242,243,244,245,246,247,248,249,250),IRS
  200 WRITE (NOUT,600)
      GO TO 12
  201 WRITE (NOUT,601) X(I)
      GO TO 12
  202 WRITE (NOUT,602) X(I)
      GO TO 12
```

```
203 WRITE (NOUT,603) X(I)
    GO TO 12
204 WRITE (NOUT,604) X(I)
    GO TO 12
205 WRITE (NOUT,605) X(I)
    GO TO 12
206 WRITE (NOUT,606) X(I)
    GO TO 12
207 WRITE (NOUT,607) X(I)
    GO TO 12
208 WRITE (NOUT,608) X(I)
    GO TO 12
209 WRITE (NOUT,609) X(I)
    GO TO 12
210 WRITE (NOUT,610) X(I)
    GO TO 12
211 WRITE (NOUT,611) X(I)
    GO TO 12
212 WRITE (NOUT,612) X(I)
    GO TO 12
213 WRITE (NOUT,613) X(I)
    GO TO 12
214 WRITE (NOUT,614) X(I)
    GO TO 12
215 WRITE (NOUT,615) X(I)
    GO TO 12
216 WRITE (NOUT,616) X(I)
    GO TO 12
217 WRITE (NOUT,617) X(I)
    GO TO 12
218 WRITE (NOUT,618) X(I)
    GO TO 12
219 WRITE (NOUT,619) X(I)
    GO TO 12
220 WRITE (NOUT,620) X(I)
    GO TO 12
221 WRITE (NOUT,621) X(I)
    GO TO 12
222 WRITE (NOUT,622) X(I)
    GO TO 12
223 WRITE (NOUT,623) X(I)
    GO TO 12
224 WRITE (NOUT,624) X(I)
    GO TO 12
225 WRITE (NOUT,625) X(I)
    GO TO 12
226 WRITE (NOUT,626) X(I)
    GO TO 12
227 WRITE (NOUT,627) X(I)
    GO TO 12
228 WRITE (NOUT,628) X(I)
    GO TO 12
229 WRITE (NOUT,629) X(I)
    GO TO 12
230 WRITE (NOUT,630) X(I)
    GO TO 12
231 WRITE (NOUT,631) X(I)
    GO TO 12
232 WRITE (NOUT,632) X(I)
    GO TO 12
233 WRITE (NOUT,633) X(I)
    GO TO 12
234 WRITE (NOUT,634) X(I)
    GO TO 12
235 WRITE (NOUT,635) X(I)
    GO TO 12
236 WRITE (NOUT,636) X(I)
    GO TO 12
237 WRITE (NOUT,637) X(I)
    GO TO 12
238 WRITE (NOUT,638) X(I)
    GO TO 12
```

```
239 WRITE (NOUT,639) X(I)
    GO TO 12
240 WRITE (NOUT,640) X(I)
    GO TO 12
241 WRITE (NOUT,641) X(I)
    GO TO 12
242 WRITE (NOUT,642) X(I)
    GO TO 12
243 WRITE (NOUT,643) X(I)
    GO TO 12
244 WRITE (NOUT,644) X(I)
    GO TO 12
245 WRITE (NOUT,645) X(I)
    GO TO 12
246 WRITE (NOUT,646) X(I)
    GO TO 12
247 WRITE (NOUT,647) X(I)
    GO TO 12
248 WRITE (NOUT,648) X(I)
    GO TO 12
249 WRITE (NOUT,649) X(I)
    GO TO 12
250 WRITE (NOUT,650) X(I)
    GO TO 12
 13 WRITE (NOUT,503)
 12 ISPACE = IX(I+1) - IX(I) -1
    IF (ISPACE) 18,18,801
801 DO 802 J = 1,ISPACE
802 WRITE (NOUT,503)
 18 CONTINUE
291 WRITE (NOUT,504)
    WRITE (NOUT,505) XSCALE,YSCALE
    WRITE (NOUT,506)
    DO 15 I = 1,50
    WRITE (NOUT,507) X(I),Y(I),IX(I),IY(I)
 15 CONTINUE
C
501 FORMAT (1H1,45X,'Y-AXIS (ACTUAL Y-VALUE/',1P1E9.3,')',/,
   1        13X,'0',8X,' 5',8X,'10',8X,'15',8X,'20',
   2        8X,'25',8X,'30',8X,'35',8X,'40',8X,'45',8X,'50')
502 FORMAT (1H , 12X,'I---------I','---------I',
   1        '---------I','---------I','---------I',
   2        '---------I','---------I','---------I',
   3        '---------I','---------I')
503 FORMAT (1H ,12X,'I')
504 FORMAT (1HO,15X,'SCALING FACTORS :',//,
   1        18X,'INDEPENDENT VARIABLE S.F.',
   2        '  DEPENDENT VARIABLE S.F.')
505 FORMAT (1HO,20X,2(1PE10.3,17X))
506 FORMAT (1H1,10X,'   X(I)   ',4X,'   Y(I)   ',4X,
   1        'IX(I)',2X,'IY(I)')
507 FORMAT (10X,2(1PE10.3,4X),2(I5,2X))
600 FORMAT (2X,1PE10.3,1X,'0')
601 FORMAT (2X,1PE10.3,1X,'I',1X,'1')
602 FORMAT (2X,1PE10.3,1X,'I',3X,'2')
603 FORMAT (2X,1PE10.3,1X,'I',5X,'3')
604 FORMAT (2X,1PE10.3,1X,'I',7X,'4')
605 FORMAT (2X,1PE10.3,1X,'I',9X,'5')
606 FORMAT (2X,1PE10.3,1X,'I',11X,'6')
607 FORMAT (2X,1PE10.3,1X,'I',13X,'7')
608 FORMAT (2X,1PE10.3,1X,'I',15X,'8')
609 FORMAT (2X,1PE10.3,1X,'I',17X,'9')
610 FORMAT (2X,1PE10.3,1X,'I',19X,'10')
611 FORMAT (2X,1PE10.3,1X,'I',21X,'11')
612 FORMAT (2X,1PE10.3,1X,'I',23X,'12')
613 FORMAT (2X,1PE10.3,1X,'I',25X,'13')
614 FORMAT (2X,1PE10.3,1X,'I',27X,'14')
615 FORMAT (2X,1PE10.3,1X,'I',29X,'15')
616 FORMAT (2X,1PE10.3,1X,'I',31X,'16')
617 FORMAT (2X,1PE10.3,1X,'I',33X,'17')
618 FORMAT (2X,1PE10.3,1X,'I',35X,'18')
619 FORMAT (2X,1PE10.3,1X,'I',37X,'19')
```

```
  620 FORMAT (2X,1P1E10.3,1X,'I',39X,'20')
  621 FORMAT (2X,1P1E10.3,1X,'I',41X,'21')
  622 FORMAT (2X,1P1E10.3,1X,'I',43X,'22')
  623 FORMAT (2X,1P1E10.3,1X,'I',45X,'23')
  624 FORMAT (2X,1P1E10.3,1X,'I',47X,'24')
  625 FORMAT (2X,1P1E10.3,1X,'I',49X,'25')
  626 FORMAT (2X,1P1E10.3,1X,'I',51X,'26')
  627 FORMAT (2X,1P1E10.3,1X,'I',53X,'27')
  628 FORMAT (2X,1P1E10.3,1X,'I',55X,'28')
  629 FORMAT (2X,1P1E10.3,1X,'I',57X,'29')
  630 FORMAT (2X,1P1E10.3,1X,'I',59X,'30')
  631 FORMAT (2X,1P1E10.3,1X,'I',61X,'31')
  632 FORMAT (2X,1P1E10.3,1X,'I',63X,'32')
  633 FORMAT (2X,1P1E10.3,1X,'I',65X,'33')
  634 FORMAT (2X,1P1E10.3,1X,'I',67X,'34')
  635 FORMAT (2X,1P1E10.3,1X,'I',69X,'35')
  636 FORMAT (2X,1P1E10.3,1X,'I',71X,'36')
  637 FORMAT (2X,1P1E10.3,1X,'I',73X,'37')
  638 FORMAT (2X,1P1E10.3,1X,'I',75X,'38')
  639 FORMAT (2X,1P1E10.3,1X,'I',77X,'39')
  640 FORMAT (2X,1P1E10.3,1X,'I',79X,'40')
  641 FORMAT (2X,1P1E10.3,1X,'I',81X,'41')
  642 FORMAT (2X,1P1E10.3,1X,'I',83X,'42')
  643 FORMAT (2X,1P1E10.3,1X,'I',85X,'43')
  644 FORMAT (2X,1P1E10.3,1X,'I',87X,'44')
  645 FORMAT (2X,1P1E10.3,1X,'I',89X,'45')
  646 FORMAT (2X,1P1E10.3,1X,'I',91X,'46')
  647 FORMAT (2X,1P1E10.3,1X,'I',93X,'47')
  648 FORMAT (2X,1P1E10.3,1X,'I',95X,'48')
  649 FORMAT (2X,1P1E10.3,1X,'I',97X,'49')
  650 FORMAT (2X,1P1E10.3,1X,'I',99X,'50')
      RETURN
      END
/*
```

NRC FORM 335 (7-77)

U.S. NUCLEAR REGULATORY COMMISSION

BIBLIOGRAPHIC DATA SHEET

1. REPORT NUMBER *(Assigned by DDC)*
NUREG/CR-0009

4. TITLE AND SUBTITLE *(Add Volume No., if appropriate)*
Technological Bases for Models of Spray Washout of Airborne Contaminants in Containment Vessels

2. *(Leave blank)*

3. RECIPIENT'S ACCESSION NO.

7. AUTHOR(S)
A. K. Postma, R. R. Sherry, P. S. Tam

5. DATE REPORT COMPLETED
MONTH: Oct. YEAR: 78

9. PERFORMING ORGANIZATION NAME AND MAILING ADDRESS *(Include Zip Code)*
Benton City Technology
Route 1, Box 1281
Benton City, Wa. 99352

DATE REPORT ISSUED
MONTH | YEAR

6. *(Leave blank)*

8. *(Leave blank)*

12. SPONSORING ORGANIZATION NAME AND MAILING ADDRESS *(Include Zip Code)*
Accident Analysis Branch
Division of Site Safety & Environmental Analysis
U. S. Nuclear Regulatory Commission

10. PROJECT/TASK/WORK UNIT NO.

11. CONTRACT NO.

13. TYPE OF REPORT
Consultant

PERIOD COVERED *(Inclusive dates)*

15. SUPPLEMENTARY NOTES

14. *(Leave blank)*

16. ABSTRACT *(200 words or less)*

This report summarizes the technological bases underlying the radioactivity washout model used by the NRC staff. The material contained in this report may be found in dozens of documents, some of those are not easily obtained. This report attempts to present all pertinent information in detail, while referencing the sources of such information. Appendix A to this report describes the computer code SPIRT. This code employs the models presented in the report and is used routinely by the NRC staff to evaluate iodine removal functions by containment spray systems.

Despite its comprehensive nature, this report does not contain information on the design of spray systems, nor does it endorse any particular spray system design.

17. KEY WORDS AND DOCUMENT ANALYSIS

17a. DESCRIPTORS

17b. IDENTIFIERS/OPEN-ENDED TERMS

18. AVAILABILITY STATEMENT
Unlimited

19. SECURITY CLASS *(This report)*

20. SECURITY CLASS *(This page)*

21. NO. OF PAGES

22. PRICE
$

UNITED STATES
NUCLEAR REGULATORY COMMISSION
WASHINGTON, D. C. 20555

OFFICIAL BUSINESS
PENALTY FOR PRIVATE USE, $300

POSTAGE AND FEES PAID
U.S. NUCLEAR REGULATORY
COMMISSION

U.S. MAIL

120555003927 2 AN
US NRC
SECY PUBLIC DOCUMENT ROOM
BRANCH CHIEF
PST LOBBY
WASHINGTON DC 20555